University of Trento
University of Brescia
University of Padova
University of Trieste
University of Udine
University IUAV of Venezia

Ph.D. Candidate
Andrea Rao

BIOMETRICS IN WEARABLE PRODUCTS: REVERSE ENGINEERING AND NUMERICAL MODELING

Advisors
Ing. Ilaria Cristofolini
Ing. Matteo Benedetti
Prof. Vigilio Fontanari

2011

UNIVERSITY OF TRENTO
Graduate School in Structural Engineering
Modelling, Preservation and Controls of Materials and Structures
XXIII Cycle

Ph.D. Program Head: prof. D. Bigoni

Final Examination: 25 March 2011

Board of Examiners:
Prof. Roberto Oboe, Università degli studi di Padova
Prof. Robert Mc Meeking, University of California
Prof. Ettore Pennestrì, Università degli studi di Roma Tor Vergata
Prof. Antonio De Simone, SISSA

Summary

The Reverse Engineering (RE) techniques and the Finite Element Modelling (FEM) are widely used tools in many scientific fields. They were firstly developed for the mechanics but in the last times became common for other disciplines. In the thesis these techniques are used for the customization of the wearable products. It is possible to observe that the geometry of whatever wearable product is fundamental for the comfort. In particular, starting from the need of wearable product it is possible to analyse the relative body part and to study the products most appropriate interface geometry to maximize the comfort. The related disciplines are biometrics, biomechanics and anthropometry. In the thesis four different non-contact RE techniques are taken into account: shape from stereo, shape from silhouette, shape from laser and range finding. The first instrument which has been developed is based on the multi stereo vision, focusing the attention to the data filtering and to the generation of the solid model represented by mesh. The second instrument is based on the model generation starting from the silhouette. These two techniques are compared to another laser instrument available on the market. The tolerance on the reconstruction give an error on the total length of the foot of about 2 mm. The tolerance is acceptable for the study of a footwear product anyway it is not sufficient for a scientific research. For this reason a fourth RE system based on range finding is studied. A lot of possible methods were analysed, the multifrequencies, belonging as Fringe Projection Profilometry (FPP) group, has been considered the best compromise between precision, accuracy and elaboration times. An instrument has been developed which in few seconds performs the reconstruction using common, cheap products such as a projector and a camera. The use of the aforementioned RE techniques allowed to adequately reconstruct the geometrical model of the foot, then the deformation of the foot is studied using a Finite Element Analysis (FEA). A model characterized by nearly 200000 elements has been developed. The deformations are congruent with literature data. Anyway, considering the complex validation process of the FE model, caused by the difficulties on measuring the real displacement of the foot under loading condition, a direct matching between the acquired geometry and the final shape of the wearable product has been preferred. A function, capable to analyse the fitting between foot and shoe, through a coefficient called comfort index has been developed.

Sommario

Le tecniche di Reverse Engineering (RE) e la modellazione numerica agli elementi finiti (Finite Element Method, FEM) sono degli strumenti molto diffusi in vari settori scientifici. Nascono per la meccanica ma negli ultimi tempi vengono sempre più utilizzati anche in altri ambiti. Nella tesi queste tecniche vengono adottate per studiare la personalizzazione dei prodotti indossabili. È possibile notare che la geometria di un qualsiasi prodotto indossabile è fondamentale per il comfort. In particolare nello studio di un prodotto indossabile si analizza la parte del corpo interessata e si definisce la geometria di interfaccia più idonea per massimizzare il comfort. Le discipline interessate sono dunque la biometrica, la biomeccanica e l'antropometria. Nella tesi sono stati presi in considerazione quattro diversi metodi di RE non a contatto: shape from stereo, shape from silhouette, shape from laser e range finding. Il primo strumento sviluppato è basato sulla multi stereo visione, l'attenzione è stata posta sul filtraggio dei dati e sulla generazione del modello solido rappresentato da mesh. Il secondo strumento si basa sulla generazione del modello partendo dalla silhouette. Questi due sono stati confrontati con uno strumento laser disponibile sul mercato. Il confronto evidenzia un errore sulla lunghezza totale del piede di 2 mm. Tolleranza accettabile per lo studio di un prodotto confortevole ma non sufficiente per l'ambiente della ricerca. Si è scelto quindi di studiare un quarto sistema di ricostruzione basato sul range finding. Vari metodi sono stati analizzati, tuttavia la multifrequencies, sottogruppo del Fringe Projection Profilometry (FPP), è stata considerata come il migliore compromesso tra precisione, accuratezza e tempi di elaborazione. È stato realizzato uno strumento che, in pochi secondi, esegue una ricostruzione affidabile con tolleranze di 0.2 mm con prodotti tipici della grande distribuzione come proiettore e macchina fotografica. Dopo l'analisi della geometria, mediante tecniche di RE, si è passati allo studio della deformazione del piede sotto carico mediante un'analisi agli elementi finiti. È stato sviluppato un modello lineare contente circa 200000 elementi. Le deformazioni risultano congrue con quanto trovato in bibliografia. Comunque, considerando il complesso processo di validazione del modello agli elementi finiti, causato dalle difficoltà nel misurare gli spostamenti reali del piede in condizioni di carico, si è preferito confrontare direttamentre il modello acquisito e la forma finale del prodotto. Una funzione, capace di analizzare il fitting tra piede e forma, chiamato indice di comfort, è stata definita.

To Susanna

Acknowledgements

I would like to thank my family and my dear friends for their invaluable help during these last incredible six months...

Trento, March 2011

Andrea Rao

Published papers

The main results presented in this thesis have been summarized in the following papers:

1) Cremaschi A., Olivato P., Rao A., "Manufacturing upon knowledge: a new approach to engineering wearable products". 2007. Proceedings of "Mass Customization Personalization (MCPC 2007)", Massachusetts Institute of Technology (MIT), Boston, 7th-10th October 2007.

2) Rao A., Sartor L., Cristofolini I., Fontanari V., "Progettazione di una protezione integrata nei guanti da moto". Proceedings of "AIAS 2008", La Sapienza, Rome, 10th-13th September, 2008.

3) Rao A., Fontanari V., Cristofolini I., "From the Computerized Tomography of the foot to the discretization of the domain for the Finite Element Analysis ". Proceedings of "TCN CAE 2008", Venice, 16th - 17th October, 2008.

4) Rao A., "Ricostruzione della superficie esterna del piede mediante tecnica di stereo visione multipla". Proceedings of "AIAS 2009", Politecnico, Turin, 9th-11th September, 2009.

5) I. Cristofolini, A. Rao, C. Menapace, A. Molinari, "Influence of sintering temperature on the shrinkage and geometrical characteristics of steel parts produced by Powder Metallurgy ". Journal of Materials Processing Technology, 210 (2010) 1716-1725.

6) Rao A., Fontanari V., Cristofolini I. De Monte G., "Instruments to measure human feet using Reverse Engineering techniques". Proceedings of "SEM 2010", Indianapolis, 7th-10th June, 2010.

7) Cristofolini I., Pilla M., Rao A., Molinari A., Libardi S., "Dimensional and geometriacal control of PM parts sitered at low and high temperatures". Proceedings of the 2010 International Conference on Powder Metallurgy Particulate Materials, June 2730, Hollywood, FL, USA.

8) Rao A., Fontanari V., Cristofolini I. De Monte G., "Un esempio applicativo di Reverse Engineering in biomeccanica clinica". Proceedings of "AIAS 2010", Maratea (Potenza), 7th-10th September, 2010.

9) Fontanari V., Avalle M., Peroni L., Monelli D. B., Rao A., "Analisi della risposta ad impatto di poliuretani termoplastici". Proceedings of "AIAS 2010", Maratea (Potenza), 7th-10th September, 2010.

10) Cristofolini I., Pilla M., Rao A., Pederzini G., Salemi A., Crosta R., Molinari A., "Optimisation of powder compaction to improve the dimensional characteristics of PM steel parts". Proceedings of the PM 2010, Firenze, 10th-14th October, 2010.

11) Molinari A., Santuliana E., Cristofolini I., Rao A., Libardi S., Marconi P., "Surface modifications induced by shot peening and their effect on the plane bending fatigue strength of a CrMo steel produced by powder metallurgy". Materials Science and Engineering A, 528 (2011) 29042911.

In the frame of this work some theses are considered fundamental:

- Andrea Lorenzi, master's thesis, "Digitalizzazione del piede umano con tecniche di Reverse Engineering";
- Luciano Sartor, bachelor's thesis, "Progettazione di una protezione integrata nei guanti da moto";
- Paolo Olivato, PhD's thesis, "Per una ergonomia della calzatura";
- Matteo Perini, mater's thesis, "Implementazione di tecniche FPP (Fringe Projection Profilometry) nella ricostruzione di superfici free form";
- Giuliano Cicolini, master's thesis, "Progettazione di protezioni per la schiena dei motociclisti".

Contents

Chapter 1

Introduction

Biometrics is the science technique of measuring and analysing biological variables using statistical and mathematical methods. Biometrical data of whatever living being are obtained measuring different characteristics of the body and the biomechanical behaviour. The scientific research is oriented to the identification of a living being through characteristics or behaviours. These characteristics are difficult to alter such as fingerprints, eye retinas and irises, voice patterns, etc. Close to biometrics, anthropometrics is different for few details; it refers only to the measurement of the human body for the purposes of understanding human physical variables. It is a direct support of anthropology and it is characterized by a series of applications; one of them is ergonomics. At the same time biomechanics analyses the behaviour of living being with relation to the loads applied. This thesis is developed in a field related to these three sciences, that means to wearable products. The term wearable products is referred to all the objects touching the skin of the human body, which are characterized by a surface of interface with it. The purpose of this work is to design comfortable wearable products starting from a fundamental observation: it is possible to obtain a wearable product more or less comfortable varying the shape of interface with the body. The present dissertation is aimed at developing a new methodology based on the RE approach able to accurately rebuild human body parts, thus making it possible to manufacture wearable products. In order to qualify and validate this procedure, foot RE analysis has been faced. Foot represents one of the most crucial human body parts. The comfort is paramount importance; in addition human foot is characterized by very complex surfaces. Accordingly, it probably represents the best test for establishing the accuracy of the novel

approach. In particular, a generic wearable product can be offered in sizes, so their it is characterized by fixed proportions, e.g. a footwear size 40 has a fixed ratio of length and width. The adoption of grading development allows economies of scales. On the contrary it creates fit problems between shoe and foot. It is possible to note that:

- Whatever individual is always asymmetric;
- Standard systems of grading are not adopted. Generally companies use internal standard derived from experience;
- Grading operation starts from a size and calculates others using a proportion; given a length one width only is derived;
- It is difficult to define a population; different ethnic groups are identified by different shapes.

Current researches in biometrics and anthropometrics are based on technical products aimed at a specific and not generic purposes such as military, sporty and for corrections of posture. In addition it is difficult to characterize 3D geometries for entire parts of the body (hand, foot and head), so that linear measures are often considered. Acquisition procedures are not automatic and frequently they are used only for research scopes. As a consequence they can be applied for limited samples of individuals. From these observations, it is possible to deduce that it is important to analyse an entire geometry, such as a whole upper limb considering both biometrics (through Reverse Engineering, RE) and biomechanics (through numerical analysis) with rapid, automatic and precise methods. For the above mentioned reasons the work evolves on the following steps:

- Analysis of the whole human body geometries by Reverse Engineering (RE) techniques;
- Numerical analysis of the foot under loading conditions using Finite Element Method (FEM);
- Analyses of the foot dimensions and comparison to shoes to optimize the comfort.

1.1 State of the art

Reverse Engineering (RE) of shapes aims to create an appropriate digital representation of existing objects from sets of measured data points. Three-dimensional CAD models are the industry standard communication tool for manufacturing and design. By converting physical parts through 3D scanning to a CAD format, efficiencies can be obtained in areas such as product development, manufacturing technology, enterprise communication, market evaluation and time to market (Lerch et al., 2007). Classically used in many areas of engineering, in the last years the utility of RE processes found interesting applications in medical sciences and biomechanical related applications (Viceconti et al., 1999), (Mahaisavariya et al., 2002), (Lin et al., 2005), (Popov and Onuh, 2009). There are a lot of different 3D surface digitalization devices, which can be divided into different groups depending on various characteristics: technology (e.g. laser scanning or white light projection), configuration (e.g. fix or on CMM/robot/arm) or type of measurement (e.g. surface scanning or profile scanning) (D'Apuzzo, 2006). Certainly all these different 3D surface digitalization technologies have advantages and disadvantages. This is a reason because a large group of 3D measurement systems is made by solutions customized for specific applications; the systems are optimized for the acquisition of particular objects and are designed according to the specific task. Some of the most established technologies for 3D reconstruction of biological materials in medicine are CT (Computer Tomography) or MRI (Magnetic Resonance Imaging) scanning; these techniques provide with a good precision both surface and internal data of the scanned subject, but they are very expensive. Moreover CT scans implies radiation exposure of the subject and operators. When only external surface information of the subject is required, less expansive alternatives than CT/MRI scans are laser scanning (Lerch et al., 2007), projection of light patterns or combination modelling and image processing technologies. These technologies do not require object contact and have no adverse effects for biological materials. Now there are many technologies available (D'Apuzzo, 2006): shape from stereo, shape from silhouette, shape from laser, Active range-finding. They will be briefly described in the following paragraphs.

1.2 Shape from stereo

The problem of determining a point's 3D position from a set of corresponding image locations and known camera positions is known as triangulation. Stereo and Active range-finding are related with triangulation (Tomasi and Kanade, 1992), (Schmid and Zisserman, 1997). Stereo reconstruction techniques can convert a pair of images into a depth map or a sequence of images into a 3D model (Szeliski, 2010). In computer vision, the topic of stereo matching has been one of the most widely studied and fundamental problems (Marr and Poggio, 1976), (Barnard and Fischler, 1982), (Dhond and Aggarwal, 1989), (Brown et al., 2003) and (Seitz et al., 2006) and continues to be one of the most active research areas. In order to estimate 3D coordinates of object surface point and to construct its 3D model it is necessary to find 2D coordinates of each point of a pattern, projected or imposed on the object, in left and right images and solve the task of stereoscopic identification of correspondent points. This technique is based on the epipolar geometry, or the geometry of stereo vision. When two cameras view a 3D scene from two distinct positions, there are a number of geometric relations between the 3D points and their projections onto the 2D images that lead to constraints between the image points. These relations are based on the assumption that the cameras can be approximated by the pinhole camera model. This is a common model which represents projection operation by rays that emanate from the camera, passing through its focal point. Each camera captures a 2D image of the 3D world. This conversion from 3D to 2D is referred to as a perspective projection. These two images identify the same point, on the images they are called epipolar points. Both epipolar points, in their respective image planes lie on a single 3D epipolar line. The epipolar line is a function of the 3D point. All epipolar lines in one image must intersect the epipolar point of that image (Fig. 1.1).

As an alternative visualization, consider the points X, O_L and O_R that form a plane called the epipolar plane. The epipolar plane intersects each camera's image plane where it forms epipolar lines. All epipolar planes and epipolar lines intersect the epipole regardless of where X is located. The epipolar geometry allows to define for each point, observed in one image, the same point observed in the other image on a known epipolar line. Observing the point in an image the correspond line on the other image must intersect the same point. The coordinates of the points depend on the position of the point respect to the epipolar line. The point can intersect the line near, or far, from the other camera. This epipolar constrain, between two cameras, is

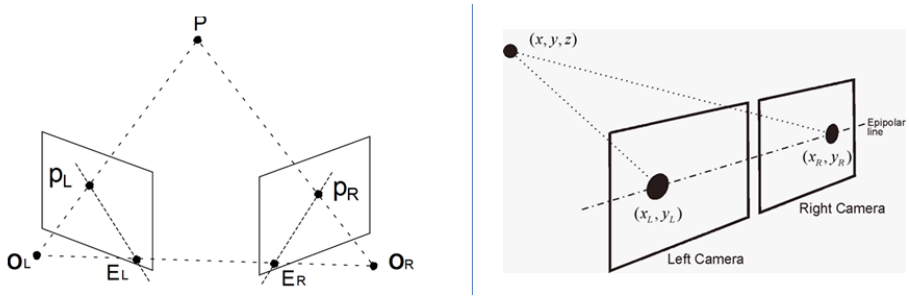

Figure 1.1: The physical principle of the stereo vision. Two cameras, with their respective focal points O_L and O_R, observe a point P. The projection of P onto each of the image planes is denoted p_L and p_R. Points E_L and E_R are the epipoles.

defined using a calibration procedure.

1.3 Shape from silhouette

Over the years, a number of techniques have been developed to reconstruct a 3D volumetric model from the intersection of the binary silhouettes projected into 3D. The resulting model is called a visual hull (or sometimes a line hull), because it is analogous to the convex hull of a set of points. The volume is maximal with respect to the visual silhouettes and surface elements are tangent to the viewing rays (lines) along the silhouette boundaries. Silhoutte performs a foreground-background segmentation of the object of interest is a good way to initialize or fit a 3D model (Grauman et al., 2008), (Vlasic et al., 2008) or to impose a convex set of constraints on multiview stereo (Kolev and Cremers, 2008). The Visual hull is a geometric entity created by shape from silhouette 3D reconstruction technique introduced by Laurentini (1994). This technique divides the foreground and the background of a grey level image using a threshold to obtain a binary image. The foreground mask, known as a silhouette, is the 2D projection of the corresponding 3D foreground object. Along with the camera viewing parameters, the silhouette defines a back-projected generalized cone that contains the actual object. Starting from each acquired image the cone can be calculated. Intersecting two or more cones, of two or more image, a solid model can be created and it is called visual hull and defines a bounding geometry of the actual 3D object (Fig. 1.2).

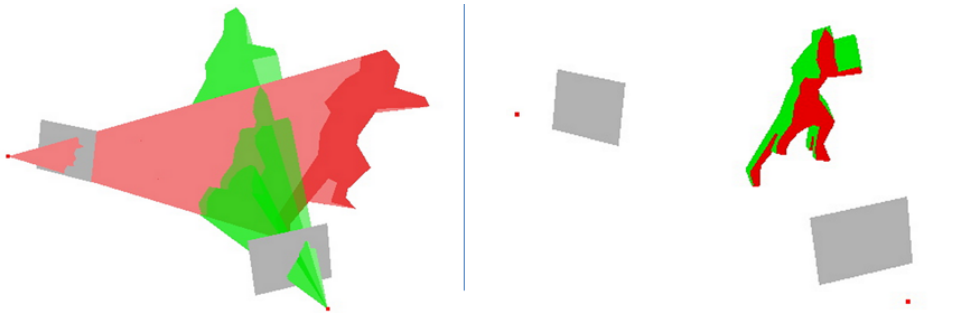

Figure 1.2: The physical principle of the silhouette. Two cameras, the cones that contains the object (left) and the visual hull solid model.

Silhouettes can often easily be extracted from images. If intrinsic parameters are known, then the visual hull can be computed by intersecting the visual cones corresponding to silhouettes captured from multiple viewpoints. The visual hull is often a good approximation to the 3D shape of the object and is useful for tasks such as 3D multimedia content creation. Although the aforementioned drawbacks approaches must be considered in the RE application thanks to the improvement proposed by Forbes et. al. (2006). The proposed technique is based on two planar mirrors and an uncalibrated camera. Two mirrors are used to create five views of the object: a view directly onto the object, two reflections, and two reflections of reflections (Fig. 1.3). Two or more images of the object and its reflections are captured from different camera positions (without altering the internal parameters) to obtain a well-distributed set of silhouettes. Starting from two mirror and a camera the system can be considered low-cost. The low-cost aspect is important but not fundamental because the attention must be paid on the calibration system. No markers or point correspondences are required. To explain the method, an analysis using only one mirror is shown from the article of Forbes et al.(2006).

"Consider a plane Π_1 that passes through the camera centres CR and CV and touches the real object at the point PR1 (Fig. 1.3, left). By symmetry, Π_1 will touch the virtual object at the point PV1 which is the reflection of PR1. Since Π_1 is tangent to both objects and contains the camera centres CR and CV , PR1 and PV1 are frontier points. They project onto the silhouette outlines on the real image at points pRR1 and pRV1. The points pRR1, pRV1 and the epipole eRV (the projection of CR into the real image) are therefore collinear, since they lie in both Π_1 and the real image plane. The bitangent

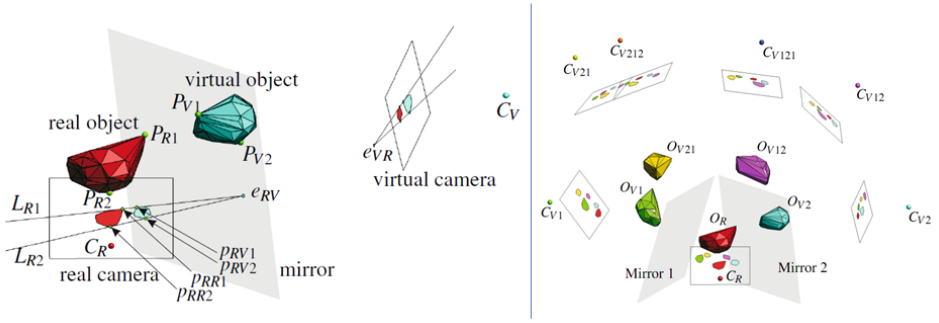

Figure 1.3: A camera viewing an object and its refrection. The epipole e_RV corresponding to the virtual can be computed from the silhouette bitangent lines L_R1 and L_R2 (left). Mirror setup showing one real and four virtual objects, and one real and six virtual camera (Forbes et al., 2006).

Figure 1.4: Two input images and resultant visul hull model of a toy locust (Forbes et al., 2006).

line LR1 passing through these three points can be computed directly from the silhouette outlines: it is simply the line that is tangent to both silhouettes. Another bitangent line LR2 passes through the epipole and touches the silhouettes on the opposite side to LR1. These tangency points lie on a plane Π_2 that is tangent to the opposite side of the object and passes through both camera centres. Provided that the object does not intersect the line passing through both camera centres, there will be two outer epipolar tangent lines LR1 and LR2 that touch the silhouettes on either side. The position of the epipole eRV can therefore be computed by determining LR1 and LR2 from the silhouette outlines; it is located at the intersection of LR1 and LR2. Note that the epipole is computed without requiring knowledge of the camera pose

and without requiring any point correspondences. We also note that by symmetry, the real camera's silhouette view of the virtual object is a mirror image of the virtual camera's silhouette view of the real object. The silhouette view observed by a reflection of a camera is therefore known if the camera's view of the reflection of the object is known."

Applying the same theory to an instrument based on the two mirrors can be obtained five silhouettes only with a single image (Fig. 1.3, right). More than one image can be considered and a better precision can be obtained (Fig. 1.4). A last degree of freedom must be defined, it is called overall scale factor. It is the unique parameter to set after the reconstruction.

1.4 Shape from laser

The active illumination to obtain the shading region has been used from the earliest days of machine vision to construct highly reliable sensors for estimating 3D depth images using a variety of rangefinding (or range sensing) techniques (Besl, 1988), (Curless, 1999) and (Hebert, 2000). One of the most popular active illumination sensors is a laser or light stripe laser. The deformation of the light stripe laser crosses the object being scanned, thus revealing its 3D shape. Instead of the light stripe laser a light source and a mobile shadow can be adopted (Bouguet and Perona, 1999). One of the most common forms of active range sensing is optical triangulation. Laser scanners create a 3D model through the triangulation of a laser line, projected onto an object from a device and acquired by a camera. The laser line is also called stripe laser and the line across the object vary its geometry. Depending on the deformation the depth can be estimated (Fig. 1.5). The scanner using reference features on the surface on the acquired surface or on the background. This technique can also use infrared Light-emitting diodes attached to the scanner which are seen by the camera through filters (Fig. 1.6). Data is collected by a computer and recorded as data points within Three-dimensional space. One of the limitations of the previous this approach is the need to capture many frames while sweeping the light over the object.

This technique gives a single range point, however to measure the whole surface of an object, relative movement of camera, object and/or projector must be carried out. A much faster scanner can be manufactured using a projector, the brightness of each pixel can be imposed. As a consequence bright and dark areas can be projected on the object. In this way shadows are created directly on the object.

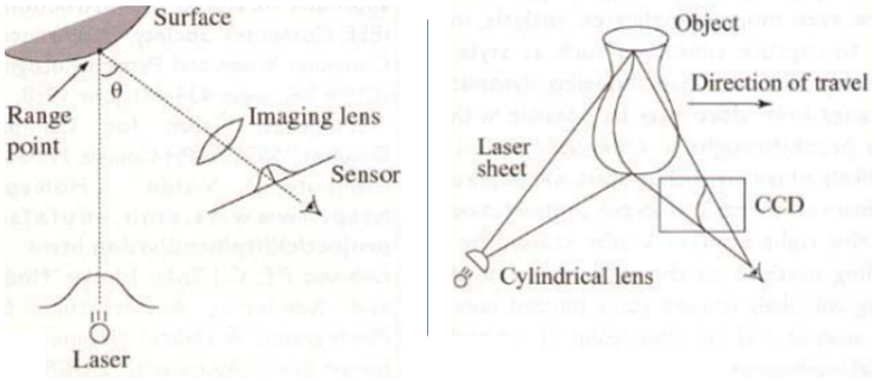

Figure 1.5: A light illuminates a region on the surface of an object. A spot light (left) and a stripe light (right).

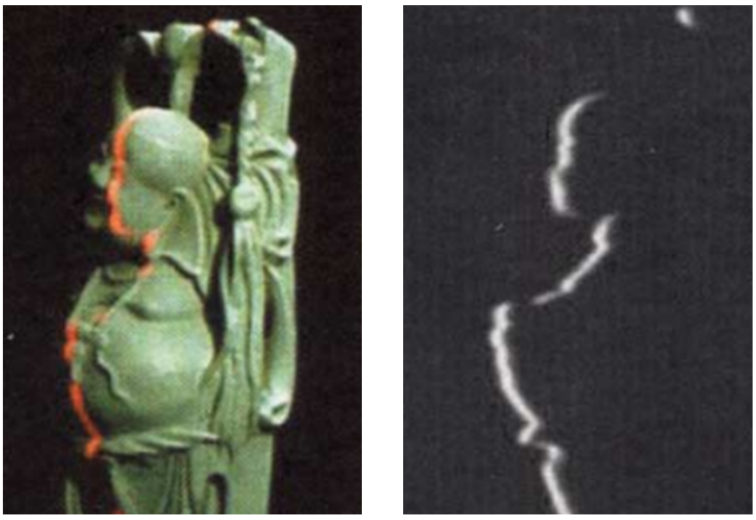

Figure 1.6: Optical triangulation using red stripe light illumination (left) and reflected light seen by a camera (right).

1.5 Active range-finding

A structured light system is similar to a stereo technique in that it only utilizes two devices for 3D shape measurement. It replaces one camera of a stereo system for the projection of a structured patterns (Salvi et al., 2004). From the

captured structured patterns, the codewords can be decoded. If the codewords are unique, the correspondence between the projector sensor and the camera sensor is uniquely identified, and 3D information can be calculated through triangulation. To reach high-speed 3D shape measurement, the structured patterns must be switched rapidly, and captured in a short period of time (Zhang, 2010). Most of the structured light systems use binary patterns, where only 0 and 1 are used for codification. The approach is characterized by several advantages, it is easy to implement, it is fast and it is robust. However, it is very difficult for this technique to reach pixel-level spatial resolution at very high speed, because the stripe width must be larger than one projector's pixel. To increase the spatial resolution without reducing the measurement speed, multiple-level codification strategies were proposed. Optimized codifications were proposed by Huang et al. (2005) and were based on a sinusoidal stripe pattern (Fig. 1.7). One of the most interesting structured light techniques is surely the Fringe Projection Profilometry (FPP).

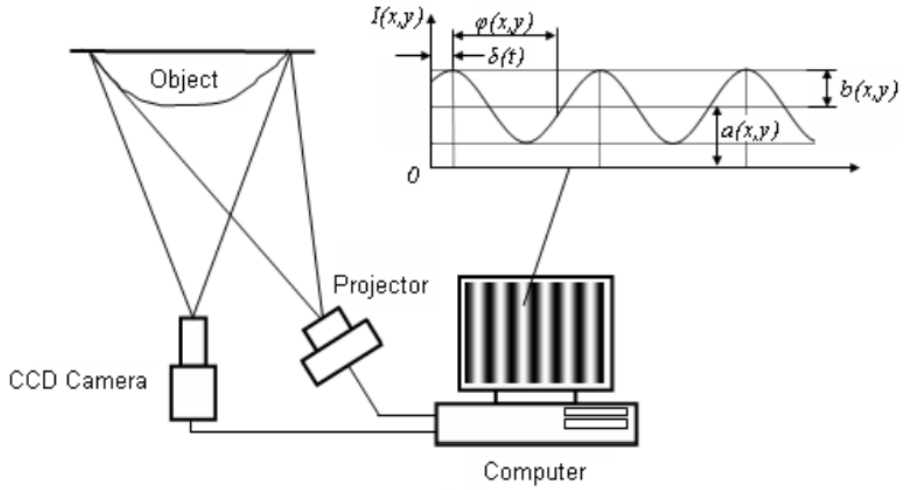

Figure 1.7: Schematic diagram of the surface measurement system based on sinusoidal fringe pattern projection.

1.6 Fringe Projection Profilometry

The technique that uses a projector to project sinusoidal patterns is called digital fringe projection technique or Fringe Projection Profilometry (FPP)

(Zhang, 2010). FPP can be divided in phase shifting and multi frequencies spatial projection. These terms indicate the projection system, in the phase shifting the fringes are transled, the phase is generally transled by 120 degrees acquiring 3 images while in the multi frequencies the fringes vary its spacial frequenty, in general acquiring in general 5 images. The number of projections (and consequent acquired images) to obtain 3D information is 3 for the phase-shifting method and 5 for multi frequenties in the analysed literature. In the last years a lot of works has been spent to improve these methods. Phase-shifting goes to real-time (60 reconstruction per second) instead multi frequenties goes to the precision. Wang et al. (2010) declare that five different fringe frequencies (1, 3, 9, 36, and 72 fringes respectively included in the projection images) were used to obtain a plane measure of 25.427, tolerance 0.18 mm, with a standard deviation of 0.08 mm. The strategy adopted to obtain such a precision was based on four topics: gamma correction of digital projection, 3D shape determination algorithm, phase unwrapping with multi-frequency fringes and system calibration with least-squares inverse approach. In a work the authors (VoMinh et al., 2010). Vo Minh et al. (2010) showed that the precision can be further increased by a different calibration method. All the FPP methods (Gorthi and Rastogi, 2010) are based on a similar flow structured as following:

1. Projection and acquisition, generating and projecting the pattern onto the object and capturing their images;
2. Fringe analysis, using fringe analysis techniques to calculate the underlying phase distribution of the acquired images;
3. Phase Unwrapping, obtaining the continuous phase distribution from wrapped phase map;
4. Calibration, conversion from image co-ordinates to real word co-ordinates and conversion from unwrapped phase to absolute height map.

In other words the 3D reconstruction involves 5 steps:

1. Sinusoidal fringe pattern generation and projection;
2. Image acquisition;
3. Image processing;
4. Fringe analysis composed by phase detection and phase unwrapping;

5. Phase to height conversion.

Schreiber and Notni (2000) showed that different measurement set-up (formed by more than one group of camera and projector) allows to measure the entire surface of an object. The power of this concept is shown by measuring the complete 3-D shape.

1.7 From the point clouds toward the solid model

All these reconstruction methods (stereo, rangefinding, silhouette, etc.) can represent the results as pointscloud, each point defined by x, y, z coordinate. The pointscloud can be transformed into a solid model using different techniques. The most important techniques are based on 3D Delaunay algorithm (Dey et al., 2001) and marching cubes algorithm (Lorensen and Cline, 1987). Commercial CAD (Computer Aided Design) programs (e. g. Catia, Dessault system) are able to automatically switch the reconstruction method by recognizing the different density. Delaunay is used for low density (points per volume) pointclouds. On the contrary marching cube is used for the high density pointscloud when a great oversampling of the surface is adoped. Commercial CAD (Computer Aided Design) programs (e. g. Catia, Dessault system) are able to automatically switch the reconstruction method by recognizing the different density. The marching cubes is based on the use of a virtual 3D uniform grid; the resolution of the grid is selected by the user depending on the application needs. It is suitable for the resampling of surfaces, the removal of high frequency details, the topological and geometric simplification of huge 3D meshes, for the fusion of multiple range maps acquired by means of 3D range scanners. The most important characteristic is the filtering of the points cloud to give a smooth surface. In this way outliers detection cannot be performed. In the Delaunay-based algorithms, the acquired points correspond on the corners of each triangle becoming to the mesh (Fig. 1.8). For this reason, outliers must be removed before the mesh generation.

1.8 Outliers detection

Outlier, defined as a result differing greatly from others in the same sample detection, is a primary step in many data-mining applications.

Outlier detection for data mining is often based on distance measures, clustering and spatial methods (Ben Gal et al., 2005). In the RE analysis

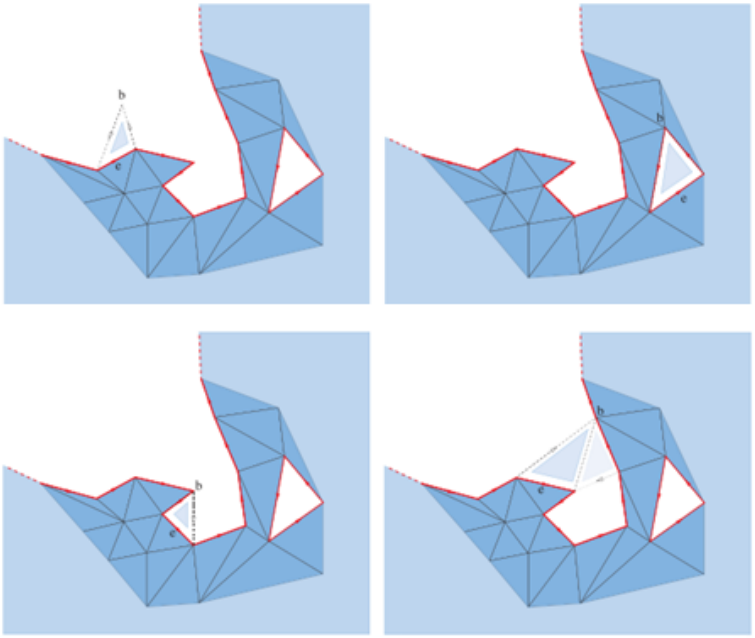

Figure 1.8: Delaunay-based tasselation for the hole filling.

ouliers can represent an error or a noise. It is therefore important to identify them prior to modelling and analysis. Within the group of non-parametric outlier detection methods there is the distance-based methods and clustering techniques. Single step procedures identify (Fig. 1.9) all outliers at once as opposed to successive elimination. In the sequential procedures, at each step, one observation is tested for being an outlier. In a sequential procedure, more than one technique can be used.

1.9 Foot measurement

Some of the available 3D scanners have been specifically developed for the digitalisation of the human foot. The foot is one of the most difficult body parts to be scanned because it has a very complex 3D shape (high curvature surfaces), it is soft and deformable. It is widely known that when a 3D scanner can carry out a good reconstruction of a foot (or a hand) then that scanner can reconstruct reasonably everything. The subject is widely studied, plenty of work has been done for example by Witana (2004), Luximon (2005), Witana

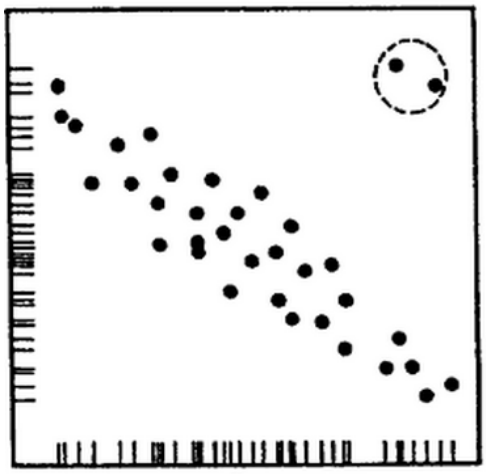

Figure 1.9: Plots of generic variables of a regression data set. Two points, indicated by dashed circle, are outliers (Ben Gal et al., 2005).

et al. (2006), Xiong et al. (2009) and Goonetilleke et al. (2009). In the last years the researches related to feet and shoes has gained prominence due to consumers' requirements for better-fitting and more comfortable shoes (Xiong et al., 2009). Footwear comfort is primarily due to the fit between foot and shoe and footwear customers take benefit from foot scanners use. The digital scanners, used in many different applications, aims at obtaining three-dimensional shapes and, as a consequence, linear and circumferential measurements. The main foot measures are shown in the figure 1.10.

Anyway the scanners can be precise and accurate, but the measurements obtained from these devices can vary depending on how an object is scanned, aligned and processed. In particular, laser scanner technologies for varying applications that claim accuracy within 1 mm. Notwithstanding the accuracy of an instrument is related to many aspects. The instrument analyses transversal sections of the foot, slice by slice with an imposed step. The minimum step is close to 0.3 mm. The acquisition performs in a few seconds, minimum 4, and during this time the foot can vary its geometry, e.g. it can pulsate or vibrate, touching a whatever human foot with the hand movements can be perceived. For these reasons the errors of the instrument is related to:

- movements during the acquisition time, in 4 s it is minimum 0.2 mm;
- different percentage of weight bearing load, during the acquisition, can

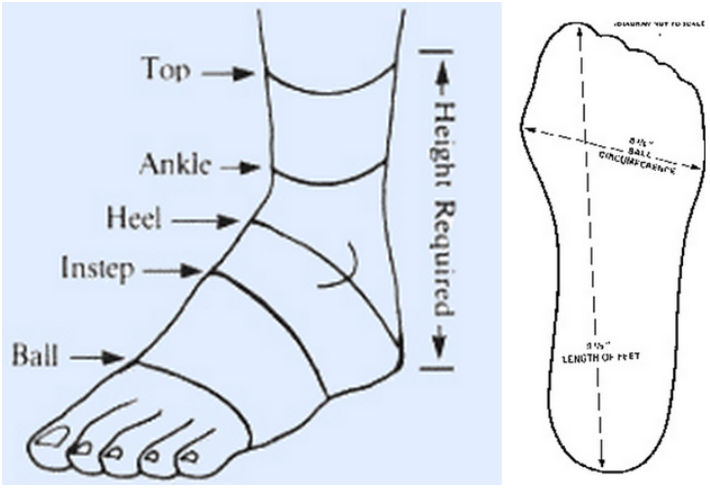

Figure 1.10: The most common foot sizes are linear dimensions and girths.

vary the foot shape, e.g. in the figure 1.11, the fat pad under the calcaneum and metatarsal heads is flatten out;

- accuracies of the instruments, based on image reconstruction, is estimated close to 0.2 mm, this is due to the reflectance of the part;
- distances between adjacent slides, imposing a minimum step of 0.3 mm, considering two extreme zone, the tip and calcaneum, this value must be multiply by 2 thus it is 0.6 mm.

Adding all the errors the total accuracy could be bigger than 1 mm.

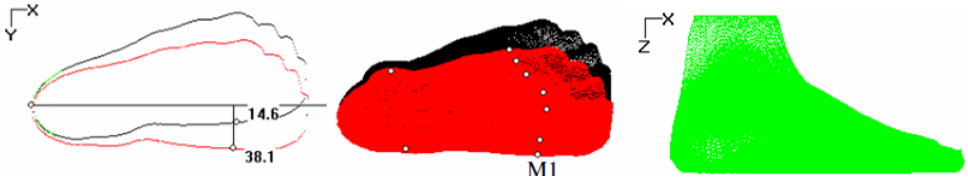

Figure 1.11: Two possible alignment of the foot based on the first metatarsal head and second metatarsal head (left and the center), lateral view of the acquired model (Xiong et al., 2009).

In particular Goonetilleke et al. (2009) studied the influence of the alignment procedure on the foot measurements. Researchers and footwear fitters

have long used differing orientations and axes to measure feet. For example, the Brannock device (Brannock web site), which has been a tool used for measuring feet from the medial side of the first metatarsal head. Most researchers use another foot axis, the line joining the pternion and the tip of the second toe (second metatarsal head). Different foot dimensions can be estimated. The results of this research show that the alignment method has a relatively small effect on measures such as foot length. The maximum difference among the three methods was less than 3 mm for all 50 participants. However, there are differences of about 5 mm in the different methods in measuring arch length. The differences between the Brannock alignment and the second metatarsal head alignment methods are relatively small. The differences in foot length and arch length measurements using these two methods are 1.5 mm and 3 mm, respectively. The ages of the participants was in a ranged between 19 to 24. Pathology free subjects are considered and bunions are usually absent in the young people. Calluses and other deformities can significantly affect the orientation of the foot axis The range of foot length was from 210 to 283 mm, these lengths seem to be small, this is typical of China ethics groups. Probably, in Europe ethnics groups, it is possible to obtain different results. The girths, measured in automatic way via software, without anatomical landmarks, can shift in the calculations. The identification of anatomical features seems to be very complex.

Luximon et al. (2005) studied a method to estimate a 3D shape of the foot starting from foot outline and the foot profile. A laser foot scanner was used and elaborations of the obtained model was performed. The foot was divided in 99 transversal sections. Each section was represented by 360 points (one for each degree). Regression was carried out and a standard foot shape was calculated. Starting from different variables two methods are proposed: the first considering the foot outline and the foot height, the second foot the outline and the foot profile. Results of the first method show that each individual foot shape can be predicted within a mean absolute error of 1.36 mm using the first method, and within a mean absolute error of 1.02 mm using the second method. In figure 1.12 sections of the foot of one subject compared with the output of different prediction methods are shown.

1.10 Anatomical features of the foot

The mechanical behaviour (especially stress and deformation) of the foot in the interaction between foot and shoe plays an important role. Many studies

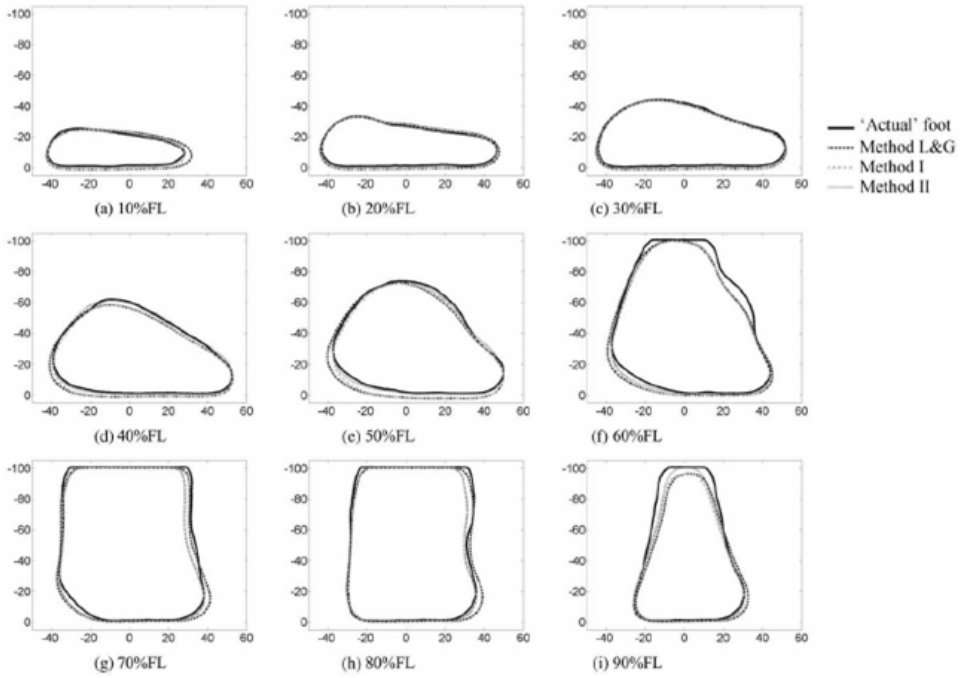

Figure 1.12: Sections of the foot of one subject compared with the output of different prediction methods. All units are mm. LeG is the method proposed by Goonetilleke's research group in a previos article (Luximon et al., 2005).

about this topic were carried out. The foot is a complex structures formed by 26 bones (Fig. 1.13), more than 20 muscles, more than 100 tendons and soft tissues. In the appendix A other images can be found on the terms used in this thesis.

Farabeuf's theory in 1870 can be considered the starting point on the studies of the biomechanical behavior. A tripod model was proposed characterized by vaults. After this, irrelevant modification of the model was introduced by Kapandji (1977) but the tripod model was accepted by the scientific communities for many years. The plantar vault acts as a shock-absorber essential for the flexibility of the gait. Any pathological condition, exaggerating of flattening its curvatures, seriously affects the support of the body on the ground and necessarily influence running, walking and the maintenance of the erect posture.

The plantar vault can be compared with architectural vault supported by

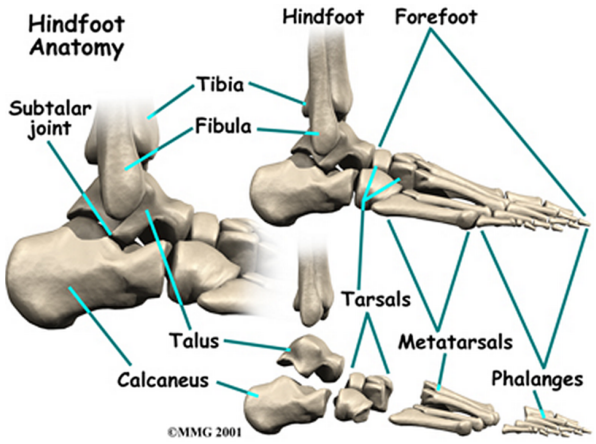

Figure 1.13: The bones of the foot.

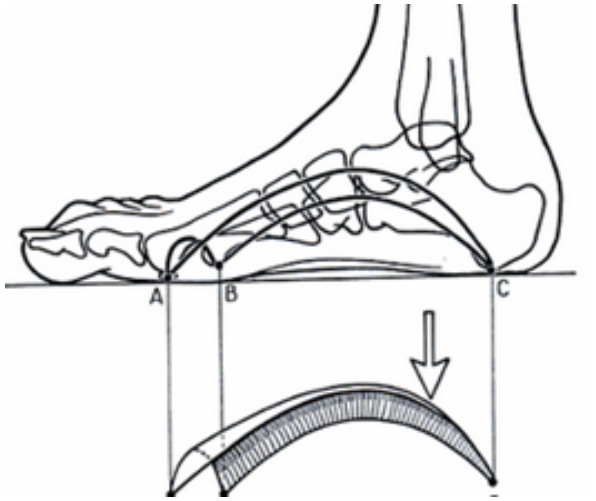

Figure 1.14: The plantar vault.

three arches. It rests on the ground at three points: head of the first metatarsal (a), head of the fifth metatarsal (b) and posteriomedial and lateral tubercles of the calcaneous (c) (Fig. 1.14). Each point is shared by two adjacent arches. The anterior arch which is the shortest and lowest stretches between the two anterior supports (a and b). The lateral arch of the intermediate length and height lies between the two lateral support (b and c). The medial arch the longest and highest and also the most important of the three static support of

the body during movements lies finally between two medial support (c and a). Medial arch and lateral arch are confirmed by the trabecolar bony architecture of the foot (Fig. 1.15). The architecture increases the mechanical property of the foot ensuring a better distribution of the stress under loading conditions.

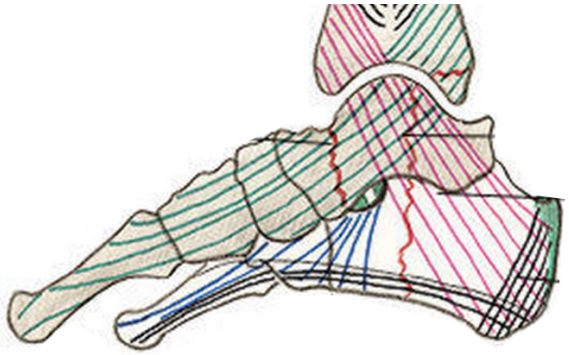

Figure 1.15: The trabecolar bony architecture, site: www.maitrise-orthop.com.

1.11 Deformations of the foot under loading static condition

The three arches under loading static condition become flat and long (stretched). Kapandji (1977) declares that the anterior arch becomes largest of about 12.5 mm. Transversal curvature decreases in the cuneiform zone and scaphoid. The longitudinal curvature in the internal arch flattens out about 4 mm, the scaphoid translates on the astragals and the distance between the talus and first metatarsal increases. Displacements of the external arch and the internal arch are similar in vertical direction. The cuboid, the calcaneus cuboid and cuboid metatarsal articulations flatten out. The distance between the talus and fifth metatarsal increases. In many conditions the foot can be constrained, in other word the points a, b, and c could be hold. In this case a rotation (abduction) between the hindfoot and forefoot can be observed and measured. Moreover in vitro the abduction under a vertical load (range 200 - 600 N) can reach a rotation of 10 degrees. This movement are confirmed by Lee (1999).

1.12 Considerations about tripod model

Many authors remarked the model originally proposed by Kapamdji. Cavanagh (1987) and Daentzer et al. (1997) claim that the tripod model is inaccurate. Firstly the plantar pressure peak on healthy subject is located between the second and the third metatarsal, so that it is difficult to hypothesize the presence of the transversal plantar arch. In this way the existence of transversal plantar arch are difficult. Secondly the alignment of the head metatarsal and plantar pressure during perambulation was studied. In healthy subjects, during the static load, the second and the fourth metatarsal head reach a lowest position then other metatarsal. In healthy subject the peak plantar pressure in metatarsal zones during the perambulation is located in the third metatarsal arch and the pressure decreases in the lateral metatarsals. These critical observations demonstrate that the plantar transversal arch in static and dynamic loads is not probable. An anterior flat foot can be considered healthy.

1.13 Calcanean and astragalic foot

One of the best model that represent the entire cinematic chain in accordance to the cinematic of all lower limb seems to be the model proposed by Pisani in 1976. This model divides the foot in two parts: the calcaneous foot and the astragalic foot (Fig. 1.16). The calcaneous foot is formed by calcaneum, cuboid, metatarsals IV and V. The astragalic foot is formed by talus, scaphoid, cuneiform, bone, metatarsals I, II and III. The calcanean foot has static function and the astragalic foot has dynamic function. In the reciprocal function a role is played by the long articular intermediary consisting of subastragalic, cuboid scaphoid, cuboid cuneiform and metatarso cuneiform. The talus is not directly linked with any muscle. The movements of talus are totally related to the adjacent bones. As a consequence the measurements of the talus in the extension and flexion (movements in the sagittal plane) are constrained to the foot (calcaneum and scaphoid), while its measurements in inversion and eversion (movement in coronal plane) are constrained to the leg. Combained actions of the dynamic and astragalic foot generate an helix (Paparella and Treccia, 1978). The transversal section of the helix is horizontal in metatarsal heads and vertical in the talus calcaneum (Fig. 1.17). In the appendix A it is shown other images (Fig. A.7) of the plantar helix are shown.

Variations of the pitch in the helix ensure the shock absorber function of

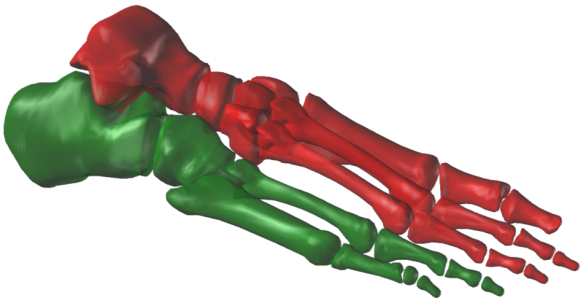

Figure 1.16: The calcaneous foot (green) and the astragalic foot (red).

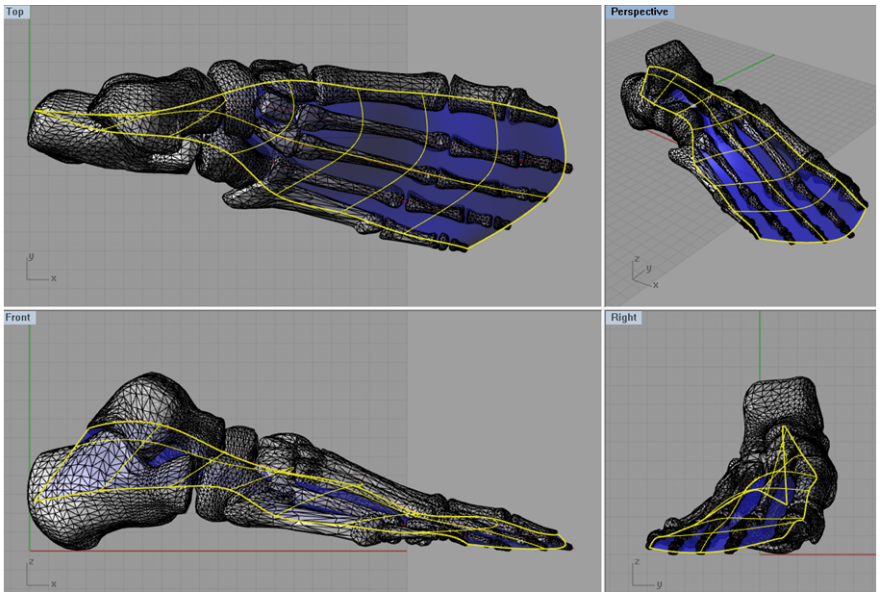

Figure 1.17: The helix model theorized by Paparella and calculated using a script implemented directly in the CAD with Visual Basic language.

the foot. During the deambulation, in the first phase (contact of the foot with the terrain) the pitch of the helix decreases. On the contrary in the last phase (unloaded foot and no-contact with terrain) the pitch of the helix increases.

This model is confirmed by different authors:

- using stereo reconstructions (Lundberg, 1989);
- verifying, through 3D video analysis that the behaviour of the foot dur-

ing the contact on the terrain is similar to a tri-dimensional rotation. As a consequence the tripod planar model is not acceptable and cannot describe the deambulation (Moseley et al., 1996);

- identifying the basic movements of the subtalar joint in the 3D space: supination and pronation, inversion and eversion, extension and flexion. (Sarrafian and Shahan, 1993)

- using internal markes in anaesthetised subjects and analysing 3d cinematic ankle and foot during deambulation. It was observed that different subjects have different orientations of three rotation axis of the foot. Inversion and eversion are prevalently related with the subtalar joint. (Arndt et al., 2004)

1.14 Considerations about the predictive models

Many researchers claim that measurements of the foot can be used to develop predictive models aimed at the displacements and the plantar pressure. Cavanagh (1997), supposed the contrary analysing correlations between skeleton characteristics and peak pressure, derived that only few variables predict approximately the 35% of variance of the pressure in some plantar zones (talus and first metatarsal) during the deambulation. As a consequence the behaviour of the foot is related with the cinematic of all the gait and is not related only with foot structure. Morag and Cavanagh (1999), using anthropometrical measures, observed that pressures in the calcaneum is a function of the cinematic, of the plantar arch and of the fat pad under the calcaneum. The fat pad is also a function of the age of the subject.

1.15 Finite Element Analysis (FEA)

The aforementioned predictive models aim at studying the relations between loading conditions, displacements, deformations and pressure. For this purpose the Finite Element Method (FEM) can be an effective tool, because it analyses a solid model of the foot, predicting the behaviour of all its parts. In the literature many papers already faced the problem by FE analysis as for example: Kato et al. (1996), Chen et al. (2003), Geffen (2003), Cheung and Zhang (2005). Several finite element models of the foot or footwear have been developed, based on certain assumptions. These assumptions include

simplified geometry, limited relative joint movement, ignorance of certain ligamentous structures, and simplified material properties. Early models were based on a simplified or partial foot shape. Analyses were conducted under assumptions of linear material properties, infinitesimal deformation, and linear boundary conditions, without considering friction and slip. Recent models have been improved in selected aspects by incorporating geometry, material, or boundary nonlinearity (eg, large model deformation, nonlinear material properties, slip/friction contact conditions). Nevertheless stress-strain constitutive laws of the materials seems to be one of the most important problem. Generally the starting point of the analysis are the geometry of each part, the constitutive laws of the materials and the applied loads and typical constraints. Other parameters have to be considered to manage the process of simulation, e.g. the element size and local mesh refinement. Thanks to numerical modelling the displacements of each part under loading condition can be studied. Validation criterion and techniques to checkout FE analysis seem to be the major problem. It was observed (Cheung et al., 2005) that a change in the constitutive law related with the plantar pressure implied variations of the model.

1.16 Outline of the research

In the last paragraph, dedicated to the state of the art, the literature was described and discussed. There are many potential topics, such as the FE of the foot and the FPP, some well-known parts such as the shape from silhouette. Starting from the aim of the thesis all the topics faced in the introduction has been developed. The aim of this work is to determine methods and tools allowing an effective modelling of human parts to be used in the design of wearable products. The flow chart (Fig. 1.18) shows how it is possible to summarize the contents of this thesis. Some of them are fixed points derived directly from the state of the art, other parts are studied, developed and implemented via software. In the flow chart on the left side each block represents an action; the starting point is a real part while the final point is a database of measurements. This is a typical RE and data management procedure for human body parts and can be adopted also for wearable products.

The flow chart combines a procedure (on the left side) and the topics (on the right side) which can be found in the thesis. This is a scheme and indicates the fundamental issues of the Reverse Engineering. Taking into account this flow chart, characterized by an input of the real part and an output of database

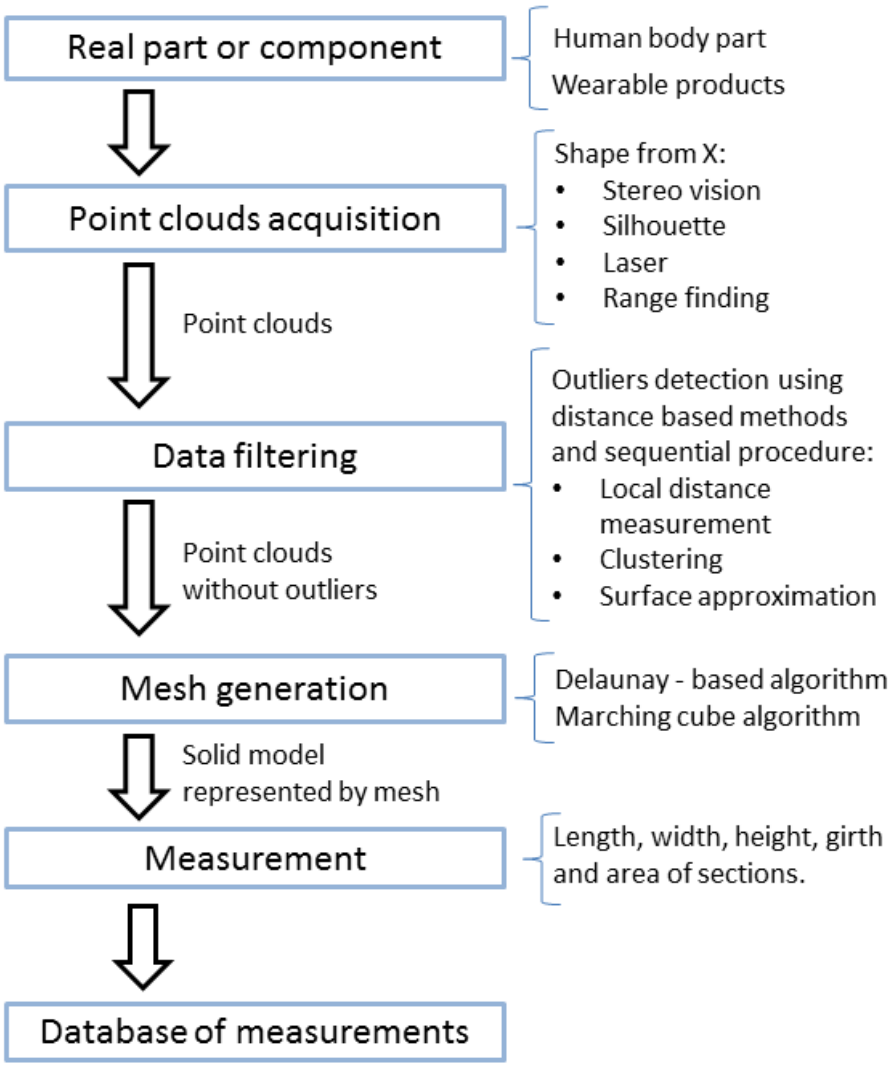

Figure 1.18: Flow chart of RE and data management procedure.

of measurement, interactions between the body part and the wearable product must be considered (Fig. 1.19).

In many products the fitting is fundamental such as spinal orthoses, shoes, gloves and helmet. The interactions can be studied through the fitting of real

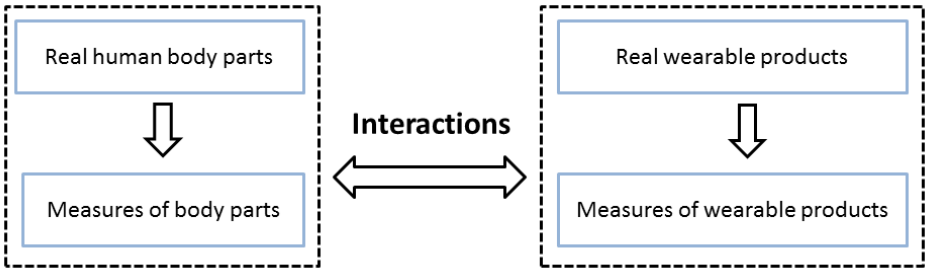

Figure 1.19: Interactions between the body part and the wearable product systems.

part geometry and the wearable product geometry to evaluate the comfort. In particular a matching strategy can be performed. The interactions, between the deformation of the human part and the deformation of the wearable product can be analysed with a numerical analysis such as FEM. Some characteristic of the human part can be discussed. A general scheme indicates the human body part correlated to the wearable product and to the real word. These three systems are in contact and a load transfer can be possible. Studying human body parts, only foot and the hand transfer loads between wearable product and the real word and they can be considered the most complex because it has all the mentioned three components (Fig. 1.20). The foot with a general ground and the hand with general object using prehensile function. Both have complex geometry however the foot is absolutely the most complex considering the shock absorber function and the applied load in many situations. For these reason the interaction between foot and shoe is very complex.

Starting from these concepts, the thesis is developed. Instruments based on RE techniques are presented in chapter two. The presented topics are related to the temporal cronological order. Requirements of the RE instruments are discussed and a first instrument, based on the multiple stereo vision was shown focusing the attention on the data filtering and mesh generation. To analyse the possibility of employing the shape from silhouette method for a 3D foot scanner another instrument was developed. After this, a comparison among stereo vision, silhouette instruments and another available on the market instrument based on shape from laser was performed. Some considerations was proposed and in conclusion a fourth method, based on Fringe Projection Profilometry (FPP) was proposed. The last instrument was considered good

enough for the reconstruction of many different human parts and wearable products and seems to be the better instrument than the others. Three instruments, stereo vision, silhouette and FPP are directly implemented using proper softwares (Matlab). Measurements on the human foot are presented in chapter three. Considering that the alignment is fundamental, a procedure was developed and differences of human foot and shoe last was analysed. A match between these parts was calculated using a fitting function able to estimate the comfort index. In this chapter a typical industrial approach was discussed while in the chapter four the biomechanical behaviour of the foot was studied through a Finite Element (FE) analysis. Chapter three and four faced the problem of the relation of human measurements and wearable products considering the shape of the parts and the deformation.

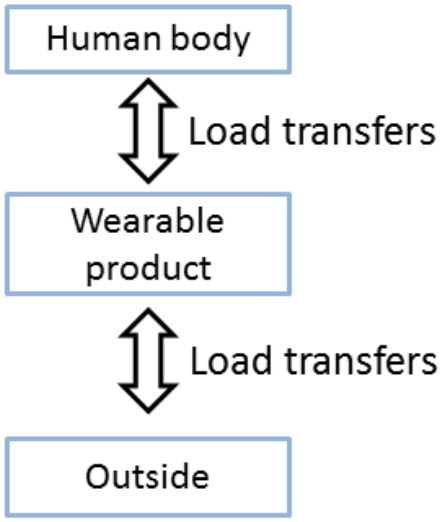

Figure 1.20: Human body part correlated to the wearable product and to the real word. The wearable products, such as the shoes, contain all the blocks and are the most complex products to study.

Chapter 2

Reverse Engineering of the human feet

In this paragraph different RE systems are presented. For the acquisition of human parts only non-contact techniques are considered; contact techniques are too slow and are affected by the deformable soft tissue. Four different 3D scanners are studied: stereo, silhouette, laser and FPP instruments. Three of them are developed directly and the last one, available on the market, is considered for a comparison. Multiple stereo vision system is developed. Filters and elaboration process of the point clouds are considered. Outliers are eliminated and mesh generation is carried out with a Delaunay-based algorithm. Silhouette instrument was developed starting from simple and cost-effective devices. A comparison between stereo vision, silhouette and laser instruments is performed. The accuracy of the multiple stereo vision, laser and silhouette method is estimated. Between stereo vision and laser the differences are around 2 mm in the evaluation of the length of the foot. This allows a good external anatomical description of the foot as required for tailored shoes but it is not a good result for the research. For this reason a new instrument is developed based on FPP to increase the precision. This allows good improvements in the RE process and an accuracy around 0.2 mm. The flow chart of this chapter is presented (Fig. 2.1).

2.1 Instrument based on multiple stereo vision

A Reverse Engineering (RE) method was developed for building up the external shape of the human foot. For this purpose, a multi stereo vision technique

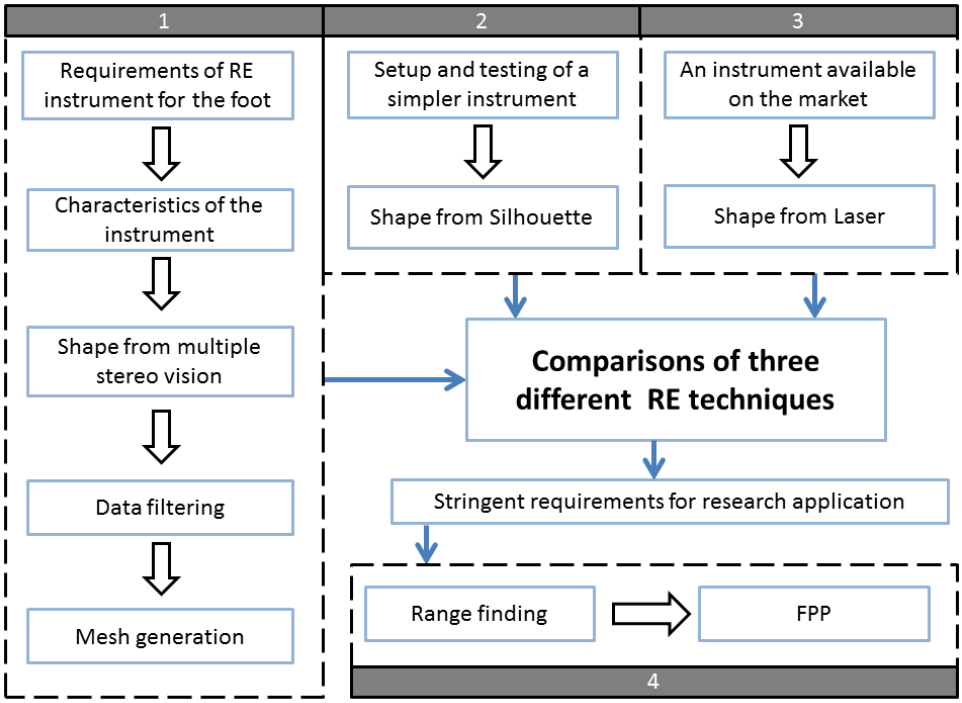

Figure 2.1: The flow chart of the RE of this chapter.

was set up to collect information about the real foot and a software was developed to automatically filter the obtained point clouds. The solid model is generated and aligned by means of a sequence of rules for an adjustment to a standard coordinate system. The procedure aims at developing a system to compare different digitalized feet related to different stages. The instrument was developed in cooperation with a company (Delta RS, Italy) and it is called Foot-o-graph ©. From the analysis of the problem the following reamrks can be drawn.

- Most of 3d scanners available on the market are based on range finding technique and they have a stripe laser, a camera, a frame and a rail. Camera and laser are mounted on a frame. The frame translates on a rail to cover the entire reconstruction zones. In this way, the acquisition is not instantaneously, in a lapse of time the cameras move on the subject and a sequence of images is acquired. During this process a human part can pulsate and vibrate. The measure of pathology free subjects (asking

to focus attentions of each subject on remain in the same position as much as possible) is characterized by a high error, as a consequence the measure accuracy is low.

- It is also important to consider the opportunity of 3d acquisitions of loaded or unloaded foot. Measuring a biomechanical complex system like the foot, with more than 100 tendons, 20 bones and soft tissue, is very difficult. The unloaded foot does not interact with other objects, the tendons are not stressed and the soft tissue is not deformed. From the medical point of view, it is prefered to perform the reconstruction considering a foot loaded with 50% or 100% of total weight. Thus the foot can be measured starting from different conditions and it is characterized by different deformations. The point of application of the load can also be on the metatarsal zone or the calcaneum. In the first case, the metatarsal arch is flatten out and the pitch of the plantar helix decreases. In the second case, the plantar arch is unloaded and the major deformation is on the fat pad under the calcaneum. Unexpectedly, the position of the applied load is related to the environment, where the instrument is used. For instance, if the instrument is close to a wall, the subjects (facing the wall) spontaneously load the calcaneum.

- The step of instruments testing, considering those available on the market, showed that subjects cannot see the foot during the acquisition phases. This is sometimes a problem because patients, especially older, show hesitation and uncertainty when they put their foot in a dark box. This point is not so important for the research but is fundamental for the design process of a product.

Starting from these considerations, a new instrument was developed. Main objectives were:

- simultaneous acquisition of all the information for the reconstruction;
- fixed cameras (no sliding rail);
- open instrument to avoid claustrophobic effects;
- free external light condition during acquisitions;
- unloaded foot.

To limit the uncertainty variables related to the percentage of weight adopted and the position of the load, the condition of unloaded foot during acquisitions was chosen. This is a limiting condition, anyway it is preferred because it ensures the repeatability of the measurements.

2.1.1 Characteristic of the instrument

Stereo vision techniques were adopted to meet the defined requirements. More than one couple (composed of two cameras) was used for instantaneous reconstructions the 3D shape of the foot. A preliminary study (via solid modelling) identified that the minimum number of couples is 7. This means 14 cameras able to cover the whole surface of the foot. The acquired image was also elaborated through an algorithm of multi stereo vision. Cameras are characterized by fish eye lens to reduce the size of the instrument by decreasing the distance between the foot and the camera. In this way external dimension can be considered acceptable (0.80 m X 0.70 m X 0.80 m) and ensures easy transport. The identification of the foot, through a 3D point cloud, is related to a socket. The socket is formed by circular markers characterized by different colours. This is fundamental, for recognizing the position of markers and obtain a correct definition of the points cloud. Software elaborations play an important role considering the calibration of the system and patterns recognition. Thus markers are adopted as spot for the identification in the image analysis. The recognition is correlated with the identification of the position in the image. In a couple of cameras (Fig. 2.2) the same marker is in a different position on both right image and left image. The difference is proportional to the depth of the marker in the real space. Using this characteristic and an appropriate calibration system, a point cloud (Fig. 2.3) can be measured starting from image discretized in pixel.

Calibrations of a multiple stereo vision system can be performed in three steps:

- Intrinsic parameters: correction of lens deformations;
- Extrinsic parameters: relative positions of cameras;
- Synchronization: relative position of all couples of cameras.

Intrinsic and extrinsic parameters can be calculated using the Zhang's technique (**?**)ZangCalib) based on mapping the acquired images. The compensation occurs by moving a grid in a field of view common to both couples.

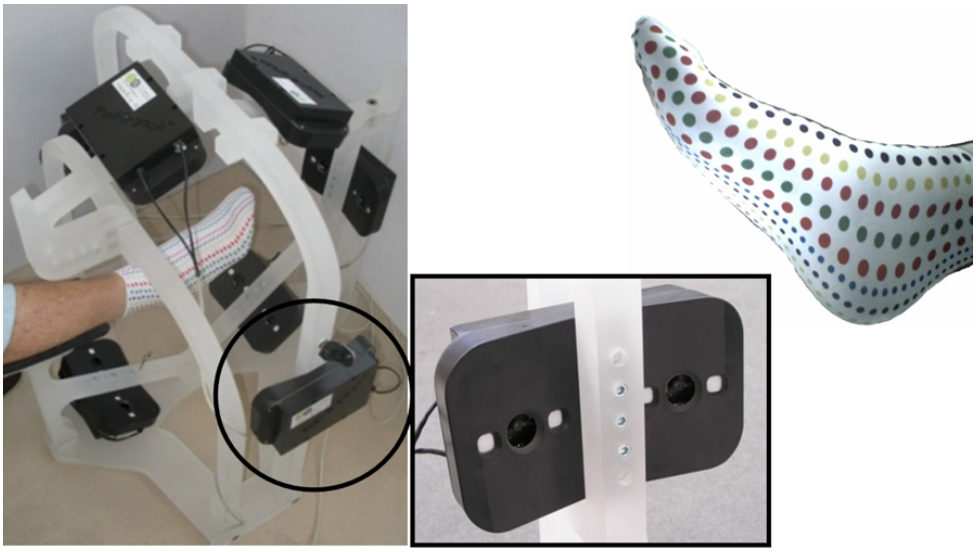

Figure 2.2: The instrument (left), a couple composed by two cameras (center) and the socket (right).

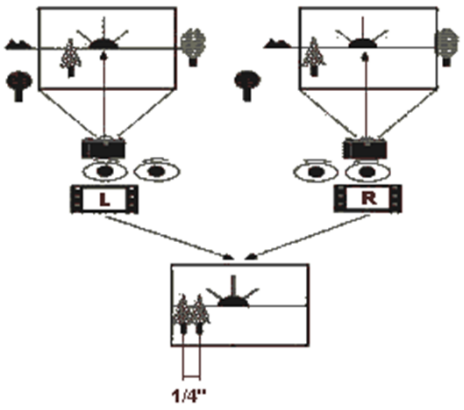

Figure 2.3: A functional scheme of the stereo vision technology, The depth is proportional to the differences of the position of the object between the right (R) and left (L) image. The three is nearest than the sun, its position is different between the right and the left camera. The sun is very far and it is at the same position in the right and in the left camera.

The process permits to relate scenes of both right and left camera and aims obtaining the depth (z axis) by triangulation. The algorithm localizes a point (centroid of each marker) in x, y and z coordinate. It is possible to deepeen this topic considering that only one line can be obtained between a marker viewed by left camera and right camera. This line can be connected to a third point on the real object using a plane called epipolar plane. During the calibration the extrinsic parameter is calculated. The difficuty of this part is to isolate univocally the same marker viewed by the right and the left camera. Errors occurring in this phase affect the reconstruction. In other words, if the obtained coordinates are not correct, inexact points, called outliers, can be created. The synchronization of the system can be seen as the fusion of data derived from each single couple of cameras. Each couple measures markers, found in common fields of view of the two cameras of the couple, obtaining a single point cloud. Contributions of each couple provide a point cloud representing all the foot.

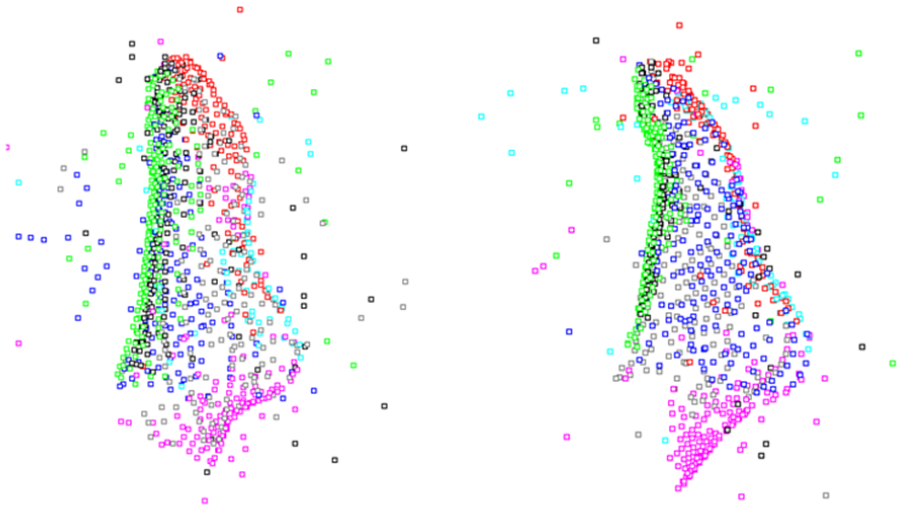

Figure 2.4: Examples of acquired point clouds.

2.1.2 The socket

The pattern is directly imposed on the socket. Each marker is circular for an easy identification using the image analysis. The colors of the markers allow to separate the pattern in groups. The same color is repeated along

a direction. The epipolar line must be always orthogonal to this direction. This concept is necessary to isolate univocally the same marker viewed by the right and the left camera. Euclidean distance among the markers is about 6 mm. Connecting the centroid of the markers, equilateral triangles are generated. As a consequence colors are necessary for minimizing the errors and the relative position on the socket is important to generate a regular mesh. Doctors accepted this coverage and it is defined such as positive contribution. Advantages regard reconstructions on damaged feet or characterized by colour variations on the surfaces. Thus difficult surfaces (using whatever image analysis techniques) can be covered by a socket. An example of reflective surface is represented by the nail. In addiction rough geometry variations of feet are also filtered by the socket.

2.1.3 Elaborations of acquired data

The obtained data through multiple stereo vision technique are point cloud defined in the space using global coordinates. Each point corresponds to a marker printed on the socket. Obtained point clouds must be elaborated considering that acquired data are not able to measure anthropometrical characteristics (e.g. length of the foot or ball girth). Data filtering is the first operation. In the point cloud outliers must be removed. Outliers derive from non-correct correspondence between markers viewed by the right and the left right camera. Two different markers are improperly matched. In this case, an error occurs identifying an incorrect depth. After data filtering mesh generations from point clouds are performed. This operation permits to represent the solid model by groups of triangular faces.

Data filtering aims to obtain a correct points cloud. All measured points must represent the real foot. Non-parametric outliers detection methods are adopted, in particular distance-based and clustering techniques (Ben Gal et al., 2005). Single step procedures identify all outliers at once as opposed to successive elimination while considering the high percentage of the outliers a sequential procedure is used and more than one technique are considered. At the beginning a distance-based methods was implemented, after this a clustering techniques was used and at the end a refinement was carried out with fitting polynomial surfaces (Fig. 2.5). Applied filters discard outliers step by step starting from data of each couple. First step provides to discard farest points (high distance from the object) while last step removes points close to the real surface of the object.

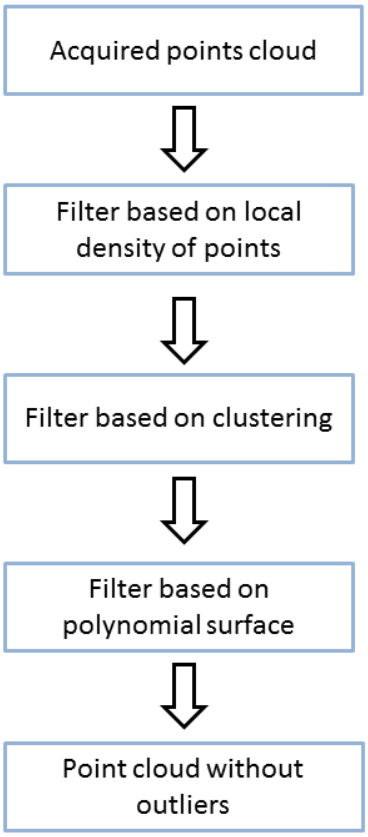

Figure 2.5: Flow chart of the filtering procedure.

Filter based on local density of points

First filter acts on the density of points in the 3D space. The condition to discriminate whether the point is an outlier is related to point density of the analysed volume. The domain of points is divided into portions and each portion is checked as clarify later. In each portion it must exist (or not) more than a certain number of points, in this case the point of the portion is accepted (or discarded). Parameters to calibrate the filter are the number of points inside the portion (threshold number of points) and dimensions of portions. They depend on both the acquisition system and the precision of the multiple stereo vision algorithms. Obtained results indicate an ellipsoidal

portion of the considered domain. The minor axis of the ellipsoid is located on the z axis (depth in the stereo reconstruction) because in this direction the stereo reconstruction errors are larger. In the example of figure 2.7 an ellipsoid is generated (major axis 40 mm and minor axis 20 mm), centroid located on each acquired point. Each point is not discarded if at least four points lie inside the corresponding ellipsoid. Results of the statement can be: the point belongs to the point cloud or the point is an outlier, in this latter case it is discarded. Statements are repeated until all measured points are analysed (Fig. 2.6).

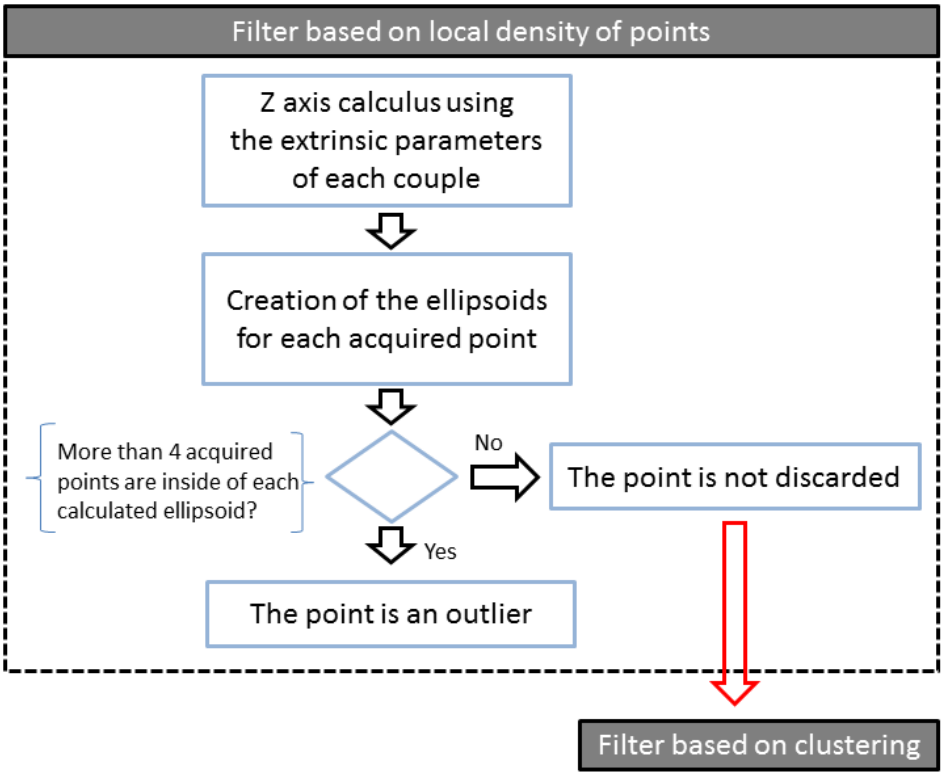

Figure 2.6: Flow chart of the filter based on local density of points.

Filter based on clustering

A k-means clustering algorithm (Ben Gal et al., 2005) is adopted to discern other outliers. k-means clustering is a method of cluster analysis which

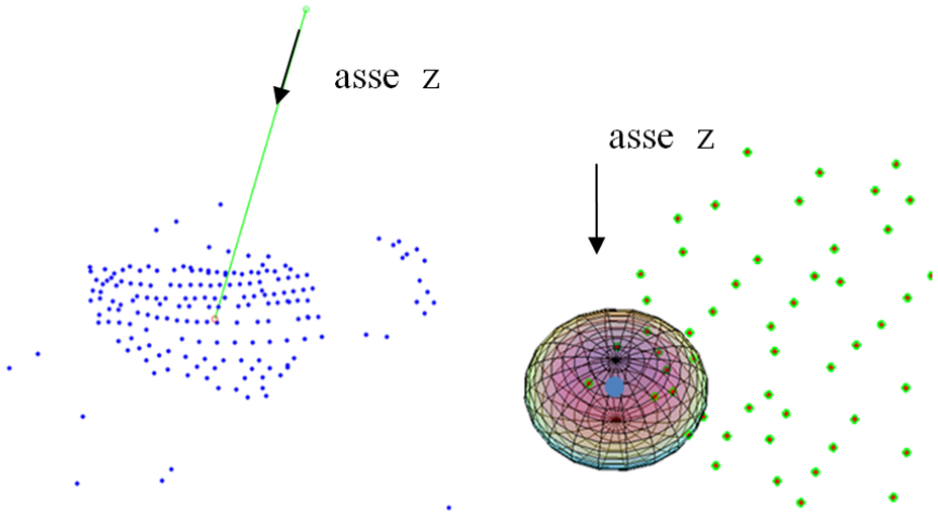

Figure 2.7: Filter based on loacal density of points.

aims to partition n observations into k clusters in which each observation belongs to the cluster with the nearest mean. n observations correspond to n acquired points and k cluster the number of final groups. In the algorithm, Euclidean distances and a k cluster are imposed. Separations into groups are performed and the example represented in the figure 2.8, four different groups are considered and groups containing less than 5 points are discerned.

The algorithm steps are:

- choose the number of clusters;
- randomly generate k clusters and determine the cluster centers;
- assign each point to the nearest cluster center, calculated using the Euclidean distance;
- recompute the new cluster centers;
- repeat the two previous steps until the convergence is met, generally in maximum 10 iterations. The main advantages of this algorithm are its simplicity and speed which allows it to run on large datasets. The disadvantage is that the resulting clusters depend on the initial random assignments, during the analyses this situation never occur. There is a very remote possibility that the initial random assignments compromise

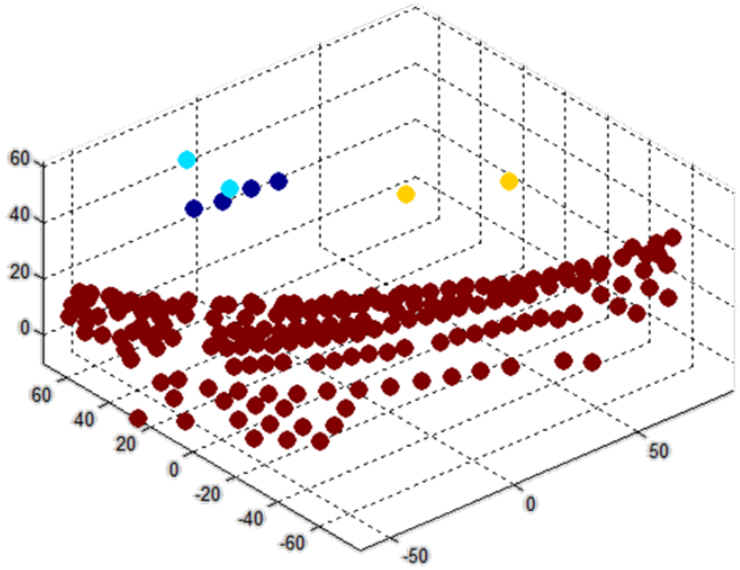

Figure 2.8: Filter based on clustering.

the final result, the ouliers detected using this technique are clearly grouped with centroids of each group very distant.

Filter based on polynomial surfaces

After the first local density filter and the second clustering filter, a third filter based on polynomial fitting was used. Starting from the points cloud, obtained with the clustering filter, an interpolated surface was calculated using a third degree polynomial function. This filter is adopted assuming that the surface of the foot is sufficiently smooth. A couple of cameras must reconstruct zones with a polynomial surface (third degree) characterized by a limited number of minima (and maxima) and inflexions. Distances between the generated surface and acquired points are calculated. The statement of the filter is related to calculated distances. A threshold distance in the filter is a parameter. In the example in figure 2.10 the threshold lenght is imposed (5 mm) and points characterized by distance major than 5 mm are discarded. The flow chart of this filter is presented in the figure 2.9.

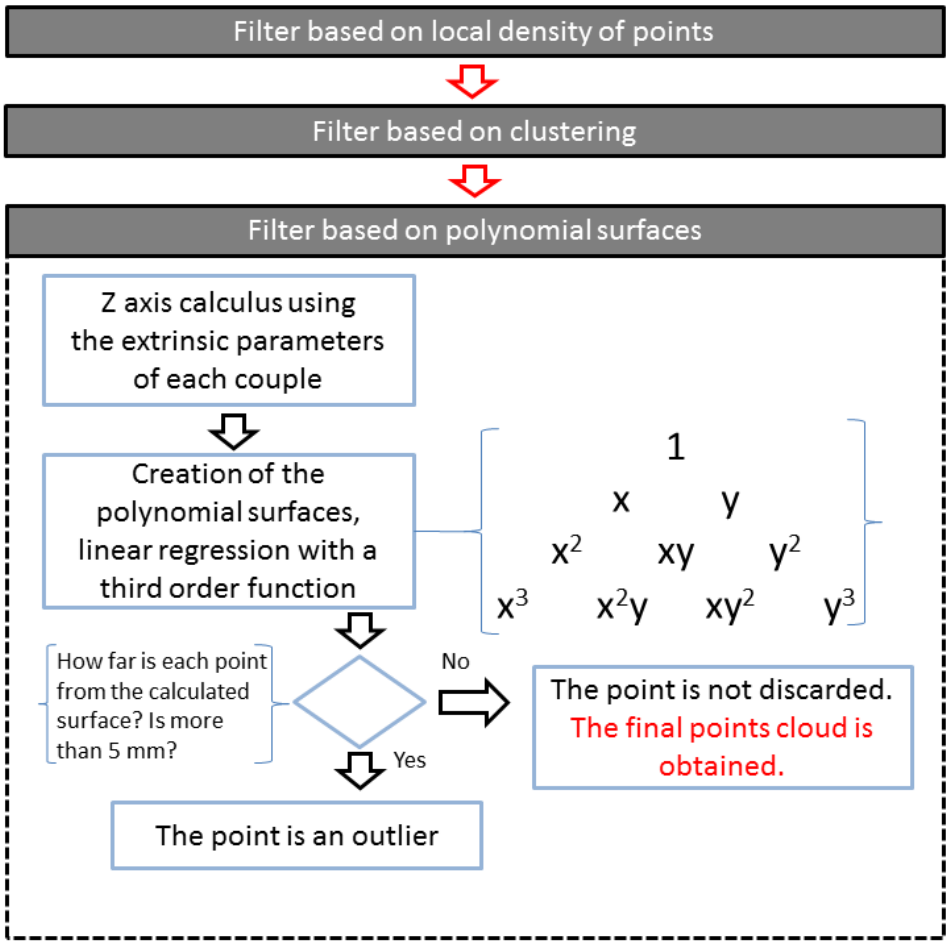

Figure 2.9: Flow chart of the filter based on polynomial surfaces.

2.1.4 Final points cloud

After filtering on acquired points, final operations consist on the fusion of all partial results of each single couple. In this way from partial results a whole 3d representation of the foot (Fig. 2.11) is obtained using roto-translation matrix previously defined by synchronization. The synchronization matrix, dimension four columns and four rows, contains the roto-translation data of each couple. It is calculated with known shape, typical a parallelepiped or a pyramid with external dimension similar to a foot. It is necessary to calibrate

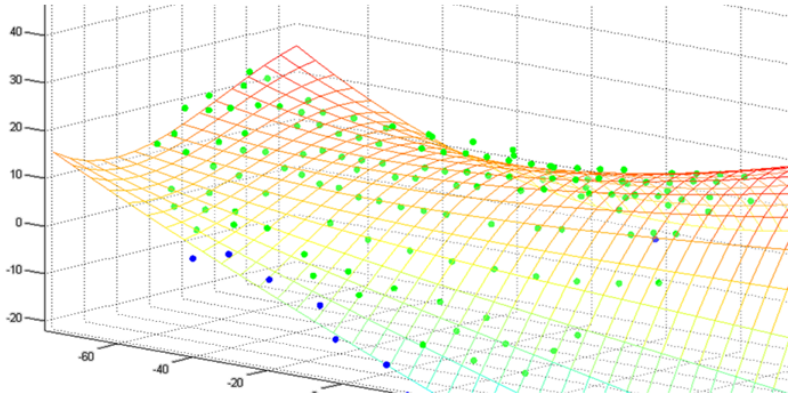

Figure 2.10: Filter based on polynomial surfaces.

the 3D space close to the region of interest. Recognizing the same surface by two different couples, the position of each one is calculated in relation to the known shape. The real dimensions of known shape allows to determine the real position of each couple. This procedure is the final part of the calibration after the calculus of the intrinsic and the extrinsic parameters, it is called synchronization.

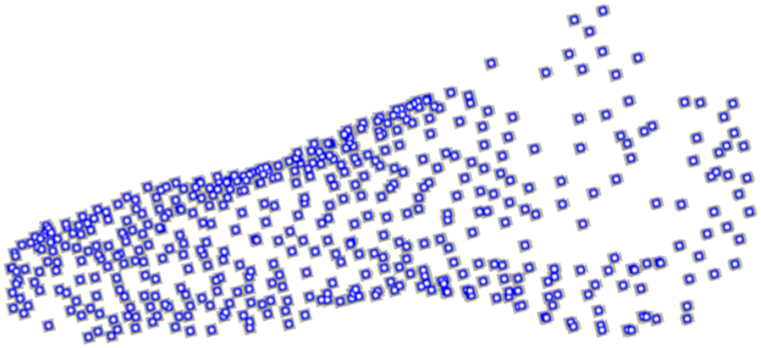

Figure 2.11: Final point clouds.

In conclusion it is not possible to adopt available (and standard) algorithms to filter the acquired point clouds by multiple stereo vision. In many conditions point clouds, which represent real feet, contain only a few points. The ratio between correct points and outlier is unfavourable. Results of re-

constructions show often a cloud formed by 1000 points characterized by 300 outlier. This means 30% of outliers.

2.1.5 Mesh generation

Mesh generation is a fundamental step to obtain a correct RE process. Many different algorithms are evaluated. In the introduction two systems are mentioned: Delaunay-based (Dey et al., 2001) and Marchi cubes (Lorensen and Cline, 1987). Merging cube acts as a low pass filter. As a consequence vertexes of the mesh do not correspond to the acquired points. In a few zones, the curvature is high (feet tip) and the marching cubes method creates a surface shorter than the real foot. As a consequence, Delaunay-based algorithms are necessary considering the density of acquired point (700 points for the whole human foot). Each vertex is positioned in the same position of the acquired points. Considerations about Delaunay algorithm have been mentioned in the introduciton. The algorithm generates, starting from a point cloud, tetrahedrons. Obtained tetrahedrons divide the domain into series of volumes. It is possible to transform series of volumes in a surface. The obtained surface can be seen as the hull of total volume. The hull is convex because Delaunay algorithm cannot reach a correct reconstruction of non-convex zones. This aspect is fundamental, considering the non-convex zones in the plantar arch and in the pathology foot.

In this thesis a new system is developed to solve the problem of the non-convex zones. It is noted that using adjustment of the original Delaunay algorithm a new Delaunay-based algorithm can be studied. Adjustments regard additions of points before the mesh generation. Points are called functional. Functional points are added and then Delaunay algorithm is performed. Tetrahedrons constrained to functional points are avoided from reconstructions. Finally non-convex surface (hull of tetrahedrons) is generated.

In figures an example of an elaboration in two dimensions can be found. Original Delaunay algorithm is shown in (Fig. 2.12). Functional point in the no-convex zone is introduced (Fig. 2.13, left). The result of Delaunay algorithm is shown (Fig. 2.13, right). It is possible to note two similar reconstructions (Fig. 2.12, right and Fig. 2.13, right) without and with functional points. The last operation (Fig. 2.14) removes triangles, attached to functional points. It is possible to note that Added functional points improve the reconstruction in the no-convex zones. Different result can be obtained varying positions of functional points. As a consequence positions must be optimized to obtain robust reconstructions. After many tests one of the best

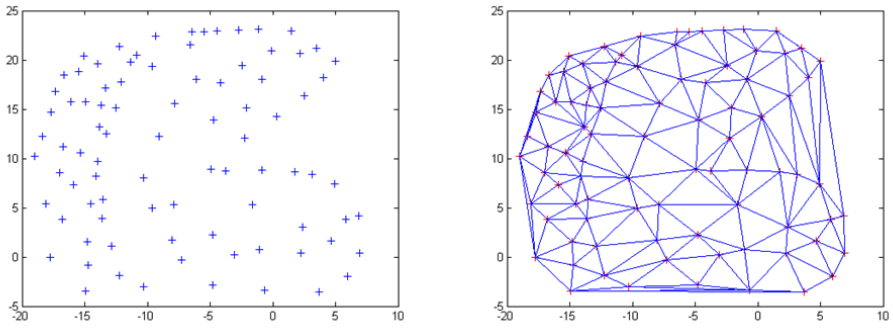

Figure 2.12: The application of the Delaunay algorithm in two dimensions, the considered point clouds input of the process (left) and the obtained mesh output of the process (right).

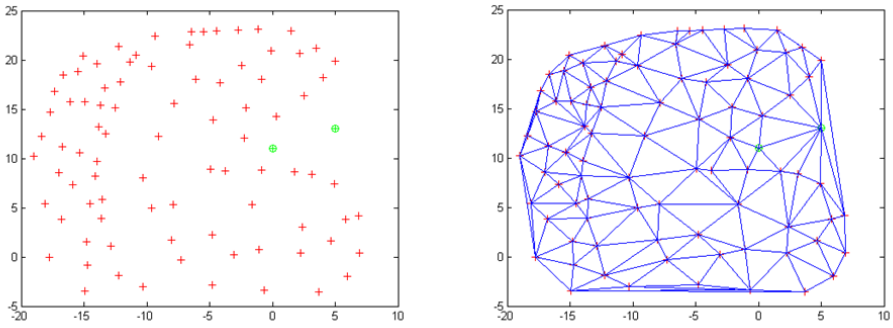

Figure 2.13: The application of the modified Delaunay algorithm, the addition of two functional points in the non-convex zone (left) and the obtained mesh (right).

positions can be calculated using offset. The functional points can be added copying acquired points (of each couple) and translating by a certain offset in the direction of the couples. This direction corresponds on z axis (depth of couples), (Fig. 2.7). In the next figure (Fig. 2.16) an offset of 70 mm is introduced. A bigger offset distances are introduced only to optimize the visualization. During real reconstructions offset distance must be 2 or 3 longer than the mean distances between markers printed on the socket. This distance assures good reconstructions in non-convex zones and unaltered reconstruc-

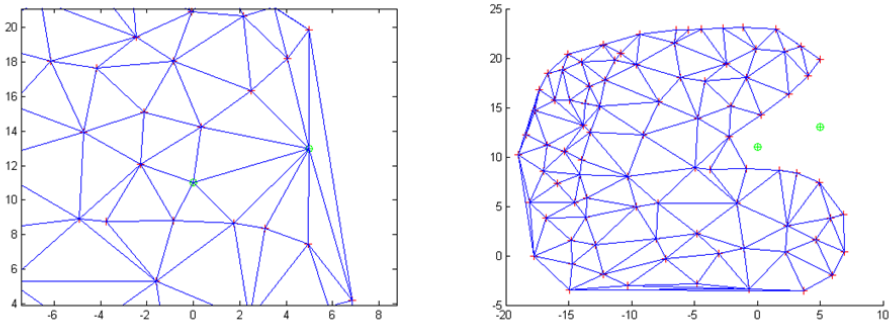

Figure 2.14: Enlargement of the non-convex zone (left) and the exclusion of the triangles related to the funcitonal points (right).

tion in convex zones.

The developed algorithm generates a solid model (represented by triangular mesh) starting from scattered points. The main characteristic of this Delaunay-based algorithm is to manage convex and non-convex zones under condition of down-sampling. Meshes are always closed and normal directions of triangles are always internal to the foot. This reconstruction algorithm can be used with low and high point density. In figure 2.16 (right) different local densities of points are correctly managed. The mesh on the calcaneum zone is coarse while the mesh on the metatarsus is fine. The elaboration time is acceptable, the developed algorithm in Matlab run in 4 seconds to complete the process. In the future, an industrialization, using a programming language (e.g. C++), could decrease one order of magnitude the calculus time. Mesh generation algorithms are sometimes unable to ensure a closed solid model. Problems are related to high curvature zones and down-sampling. Using the implemented Delaunay-based algorithm, taking into account the synchronization parameters of each couple, can be considered an effective improvement in the model generation starting from multiple stereo vision technique.

2.1.6 Conclusion of multiple stereo vision instrument

The final result is a robust instrument and always capable to reconstruct the foot despite noise coming from external environment such as variations light. A RE system was developed using a triangulation system based on images instantaneously acquired from different cameras. The obtained point cloud

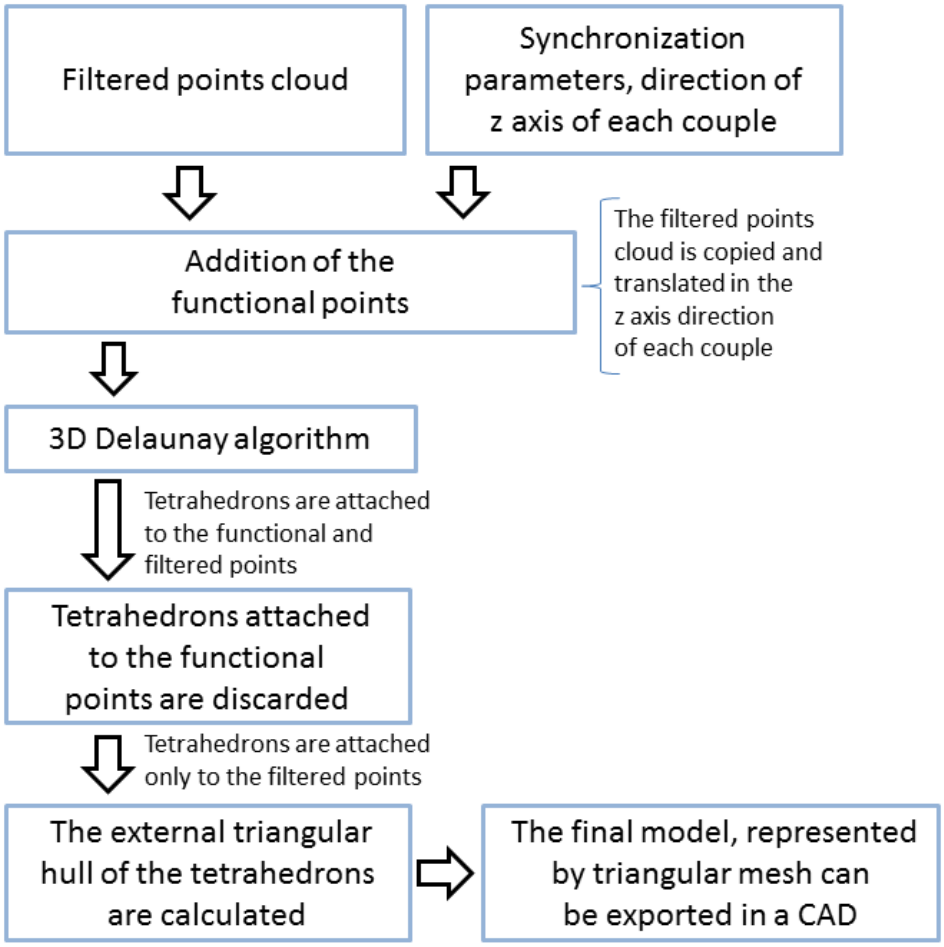

Figure 2.15: Flow chart of the mesh generation process.

through multiple stereo vision is the base for the representation of the external foot surface. For this purpose, an application was studied to automatically filter the acquired data and to generate the solid model. Accurate solid models allow to realize correct anthropometrical measures. This paragraph is focused on the system to obtain correct model as precisely as possible.

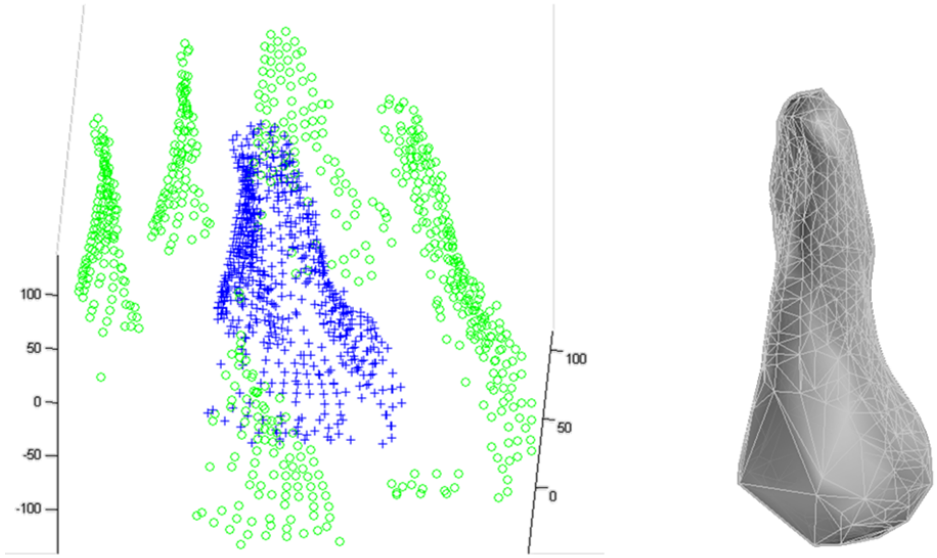

Figure 2.16: The addition of the functional points for the correction of the non-convex zones with an offset of 70 mm (left), the final model (right).

2.2 Instrument based on Silhouette

In this section an instrument based on silhouette was developed. The methods has many limitations notwithstanding is very important because it is the most simple RE method. Using the silhouette method, many different points of view must consider to obtain good reconstruction. The final model, represented by triangular mesh, indicates the hull volume of the real model. Holes cannot be reconstructed. Considering the foot with a socket, holes are absent and because everyone is covered. Starting from the algorithm described by Forbes et al. (2006) (Fig. 2.17), a system can be developed. The characteristic of the system is that the calibration is unnecessary. This technique divides the foreground and the background of a grey level image using a threshold to obtain a binary image. The foreground mask, known as a silhouette, is the 2D projection of the corresponding 3D foreground object. For this reason to maximize the contrast between the foreground and the background the foot must be white while other parts in the field of view of the camera must be black. To test the silhouette method a custom made scanner is built up. It is made up of three components:

- 2 planar mirrors, 0.7 X 0.7 m with black frame;
- 2 cameras, Canon A620 with 7.2 MPx;
- a background in black cotton tissue, 1 x 1 m;
- an elastic white socket.

The foot is placed in the middle and a sequence the acquisition can be performed. The output of the instrument is directly a triangular mesh (Fig. 2.18).

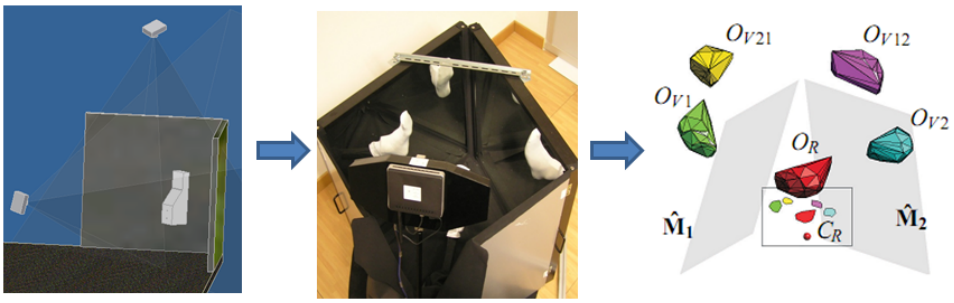

Figure 2.17: The process to obtain the silhouette model.

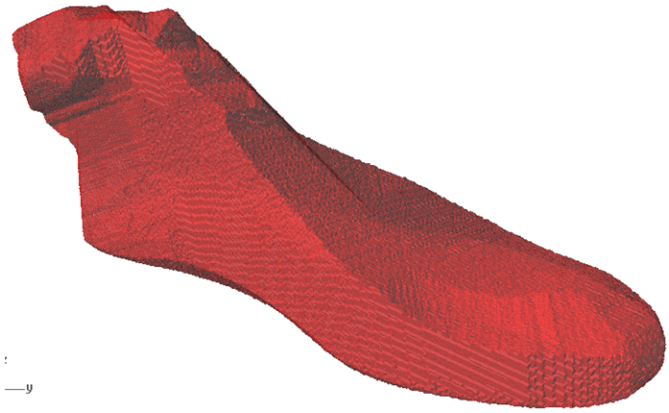

Figure 2.18: The solid model, represented by mesh, of the silhouette technology.

The instrument does not perform a good model and increasing the number of the considered images the improvements of the model are not relevant. High errors in the reconstructions, more than 3 mm can be considered common. The model is represented by the intersection of cones thus many particulars are not reconstructed. The low precision is the most disadvantage of this technique. However there are two important reasons to consider it a good starting point. First it is able to filter the obtained point clouds using other RE technique. Second it is a self-calibrated system.

In the next section, the precision of the instrument will be evaluated and compared among three different foot scanners. Deviations (on each part of the model) between known model and acquired model are evaluated.

2.3 Comparisons of three different foot scanners

The scanners used for comparisons are based on three technologies: silhouette, laser and multiple stereo vision. Using an impression casting method (phenolic foam, Podoschiuma, Podartis SRL, Italia) the foot and ankle shapes of one male subject's right foot (size 42) is captured. The level of the impression cast covers the foot up to the lateral malleolus. The negative cast is than filled with resin (Podoform H1000, Podartis SRL, Italia). The 3D scan of the non-modified positive foot cast yelds a stable and fixed comparative geometry, avoiding all problems related with scanning real feet (e.g. soft tissue deformation). To gain comparability among all the measurements in all the experiments the foot cast is covered by a socket. The stereo vision scanner needs a socket with markers. This is fundamental for the technologies of multiple stereo vision and for the silhouette. In the stereo vision, the markers are not projected on the surfaces but they are directly impressed on socket surfaces. On the contrary in the silhouette scanner the foot cast must be white to increase the contrast with the background.

2.3.1 Silhouette

To test the silhouette method a custom made scanner is built up. It is made up of three components: 2 mirrors, 2 cameras and a background in black cotton tissue. The foot cast is placed in the middle and a sequence of five acquisitions is performed. The images acquired were processed by means of the algorithm described by Forbes et al. (2006) discussed in the previous paragraph and in the introduction. The foot cast is fixed to a support in the middle of the mirrors and five subsequent scans is performed.

Figure 2.19: The scanner used for the experiment: silhouette (left), laser (centre) and multiple stereo vision (right) technologies.

2.3.2 Laser

The Laser scanner used is the Digipie (Automtica y Control Numrico S.L, Inescop, Spain) (Fig. 2.19, center). It is composed by four cameras and four stripe laser modules mounted on a sliding rail. The distance between the acquired slices is 1.37 mm. The foot cast is held on the internal support surface of the instrument. In this way each acquired slice creates a transversal section of the foot. Five scans with and five without automatic filter are obtained. The acquired points clouds is processed by the built-in software to obtain triangular meshes.

2.3.3 Multiple stereo vision

The multiple stereo vision scanner tested was the Foot-o-graph (Delta RS, Italy). It is composed of 14 cameras grouped in couples triggered synchronously. Each couple measures a part of the foot cast. To test this scanner, the white socket is substituted with a socket carrying colored markers in order to add a pattern for multiple stereo vision. In any case, this socket has the same characteristics of the previous one excepted for the coloration. The output model is represented by a triangular mesh. The algorithm to obtain this model is described in the paragraph 2.1. The foot cast is fixed directly to the frame to permit a stable acquisition. Three series of acquisitions is performed: five scans in one position, five scans after re-worning the socket and finally five

scans after repositioning the foot cast.

2.3.4 Data analysis

In order to estimate accuracy, repeatability and validity of scan methods, distance analyses is performed in Catia version 5 (Dessault Systemes), dimensional analyses is performed in Rhinoceros version 4 (McNeel) and statistics with Statistica version 9 (StataSoft).

2.3.5 Results

The foot cast and the model acquired using silhouette method is too different. The gap in some area is too large. The errors in the reconstruction is maximum 5 mm. For this reason the silhouette cannot be introduced in the scientific analysis. The analysis is carried out using two remaining scanners. The dimensional analysis is performed by Rhinoceros using the bounding box command. In order to evaluate the foot cast length and width. Additionally, two perimeter sections (transversal and longitudinal) are calculated. These two dimensions is ball girth and foot girth respectively. The dimension analysis using mesh unfiltered and filter mesh data obtained from laser scanner shows the mean values and standard deviations for length, width, ball girth and foot girth reported in Table 2.1 and Table 2.2 respectively.

	Valid N	Mean	Min	Max	Std.Dev.	Coef.Var.
Length	5	257.7	256.7	258.4	0.8	0.3
Width	5	103.6	103.0	104.1	0.5	0.5
Ball Girth	5	244.7	244.2	245.4	0.4	0.2
Foot Girth	5	603.8	602.6	604.9	0.9	0.2

Table 2.1: Laser scanner dimension analysis using mesh unfiltered data, distance in mm.

Concerning the dimension analysis obtained from stereo vision scanner of series 1, the mean values and standard deviations for length, width, ball girth and foot girth reported in Table 2.3. Finally, same parameters obtained by stereo vision scanner of series 3 are shown in Table 2.4.

The acquired data is then compared in Catia, performing a surface distance analysis. Moreover the dimensions and the geometrical characteristic of the scanned data were compared with a 3D model of the foot cast obtained by a Coordinate Measuring Machine (CMM, Global Image 07.07.07, DEA, Italy).

	Valid N	Mean	Min	Max	Std.Dev.	Coef.Var.
Length	5	256.8	255.1	258.3	1.2	0.5
Width	5	104.0	103.0	104.8	0.7	0.7
Ball Girth	5	244.5	244.2	245.1	0.4	0.2
Foot Girth	5	603.3	602.3	603.9	0.6	0.1

Table 2.2: Laser scanner dimension analysis using mesh filtered data, distance in mm.

	Valid N	Mean	Min	Max	Std.Dev.	Coef.Var.
Length	5	254.1	254.1	254.2	0.0	0.0
Width	5	105.9	104.8	106.3	0.7	0.7
Ball Girth	5	254.7	253.3	256.0	1.3	0.5
Foot Girth	5	580.3	552.8	600.8	24.3	4.2

Table 2.3: Stereo vision scanner dimension analysis using mesh series 1, distance in mm.

	Valid N	Mean	Min	Max	Std.Dev.	Coef.Var.
Length	5	255.0	254.6	255.2	0.3	0.1
Width	5	103.8	102.7	105.1	1.4	1.1
Ball Girth	5	253.4	252.2	254.0	0.7	0.3
Foot Girth	5	580.1	527.4	599.8	31.5	5.4

Table 2.4: Stereo vision scanner dimension analysis using mesh series 3, distance in mm.

CMM can measure point by point or scanning, and it guarantees an accuracy of 1.7 micron (ISO10360-2, 2001) when measuring point by point, and of 3.4 micron (ISO10360-4, 2000) when measuring by continuous scan (Dea web site). In this work, surfaces is measured by scanning mode. The precision of the CMM is more than one order magnitude larger than that of scanners. To align the reference with the models acquired, the best fit alignment of Catia is used. After alignment, the foot cast models are trimmed with a reference boundary for standardizing the comparison area. The trimline is similar to that of commercially available insoles, but in this design, the forefoot section is included. The foot models are trimmed 15 mm horizontally above the weight-bearing plane. These models are also compared in Catia performing

distance analysis in order to evaluate the differences between two geometrical entities defined by meshes. In Figure 2.20, it is possible to observe the results of distance analysis considering one laser scanner model and the reference. The color of each point was related to the gap between models. The lower and upper worst distances were -1.8 mm and 1.7 mm.

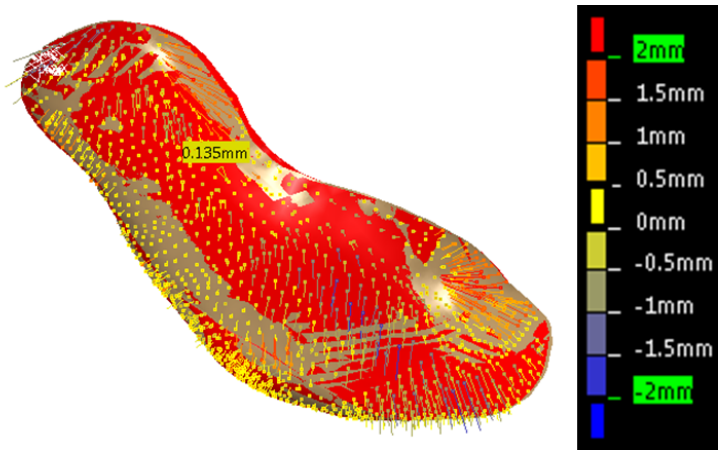

Figure 2.20: Distance analysis of one laser scanner model and reference model.

The statistical analysis shows (Table 2.5) the percentage in each single range (e.g. in the gap 0.5 - 0 mm the percentage of model was 32.1%).

Gap		% of model
2.0	1.5	1.0%
1.5	1.0	4.6%
1.0	0.5	6.9%
0.5	0.0	32.1%
0.0	-0.5	33.0%
-0.5	-1.0	17.2%
-1.0	-1.5	4.6%
-1.5	2.0	0.6%

Table 2.5: Statistical analysis of the gap between laser scanner and reference model.

In figure 2.21 it is possible to observe the results of distance analysis considering one laser scanner model and the reference. The lower and upper worst

distances were -1.4 mm and 1.6 mm. Table 6. shows the statistical analysis.

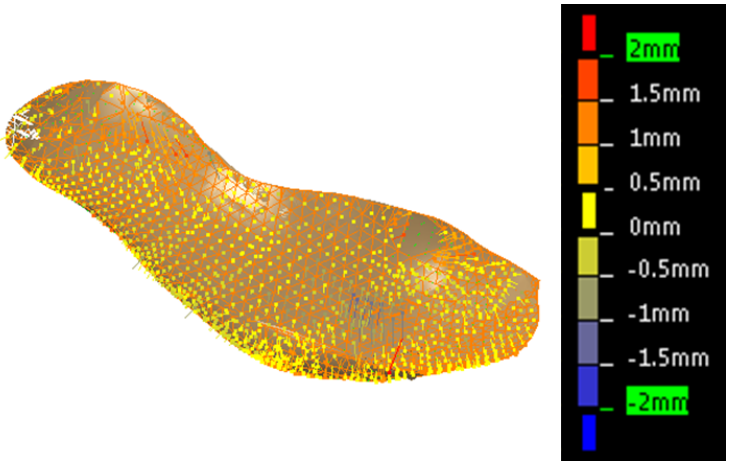

Figure 2.21: Distance analysis of one stereo vision model and reference model.

Gap		% of model
2.0	1.5	0.1%
1.5	1.0	1.0%
1.0	0.5	11.3%
0.5	0.0	41.4%
0.0	-0.5	41.0%
-0.5	-1.0	4.2%
-1.0	-1.5	1.1%
-1.5	2.0	0.0%

Table 2.6: Statistical analysis of the gap between laser scanner and reference model.

2.3.6 Discussion

As pointed out in the results, the foot cast and the model acquired using silhouette method are too different. The incongruence of these data is the reason why they are not considered in the comparison with the laser and the optical technology based scanners. Probably, the acquired data (number of Images) are too small in order to have a sufficient detailed 3D reconstruction

of the foot cast; however this methodology is unsatisfactory compared with the others two. The results of both laser and multiple stereo vision scanner could be considered good enough to have a detailed 3D reconstruction of the reference foot cast (Mundermann et al., 2005). The existing differences between these two methodologies even though around 2 mm in length allow a good external anatomical description of the foot as required for tailored shoes. The estimated width values were similar in both technologies. Both scanners show a good repeatability and a low coefficient of variation (Table 2.1, Table 2.2, Table 2.3, Table 2.4). Considering the obtained results, the multiple stereo vision scanner seems to be the better instrument to estimate the foot dimensions. It shows better coefficient of variation (excepted for the foot girth, see Table). This indicates a good repeatability. The lightly higher coefficient of variation of length estimated from the laser scanner data can be explained on the base of the acquisition step imposed (1.37 mm). As a consequence, the maximum error could be 1.37 * 2 including the tip zone and the calcaneum zone. One of the most important advantages of the laser scanner technologies is the possibility of acquiring data of one foot from different weight bearing conditions. On the contrary, with the stereo vision scanner tested, only the unloaded foot condition is possible. The laser scanner acquisition lasts few seconds. The pulsation and vibration provoked by uncontrolled muscle contractions of real feet could be a noise factor in the measurement. The laser scanner acquisition time is instantaneous. Moreover one of the disadvantages in the stereo vision system is related to the adoption of the socket, which must be used because it contains the pattern for the image recognition. The distance analysis of the laser scanner shows large portion of the model characterized by the same average distance (areas visualized in figure 2.21 by the same color), related to alignment difficulties of the automatic filtering routine.

To avoid alignment problems on both systems, a fitting algorithm based on the position of heel and metatarsal head will be discussed in the next paragraph. However, in the present work, the alignment of the stereo vision data is done with the fitting algorithm included in Catia. Considering the length of the foot estimated by the laser scanner, it decreases from 107 of unfiltered data to 104 mm of the filtered one. This is probably caused by an "highly selective" filter (Fig. 2.23) that works similarity to a low-pass. It decreases significantly the curvature of same zones. Anyway it is possible to set the filter, enable or disable, via software.

The points cloud sampling (related to the pattern on the socket) of the

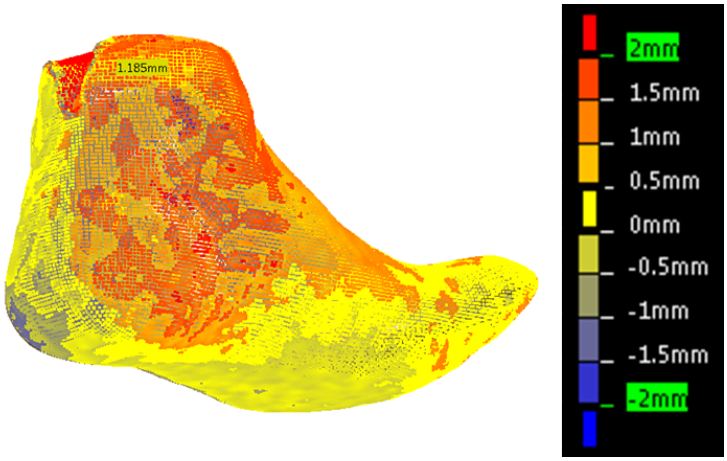

Figure 2.22: Model to model distance analysis of two laser scanner measurements.

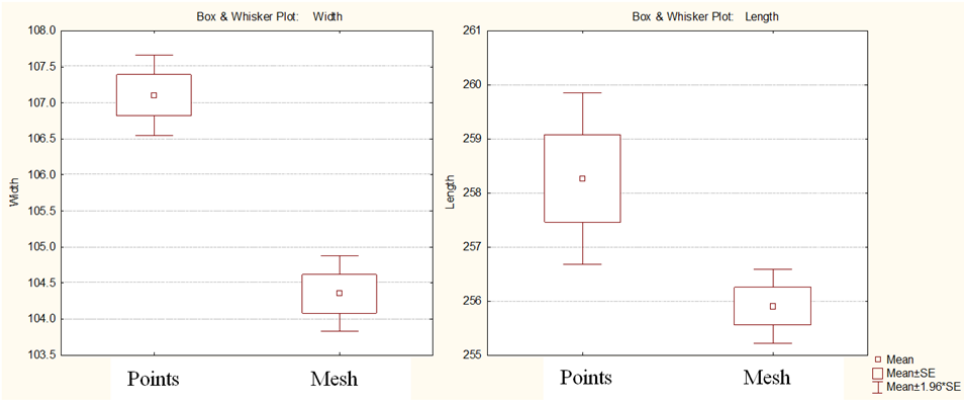

Figure 2.23: Width (left) and length (right) of points acquired by laser scanner and the mesh filtered.

stereo vision is lower than that of laser but it cannot be considered a downsampling. Anyway, the details obtained still defines a proper 3D representation of the model. However, for further calculation diminishing the number of data can be an advantage. The scanners can be useful for the 3D reconstruction of real feet, as required by the current footwear industry. This consideration is confirmed by the fact that the differences are localized prevalently in length measure and do not reflect in other important parameters related to the cus-

tom shoes (e.g. width and ball girth). The length discrepancies can be easily managed during the customization of shoes if they are systematic as in our results. The silhouette technology could support the data acquisition and filtering as pointed in Yemez et al. (2007). All the existing methods can provide unique information and the objective of the future research should be focused in combining laser, stereo and silhouette scanners in fusion techniques.

2.4 Instrument based on FPP

The main important conclusion of the last paragraph is: "The existing differences between these two methodologies (multiple stereo vision and laser), even though around 2 mm in length, allow a good external anatomical description of the foot as required for tailored shoes". As a consequence, a good representation of the foot is carried out. The reconstruction can meet requirements of the market but not more straight requirements imposed by the research, precision maximum $\pm$ 0.3 mm. This is a fundamental problem and it suggests testing another technology. In the introduction, shape from silhouette, stereo, laser and range finding was mentioned. The last one is never faced. One of the main important methods to reconstruct whatever 3d shapes is the Fringe Projection Pattern (FPP). Recently this technique has become very promising in relation to the new generation of commercial projector based on DLP (Digital Light Processing). DLP projectors are formed by mirrors actuated by capacitive systems to create the scene. The most relevant advantage is the frame frequencies, that can outcome 100 Hz. This means projections of many different fringes in a short lapse of time. Multi-frequencies systems (5 acquired images per reconstruction) can perform theoretically more than 20 reconstructions per second. A typical system is formed by projector and camera.

Instrument to measure human part are characterized by the following requirements:

- Simultaneous acquisition of all information for the reconstruction
- Fixed cameras (no sliding rail)
- Open instrument to avoid claustrophobic effects
- Free external light condition during acquisitions
- Foot unloaded (or loaded controlling the loading conditions)

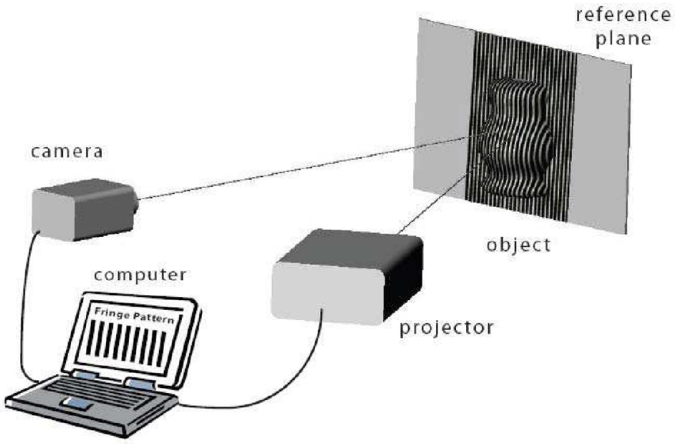

Figure 2.24: Schematic setup of a FPP system.

FPP can satisfy all the previous requirements except for simultaneous acquisitions. The same region must be acquired 5 times varying projected fringes. The acquisition time is related to the frame frequency of projector and camera. A system with a good trigger can reduce the acquisition time down to 0.1 second. FPP involves in three steps: projection of fringes, acquisition using a camera and image processing. One of the most important characteristics is the point assignment to each pixel. E.g. a 12 Mega-Pixels camera can perform reconstruction with 12 Mega-Points (12 million of points). Common FPP algorithms are related to phase-shifting and multi-frequencies methods. Phase-shifting allows to calculate in a fast way the phase using a function based on arctangent operation. The unwrap phase is slow. On the contrary multi-frequencies method adopts a relative complex system for phase detection while the unwrap operation becomes very fast and simple.

Multi-frequencies can be considered better than phase-shifting for two reasons:

1. Multi-frequencies can measure irregular geometries, phase-shifting is very robust only with smooth surfaces;

2. The precision of Multi-frequencies is declared by Zhang (2010) lower than 0.2 mm.

X and Y coordinate are functions of the position (i and j) of pixels in the CCD (or C-mos) matrix of the camera. Z is defined as depth. Consequently the Z axis is function of X and Y (or i and j) and the phase. Depth can be calculated using different formulas. At the moment the best formula seems to be Z equal fractional expression (Du and Wang, 2007) as shown in following (Eq. 2.3). One of the most important aspects is the calibration system. That must find more than 20 parameters. The equation system is not linear, so Levemberg-Marquardt algorithm must be adopted. There are two calibration methods: different known planes (with different depths) and a grid based on the Zhang method. Using different known planes, the calibration is fast and it can be performed only with a single reconstruction (formed by 5 images). Using Zhang-based method, the grid must be moved in the field of view of the camera (and projector). Vo Minh et al. (2010) propose 18 reconstructions with the grid in different positions. Zhang-based istime consuming and obtains better results. Known planes procedure is shorter and can be considered good enough. In fact this permits to reach a tolerance of $\pm$ 0.2 mm.

2.4.1 Method

The instrument is composed of: a commercial camera (Canon A620) 7.2 Mega-Pixels, a frame (section 30 x 30 mm) in aluminium and a commercial DLP projector (HP VP6100). 3D FPP reconstructions involve by 5 steps:

1. Sinusoidal fringe pattern generation and projection;
2. Image acquisition;
3. Image processing;
4. Fringe analysis composed by phase detection and phase unwrapping;
5. Phase to height conversion.

In the following each step is discussed.

1. Sinusoidal fringe pattern generation and projection

During the 3D shape measurement, a set of fringe patterns are projected onto the surfaces of the objects of interest. The surface morphology information is naturally encoded into the distorted fringe patterns, which will be captured by the camera for further processing. Normally vertical fringes are

numerically generated with a sinusoidal function. In the practise a digital projector often applies gamma decoding correction to the images and videos to enhance the visual effect. Modern projectors automatically apply a non-linear gamma decoding processing with γ in the range 2.2 and 2.6. Nevertheless, for the FPP-based 3D shape measurement, the gamma decoding will generate unwanted intensity changes to the fringe patterns and the projector fail to produce the ideal sinusoidal intensity distributions. Accurate fringe patterns to correct gamma can be expressed as

$$I = 2I_0 \left[\frac{1}{2} + \frac{1}{2} \cos(2\pi k \frac{x}{\omega} + \delta \right]^{\frac{1}{\gamma}} \tag{2.1}$$

where I is the pattern intensity at the point whose horizontal pixel coordinate is x, ω is the width of the pattern image, k is the number of fringes in the image, δ is the phase shifting amount, and I_0 is normally set to 127.5 to obtain a desired intensity in the range of 0-255 for gray scale images. In this way, the gamma problem is solved directly in the digital projection phase. Five fringe patterns are generated using γ equal to 2.4. Fringe frequencies are 1, 3, 9, 36 and 72, respectively (Fig. 2.25).

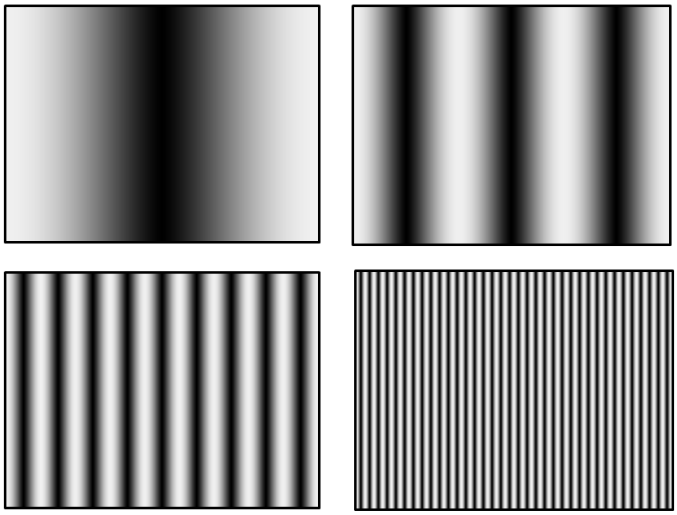

Figure 2.25: Projection fringe patterns with 1, 3, 9 and 36 fringes.

2. and 3. Image acquisition and image processing

Image acquisitions (Fig. 2.26) are performed directly via firmware of the camera. The developed firmware substitutes the original firmware. In automatic way it is possible to hold many parameters of the camera. Zoom, focal length, time, white balance, number of acquired image are directly fixed via firmware. A for statement is implemented to obtain five image in sequence triggered with the fringes imposed by the projector.

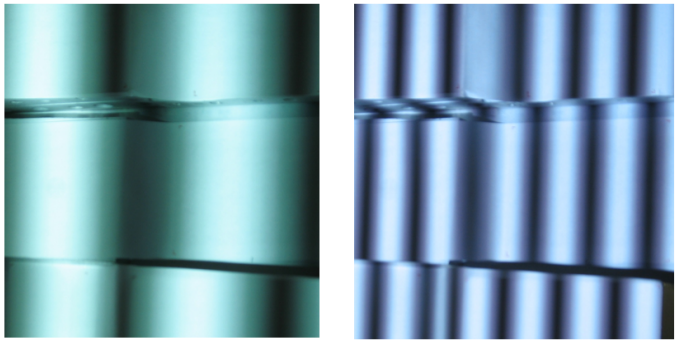

Figure 2.26: Fringe patterns captured by camera, 3 fringes (left) 9 fringes (right).

4. Fringe analysis composed by phase detection and phase unwrapping

The phase detection starts from acquired images and aims to calculate the phase of fringes. Fourier Transform Profilometry (FTP) is adopted. It is a very popular technique that is well known to people working in the field of non-contact measurement. Since Takeda proposed his technique for using the Fourier transform in analysing a fringe pattern in 1982 (Takeda et al., 1982) (Fig. 2.27), many applications have adopted this technique in order to measure 3D surface shape.

Takeda technique is developed in one dimension but it can be extended in two dimensions. Fast Fourier in two dimensions (FFT2 function) again contains the information necessary to detect the phase (Fig. 2.28, left). Hanning window must be applied and conjugate is isolated $c(f_x - f_0, y)$. Parts of the 2D FFT are filtered (Fig. 2.28, right). Inverse of the 2D FTT2 (2D iFFT) allows to calculate directly the phase (Fig. 2.29).

When the object involves complex shapes and/or multiple separated objects, the phases of the projection fringes on each object and among different

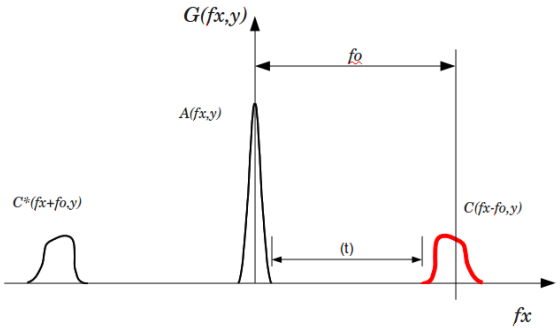

Figure 2.27: 1D FFT of a sinusoidal signal with three peaks, only the right peak C (in red) is necessary for the phase calculus, f_0 is the spatial frequency.

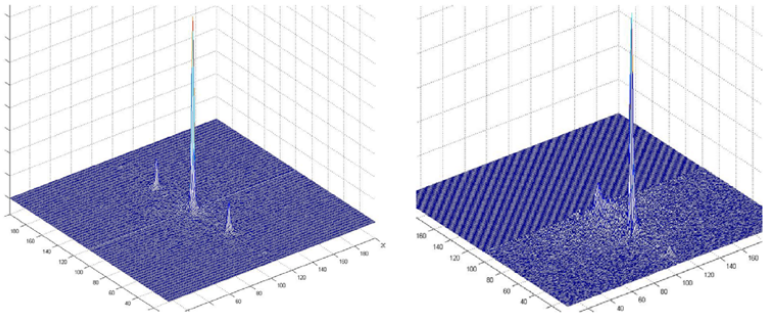

Figure 2.28: 2D FFT of the image with 32 fringes (left), Filtered 2D FFT of the image with 32 fringes (right).

objects are often discontinuous. FPP generally employ phase shifting scheme to obtain the full-field wrapped phase distributions of the projection fringes. The wrapped phase must then be unwrapped to obtain the real phase distribution.

The lowest- frequency fringe pattern with one single-fringe in the entire field can yield full-field phase distributions without a phase-unwrapping process. The unwrapped phase distributions of the higher frequency fringes can be readily calculated without a general phase unwrapping, no matter how complex the fringe patterns are. The algorithm can be expressed as

$$\phi_i^{uw} = \phi_i^w + INT\left(\frac{\phi_{i-1}^{uw}\,(f_i/f_{i-1}) - \phi_i^w}{2\pi}\right)\cdot 2\pi \quad (i = 2, 3, \ldots, n) \tag{2.2}$$

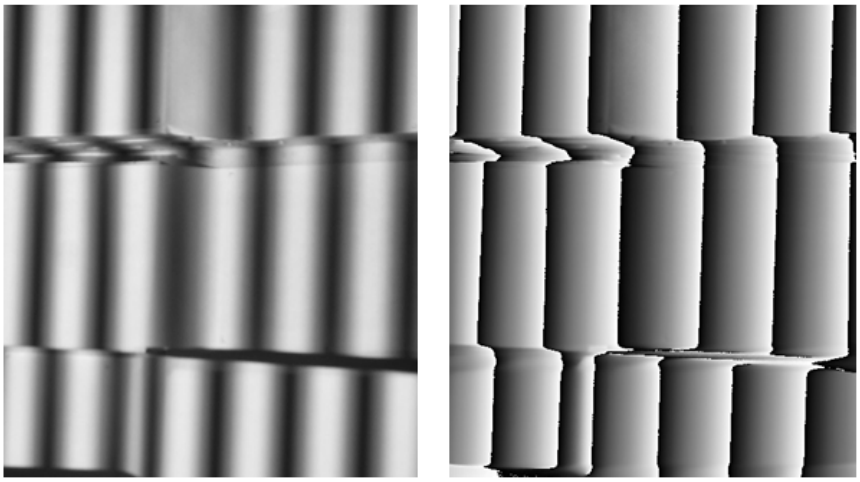

Figure 2.29: An image with 9 fringes (left) and the phi calucus (right).

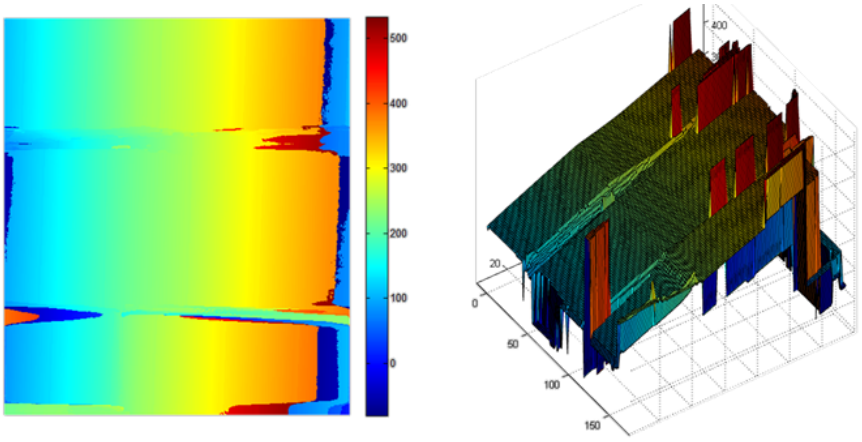

Figure 2.30: An example of unwrap, on the considered portion the phi varies from 100 to 400.

where i indicates the ith projection fringe pattern, the superscripts uw and w denote unwrapped phase and wrapped phase, n is the number of fringe frequencies, f is the relative fringe frequency. The direct phase-unwrapping approach based on multi- frequency fringe projection can obtain the full-field unwrapped phase distributions (Fig. 2.30) in a fast way. Furthermore, the ap-

proach is suitable for measuring multiple objects with complex shapes without any additional processing.

5. Phase to height conversion

The mathematical derivation of the governing equation for the 3D shape determination was discussed by Du and Wang (2007). Basically, the governing equation of the out-of-plane shape determination can be expressed as

$$z = \frac{1 + C_1\phi + (C_2 + C_3\phi)\, i + (C_4 + C_5\phi)\, j + (C_6 + C_7\phi)\, i^2 + (C_8 + C_9\phi)\, j^2 + (C_{10} + C_{11}\phi)\, ij}{D0 + D_1\phi + (D_2 + D_3\phi)\, i + (D_4 + D_5\phi)\, j + (D_6 + D_7\phi)\, i^2 + (D_8 + D_9\phi)\, j^2 + (D_{10} + D_{11}\phi)\, ij} \tag{2.3}$$

where i depends on x coordinate and j depends on y with a scale factor. To calculate the out-of-reference-plane height (z coordinate), the new coefficients C1 .. C11 and D0 .. D11, associated with the geometrical and other relevant system parameters, must be determined first. The coefficients are determined using a least-squares inverse approach based on reference planes. The phase, the position x, y and finally the depth of the planes, defined by z, it is know and these data can be adopted for the calibration process. Reference planes objects are used for the system calibration only. They are not required for 3D shape measurements. The calibration approach involves minimizing the linear least-squares through Levemberg-Marquardt algorithm. Substantially, 300 X 300 mm areas characterized by 6 aluminium planes with 6 different depths are used (from 0 to 60 mm). All the planes is covered by no-reflective material (Fig. 2.31). White paper or white colour can be adopted.

2.4.2 Experimental calibration

The distance between the camera and the reference plane is about one meter. The valid field of view is approximately 300 X 300 mm. The field of view can be easily and directly extended by decreasing the zoom of the camera and at the same time increasing the distance between the camera and the reference plane. Heights of 6 planes (Fig. 2.32) are: 0, 23.3, 30.4, 51.4 and 60.6 mm. Two zones have a height equal to zero. Five different fringe frequencies, with 1, 3, 9, 36, and 72 are projected. As indicated in the literature, two adjacent fringes are not characterized by a frequencies ratio major than 3. The 3D shape measurement results (based on the calibration) indicate that the average error is 0.01 mm. This means a good calibration system; in particular Levemberg-Marquardt Algorithm is an accurate approach. The standard deviation of the distance between correct height and reconstructed height is 0.09 mm with a

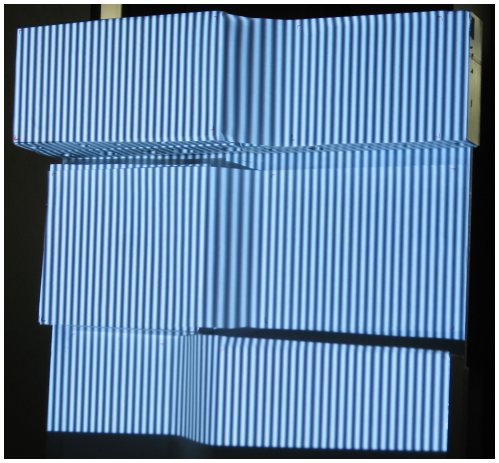

Figure 2.31: Calibration system characterized by 6 aluminium planes.

precision of 0.22 mm. The reconstruction of a shoe last shows the capability of the instrument, the mean gap between the real model and the solid model is 0.1 mm (Fig. 2.33). Some reconstructions are presented from figure 2.34 to figure 2.38.

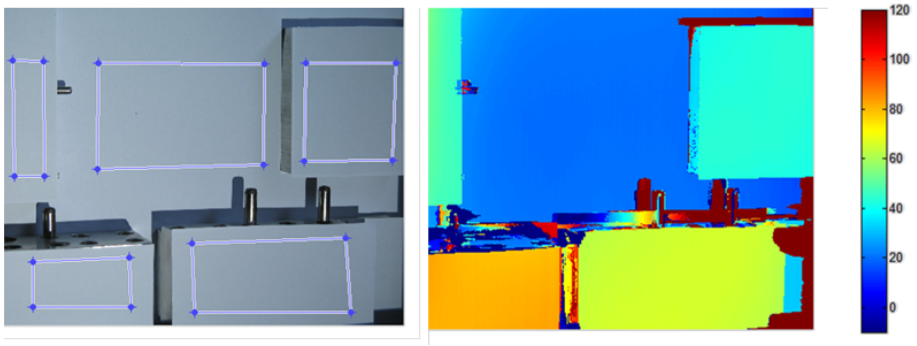

Figure 2.32: The reconstrucion of some planes using FPP.

2.4.3 FPP Conclusion

Using the same strategy, a similar system applied to a microscope it is reasonable (the projector system must be smaller). A bigger field of view, more than 2 or 3 meter, can be obtained using a powerful projector. In this case,

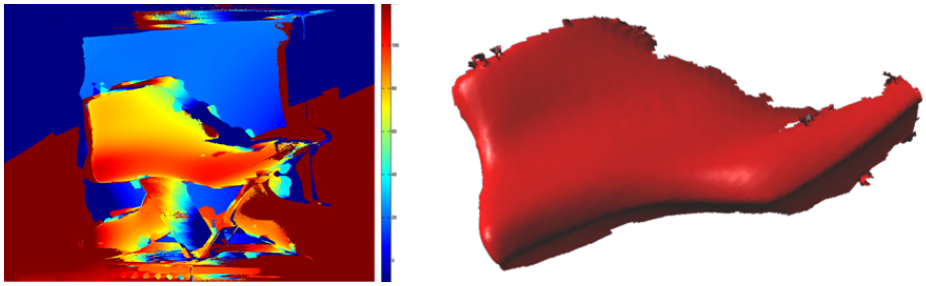

Figure 2.33: The reconstrucion of a last using FPP technique (left) and the mesh generation using a commercial software, Rhinoceros v.4 (right).

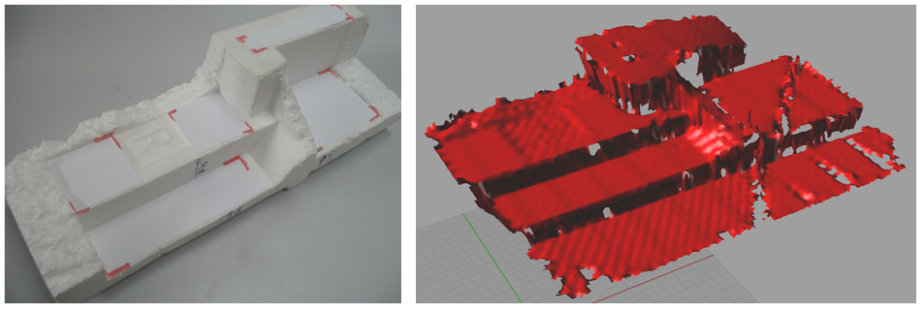

Figure 2.34: The reconstruction of a porous material, polystyrene.

the system can be adopted for reconstructuring large complex shape. The 3D shape measurement technique has also been employed to construct a complete 360 degrees object.

For each of the performed experiments, the elaboration time was around 10 seconds with a regular personal computer to acquire, analyse and elaborate 5 images (7.2 Mega-Pixels).

2.5 Conclusion

Differences between FPP and other systems (based on shape from X) are huge. Stereo vision, including Digital Image Correlation (DIC) works on patterns directly imposed on the object, or projected such us speckle. Shape from silhouette instrument does not perform a good model and increasing the number of the considered images the improvements of the model are not

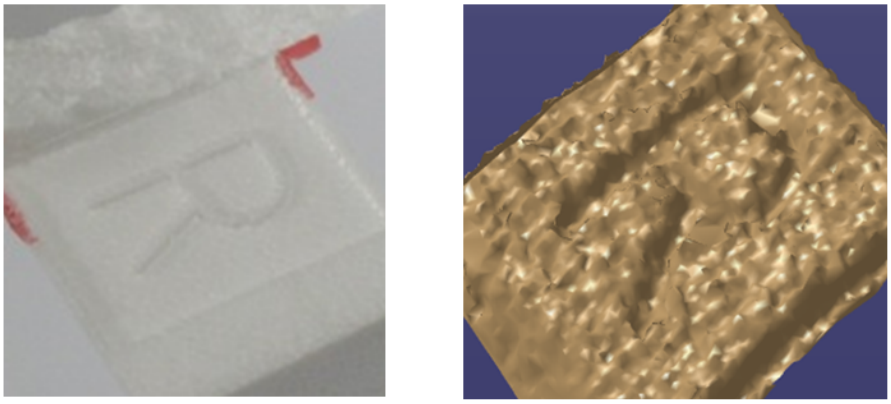

Figure 2.35: A particular of the shape in polystyrene, the letter "R" has a depth of 0.3 mm.

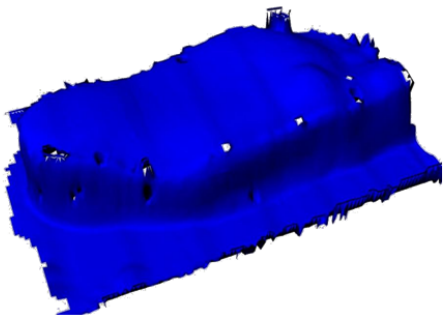

Figure 2.36: The reconstruction of an imprint (foot-mark).

relevant. High errors in the reconstructions, more than 3 mm can be considered common. The low precision is the most disadvantage of this technique. However, for two important reasons it must be considered. First it is able to filter the obtained point clouds using other RE technique, especially for the stereo vision. Second it is a self-calibrated system. Stereo vision instrument is in development and the algotithm to obtain less than 30% of outliers is a working progress. For this reason the data filtering process characterized by outliers detection must be optimized. At the moment, parameters are tested to obtain a good solid model represent by mesh but a robust process requires the optimization of all the parameters of each filter. E.g. a Design of Experiment (DoE) analysis can be performed to optimize the parameters.

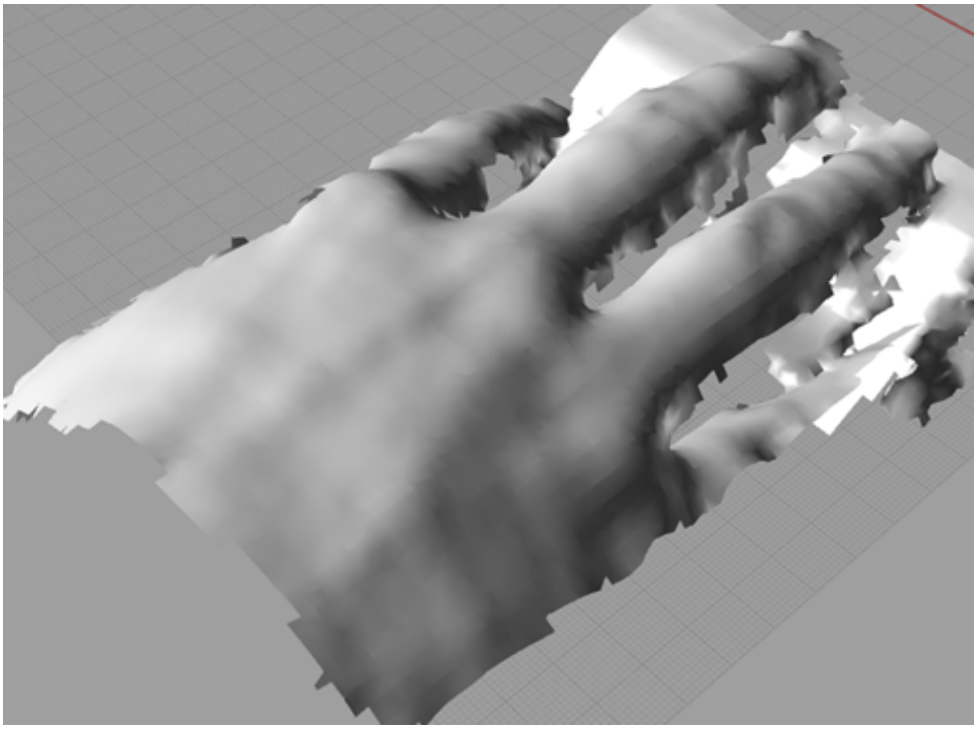

Figure 2.37: The reconstruction of the hand using mesh generation of Rhinoceros version 4.

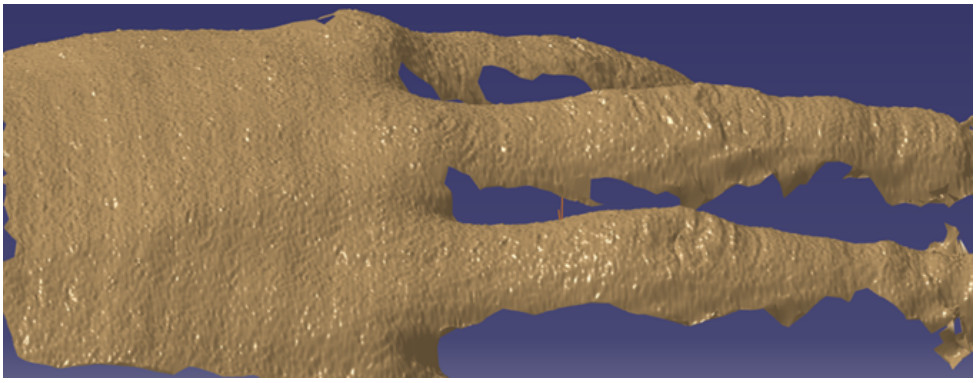

Figure 2.38: The reconstruction of the hand using mesh generation of Catia version 5, wrinkles on the phalanges can be described.

Regarding the mesh generation Delaunay-based algorithm is appropriated and able to manage convex and non-convex zones under condition of correct sampling and down-sampling. Meshes are always closed and normal directions of triangles are always internal to the foot. This reconstruction algorithm can be used with low and high point density. The mesh generation is not related to parameters but is only a function of the distance between the markers. In future, if the socket will be changed only the distance between the markers bust be varied. Anyway, in general, points sampled are univocally related to the patterns. In the DIC the pattern is typically 20 X 20 pixels and it is the minimum sampling which can be imposed in the stereo vision technique. On the contrary FPP can calculate the depth of each pixel using the mentioned relation only. Thus, computational time is short. In addition, stereo vision does not tolerate large deformations of the pattern. This means that reconstructions of high curvature surfaces could become problematic. Image acquisition process in the FPP is not instantaneous, 5 images of the same field of view in sequence are necessary. The acquisition time can be considered quick enough for human parts. As indicated in the literature, more than one FPP systems (formed by a camera and a projector) can be adopted to obtain directly the whole 3D shape information of an object, or human parts, in general, such us feet, hands and body. A bundle adjustment algorithm (again based on Levemberg-Marquardt) can manage all the information obtained by single a FPP reconstruction. At the beginning of the work, The FPP instrument was designed to develop a RE system for the foot only. The results demonstrate that many objects and different human parts can be represented using this technique. Wide range of real objects can be reconstructed. Thus, in many different fields such as medical sciences, biomechanics and in many areas of engineering can be adopted.

All the considered techniques can be adopted in the future for industrial application. In particular FPP characterized by a good accuracy and precision can be indicated for supporting the research activity in the biomechanical field. The surface acquisition of the human body parts is fundamental in each biomechanical study for the validation of the predictive models. An application regarding the custom shoes is proposed in the chapter 3, this is a typical analysis for an industrial application. A biomechanical study of the foot aims at the prediction of the displacement under loading condition. This FE model is discussed in the chapter 4. Considering all the analysed RE technique, the validation of the FE model could be performed using the FPP given that it is the more precise than the others.

Chapter 3

From the model toward the customized shoe

Shoes are one of the most difficult products to customize considering high curvature surfaces and important role of the fit between shoes and feet, while primarily primarily determines the footwear comfort. In this chapter measurements of the foot are analysed taking into account the last. Most relevant anthropometrical measures of the foot can be divided into two groups: 2d techniques and 3d techniques. 2d techniques are used by Nike and other companies and are based on profiles. The foot is positioned on a white paper. Boundaries are drafted maintaining a pen in vertical following the external profile. The outline of the foot is measured and dimensions are calculated. 3d techniques find the position of some points on the 3d solid model and then the distances between points are calculated (Fig. 3.1). These distances represent fundamental dimensions of the foot. In this paragraph 3D techniques are discussed starting from the alignment of the foot.

3.1 Foot alignment

The alignment of the model is the first operation. Therefore after the generation of the solid model (using whatever RE technique) represented by mesh, a group of algorithm presented in the following are applied to align the model. This plays an important role to univocally obtain accurate position of the foot on a standard 3d Cartesian coordinate reference system. Basic operations are roto-translation using a matrix applied directly to the solid model. A robust alignment allows to measure the same foot in different acquisition times ob-

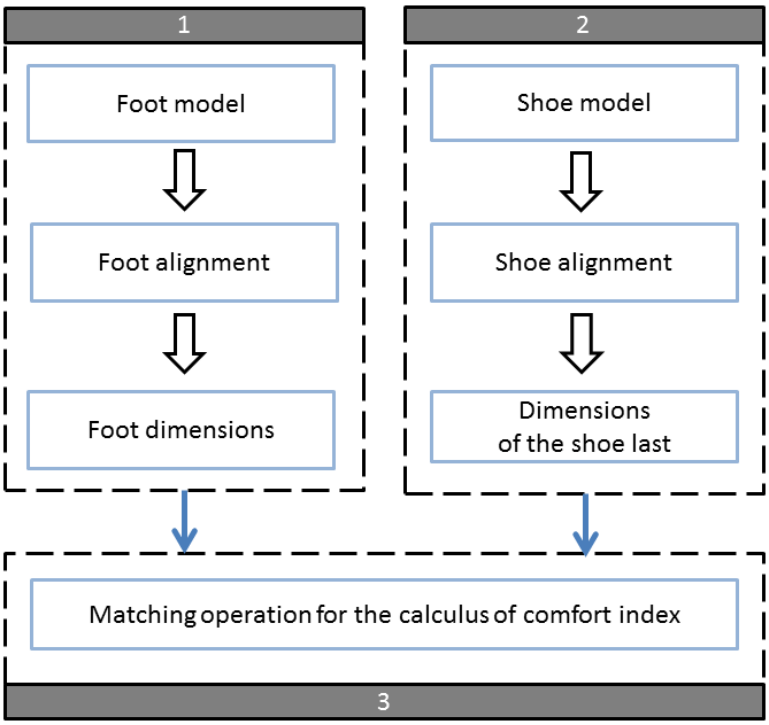

Figure 3.1: The flow chart of the RE of this chapter.

taining always the same dimensions (e.g. length and width of the foot). In different acquisition times the foot can be in a different relative position with respect to the instrument. The solid model of the foot is characterized by free-form entities related to the shapes of the human body. The geometry is not characterized by plane, holes and fundamental features typical of mechanical components. They are easy to individuate. In the free-form models, the alignment is performed using a group of rules for the minimization of distances through fundamental entities (such as a sphere for the talus zone) and fitting system with surfaces approximated by polynomial functions. The alignment is divided into two parts: the first is course, the second one is fine. The course alignment is obtained using predeterminat roto-translation to achieve an approximate position of the model. The foot model is set into a position close to the correct one. Each instrument has a typical course alignment, that can be calibrated considering the acquisition zones. In the instrument of multiple stereo vision, the foot are always inclined by an angle of 60 $\pm$ 3 degrees.

The laser scanner acquires the model and the course alignment stars from a translation along x and y axis. The z axis translation is not necessary because under the foot a glass hold the foot in the correct z position. In addition, the position of the glass corresponds to z equal to zero. This is imposed by the instrument manufacturer. The fine alignment is characterized by iterative algorithms for small roto-translations. It can be less than one degree or one millimeter. It is possible to separate these two alignments thinking that the foot is always inserted to the instrument from the same position and the foot is constrained inside a limited volume of acquisition of the instrument. A standard Cartesian coordinate system is defined according to the standards of medical environment.

- The length is defined along the x axis.
- The width is defined along the y axis.
- The height is defined along the z axis.

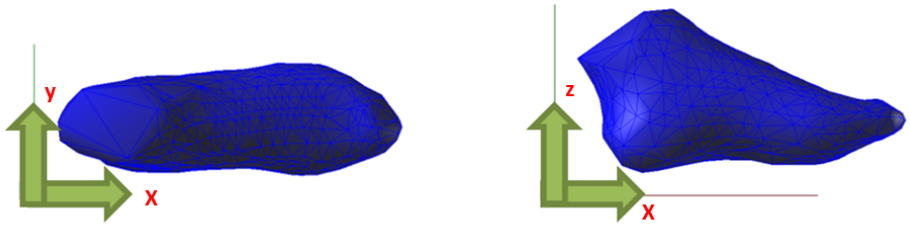

Figure 3.2: Top and front view after the course alignment process.

The coarse alignment (Fig. 3.2) depends on the manufacturer of the instrument and it is fixed at the beginning of the installation process (e.g. multiple stereo vision system needs only a rotation of y axis, laser system a translation of x, y axis). After the course alignment the fine alignment is performed. The approach begins with the correction of the rotation of x axis, y axis and z axis respectively and finally the correction of the translations. The x axis rotation is obtained selecting the metatarsal heads. Experimental analyses show that the metatarsal heads lie between 53% and 68% of the total length of the foot (Fig. 3.3) starting from pternion (defined as the extreme rear point of the talus). In the multiple stereo vision instrument, these values must be increased by about 7% because the foot is inclined with respect to the leg.

This operation is not necessary considering the foot in a different position, e.g. if the x-y plane of the foot is orthogonal with the position of the leg. Using the laser instrument, an angle of 90 degrees between leg and foot is generated and the 7% correction is omitted. Anyway, it is necessary to maintain a relaxed (and natural) position for correctly measuring the foot. As a consequence, the compensation of this length is necessary. After the selection of the metatarsal head, an ellipse is generated through a last square fitting operation. The inclination of the principal axis of the calculated ellipse is the rotation in x axis to obtain the compensation of the eversion and inversion of the foot. The y axis correction is imposed valuating the relative minimum on the talus and on the metatarsal head ("A" and "B" points in the figure 3.4). The inclination of the straight line, which lies on these two points, corresponds to the y axis correction. In this way the flexion (or the extension) is corrected. The last correction is the rotation about the z axis. The talus is fitted using a sphere and a polynomial surface (second order) is adopted for the tip of the foot. The tip conventionally comprises 15 % of the total length around the toes zones. This percentage is not important for an accurate alignment; in a range between 10% and 20% similar results are obtained. The sphere defines the "pternion" ("C" in figure 3.5) while the front point ("D" in figure 3.5) is defined as the maximum on the polynomial surface. The inclination of straight line, which lies on the "C" and "D" points, corresponds to the z axis correction. After the rotations, the last operation allows to translate the solid model. The x and y coordinates of the "C" point are imposed equal to zero, the z coordinate of the "E" point is imposed equal to zero.

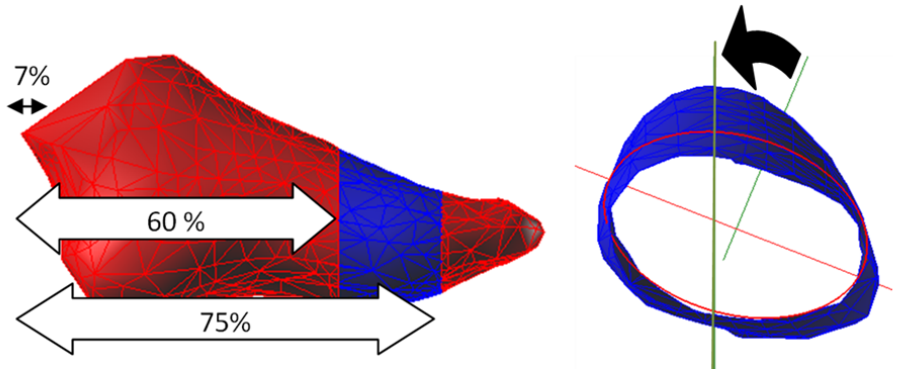

Figure 3.3: Fine alignment around x axis.

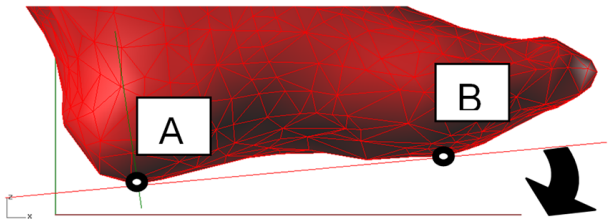

Figure 3.4: Fine alignment around y axis.

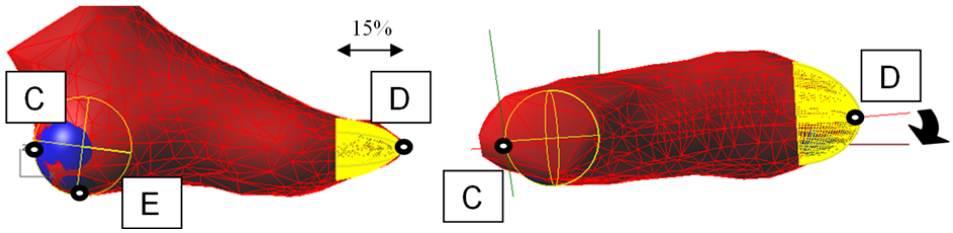

Figure 3.5: Fine alignment around z axis, in yellow the fitting between a sphere on the talus and polynomial surface on the tip.

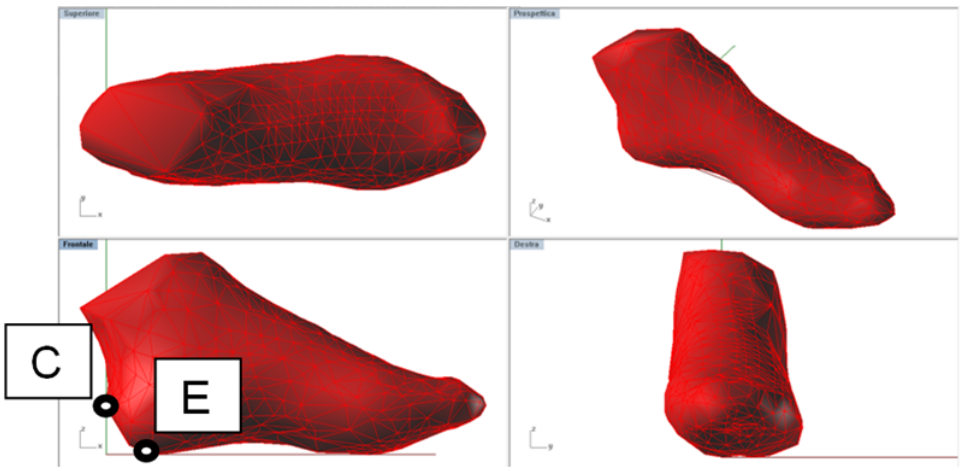

Figure 3.6: Fine alignment, final correction of the translation respect "C" and "D" points.

The aforementioned procedure allows to obtain the same position of different acquired solid model in relation with an established reference system.

This alignment, implemented in Matlab, is performed in 30 seconds. It is possible to write again the algorithm, using another computer language (such as C++), for the reduction of the elaboration time (estimated in one order of magnitude). Fundamental anthropometrical measures can be derived directly from the alignment procedure. E.g. the distance between "C" and "D" point is the total length of the foot (Fig. 3.7).

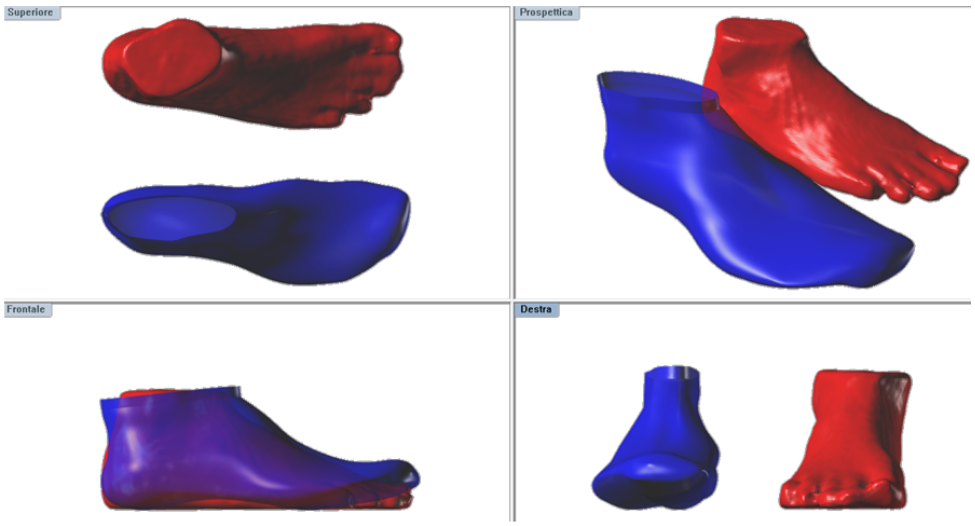

Figure 3.7: The alignments of a foot and a last using the developed application.

3.2 Anthropometrical measurements

Anthropometrical measures are widely discussed in the literature. Major problems are related to: several people are included in the research campaigns and many different strategies can be adopted to measure the foot. This thesis want to develop a method for increasing the considered people and for proposing a robust procedure. The most important methods are based on linear and girth measures. Using 3D scanners linear measurements can be calculated only in some cases where the features are always identified on the foot. Using the free-form solid model, a certain position of each relevant point of the foot cannot be exactly estimated. In many cases, especially in pathological feet, metatarsal girth cannot be correctly estimated. Different doctors can manually measure the metatarsal girth in different way and the obtained results

can be really different. For this reason, all the girths are always calculated orthogonally to the x axis (longitudinal axis) and features are always adopted only for the alignment.

3.3 Sections on the foot

5 mm spaced sections of the foot are calculated. This distance is not fixed and can be varied depending on the application requirements. In general, doctors measures manually seven girths in different sections to customize shoes for pathological feet. Using this method with a in space of 5 mm, it is possible to generate more than 50 sections of an adult foot, considering a total bigger than 300 mm. The intersection between the solid models, represented by mesh, and the plane is implemented in Matlab.

3.4 Foot dimensions

The most important dimension is the total length of the foot. In addition, width, height, girth and area of each calculated section are considered. These data are adopted for the creation of a spread sheet able to characterize the foot. Considering the possibility of managing different spread sheets of different feet, a database can be created for many purposes:

- monitoring a human part, in this case the foot, of an ethnic group;
- studying a group of customers;
- evaluating progressions of pathologies;
- calibrating products of a company for the future;
- measuring sizes of a foot for a custom shoe;
- comparing the measured foot with shoes available in a store;

3.5 Shoe dimensions

Shoe dimensions must be taken in the same position with respect to the foot. E.g. the length of both foot and shoe must be measured using the same criteria and in the same position. The present thesis begins from the concept of finding a good fitting between shoe and foot. The shoe is originated starting from the

last. For this reason, the dimensions are not directly investigated on the shoe but on the last. Starting from the physical shape of the last, whatever RE system, regardless of contact or non-contact techniques, can be used to achieve a solid model of a last. Different methods are tested for the reconstruction of the last; among them CMM (contact), stripe laser (non-contact) and FPP. FPP (Fig. 3.8) seems to be the better compromise between precision and acquisition time. After the reconstruction, the obtained solid model is aligned using the same procedure adopted for the foot. Finally transversal sections are carried out and dimensions of the last are inserted to a spread sheet. In this way, a second database can be created.

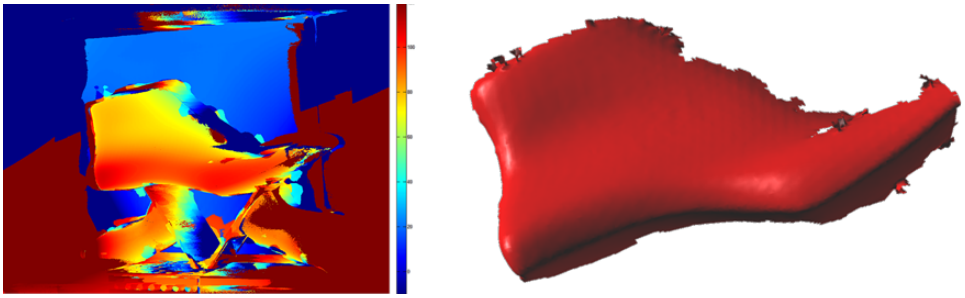

Figure 3.8: The reconstrucion of a last using FPP technique (left) and the mesh generation using a commercial software, Rhinoceros v.4 (right).

3.6 Comfort index

The first database regards the measured feet while the second the measured lasts. In general, whatever foot, contained in the database, can be compared with whatever last on the database. The comparison is similar to a matching operation where similarities are analysed. Therefore, starting from foot dimension, it is possible to make a comparison among different footwears. For this purpose, a function is developed to understand the correspondences between the foot and the last. The function allows to calculate a coefficient, called comfort index. The larger the comfort index is the better fitting between shoe and last. The function contains parameters and measurements of the section. Calibration of parameters is very complex because they must take into account the opinions of doctors (for ergonomics) and shoemakers. In addition, different companies want to consider different parameters in relation to different standard and different ethnic groups.

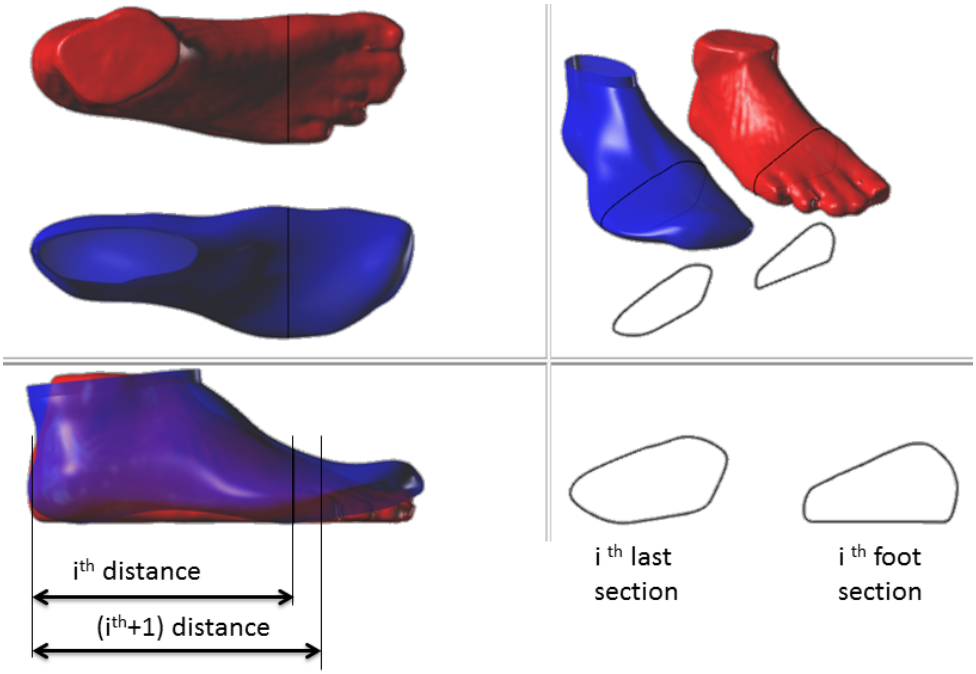

Figure 3.9: The sections of a foot and a last using the developed application.

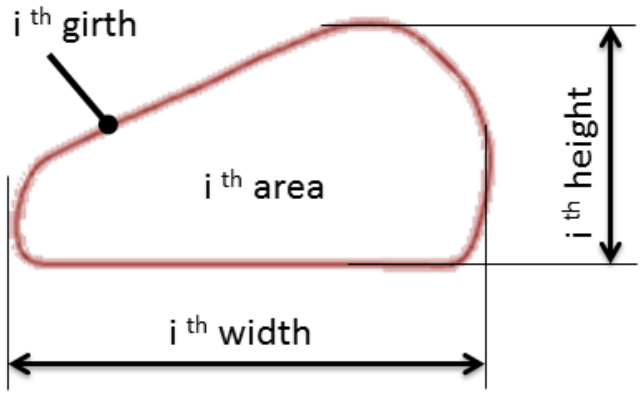

Figure 3.10: The calculated measures of each section: width, height, girth and area.

Num.	dist.	area	girth	width	height
1	115	3325	234	78.2	57.2
2	120	3291	221	71.6	69.5
3	125	3263	219	73.4	66.8
4	130	3231	218	75.3	64.0
5	135	3197	217	77.1	61.3
6	140	3154	216	78.8	58.5
7	145	3100	215	80.4	55.6
8	150	3031	214	81.7	52.8
9	155	2940	212	82.6	50.1
10	160	2826	210	83.0	47.3
11	165	2689	206	83.0	44.1
12	170	2533	202	82.4	41.3
13	175	2372	197	81.4	38.6
14	180	2224	193	80.1	36.2
15	185	2085	188	78.5	34.2
16	190	1953	182	76.6	32.5
17	195	1827	177	74.3	31.1
18	200	1707	171	71.8	29.9
19	205	1591	165	69.0	28.7
20	210	1475	158	65.9	27.7
21	215	1361	151	62.4	26.7
22	220	1248	144	58.8	25.9
23	225	1125	135	54.7	24.8
24	230	991	126	50.3	23.5
25	235	491	98	50.3	23.5
26	240	291	76	20.3	13.5

Figure 3.11: The table extracted from the GUI of the developed application shows the trasversal section of a last. The spaced sections is 5 mm, starting from 115 mm (distance from the pternion) to 240 mm. Area, girth, width, height of each section are in mm.

3.7 Conclusion

The parameters of the comfort index function cannot be published in this thesis because they are considered confidential. Anyway, several considerations can be proposed.

- The length of a shoe is always lightly longer than the foot.
- The zone of metatarsal head must totally match the shoe. Whatever differencies in the girth cause a non-comfort sensation.
- It is better to allow generous gap near the toes.

- The alignment of the sections, indistinctly in the rear or in the front of the foot, seems to be poorly influence on the perceived comfort.

Different companies could develop different functions for the calculus of the index comfort considering dissimilar typologies of customers. In fact, people think sometimes to buy a shoe of a certain trade market since that trade mark is more comfortable. In this case a certain group of shoes is comfortable only for a certain group of people.

Usually, many people do not judge the footwear from its comfort but only from its aesthetic characteristics. Additionally, the routine to test different shoes often appears such as a rite. Therefore this method, which analyses only the geometries, shows criticalities related to the cultural standards. In general, people prefer to test different shoes starting from their size (e.g. number 40) but the time dedicated to a 3d scanner seems to be time wasted. In addition, many times in the post-sale after a week (or a month) the footwear modifies its geometry and the perceived comfort increases. Shoes have this typical behaviour if quality components (leather) are used. At the beginning, the perceived sensation is non-comfort but after sometime the footwear shows enormous adaptive capabilities. For these reasons, the measurement system can be a powerful tool for a total customization of the footwear especially indicated for medical purposes. The mass customization could be considered in the future. In the clinical case, the function of the footwear is predominant with respect to the aesthetic factors. It is possible to find a scheme, in the appendix B, used by one of the major Italian companies of orthopaedics. It is important to note that more than 50 variables must be considered related to patient, last, plantar, models, upper, girth and 2D profiles of left and right foot, sole and other details. This company measures the foot in manual way and creates the orthopaedic footwear customized so as to meet the geometrical requirements of the single patient. In medical field, measures are fundamental and the custom product is made directly from the dimensions for the correction of the pathology. Measurements are also fundamental related to the possibility of monitoring pathology, e.g. the diabetic foot. For the last case the database is necessary to analyse the foot dimension during the evolution of the pathology with the aim of studying the effect of a pharmacologic cure.

Chapter 4

Finite Element (FE) analysis of the foot

The work is focused on the study of the biomechanical behaviour of the foot by means of Finite Element (FE) modeling. This is a crucial task in a research project aimed at studying wearable product, shoes in particular. For this purpose, a foot scanning is performed and the behaviour of the foot under typical loading is predicted. The FE Method can be an effective tool, because analyses a solid model of the foot, predicting the behaviour of all its parts. This paragraph will present an automatic procedure to preprocessing of a FE analysis of the foot, starting from information obtained from clinical exams, such as Computerized Tomography (CT) and Magnetic Resonance Magnetic resonance imaging (MRI). The CT (or MRI) produces a DICOM format file that can be converted into Solid To layer (STL) format via commercial software. Starting from the STL file, a solid model is generated, requiring a regular FE meshing. This solid model can be automatically rebuilt by means of appropriate seam curves on the external surface as shown in the figure 4.1. Simulations ware performed to test the efficiency of the procedure. In particular the slip between the talus and calcaneus on the calcaneal articular surface of talus during the deambulation was simulated. Part of this paragraph starts the article presented at TCN CAE international conference, list of published paper n. 3. A medical exam, CT or MRI, is adopted for the reconstruction of the internal parts while a RE technique could be adopted for the validation of the model. In particular the displacement under loading condition can be estimated and compared with the numerical model.

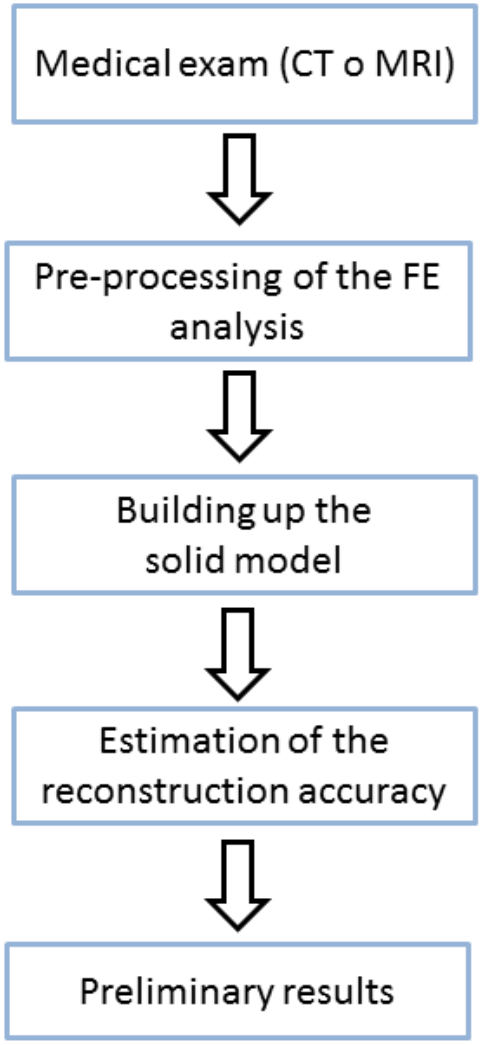

Figure 4.1: The flow chart of the RE of this chapter.

4.1 Introduction

The traditional approach to shoes production starts by building the last, e.g. the form used by shoemaking to shape a shoe. This shape needs to fit the foot. In production, the sole and upper are added to the last. The last is one of the most important issues to make a comfortable shoe. Industrial manufacturing

is based on a series of standard lasts, on the contrary the focus point of the tailored manufacturing process is the customer's foot. The MC process (Fig. 4.2) starts from customer foot measurement using a three dimensional scanner in order to generate the virtual model. The manufacturing of the custom shoes is based on the elaboration of this virtual model.

Figure 4.2: The process to obtain custom shoes.

Figure 4.3: The scanner of the foot (left) and the last in-between the sole and the upper (right).

The foot and the last have dissimilar shape. The foot is scanned unloaded (Fig. 4.3) in the multiple stereo vision (Foot-o-graph, Delta RS, Italy), in a relaxed position to ensure the reliability of the measure. On the contrary, during the deambulation (or the normal daily activity) the foot varies its form. This means that the last must take into account the deformation during the load phase of the foot (perambulation). The displacement of the foot during the perambulation can be investigated considering the biomechanical behavior using a predictive numerical approach. This approach is based on the hypothesis that similar external shape (measured by the scanner) of the foot shows

similar displacements fields. This hypothesis will be validated by comparing the results of theoretical models with experimental measurements that will be carried out on the loaded foot under laboratory controlled conditions. In biomechanics, many approaches, such as plantar and transverse metatarsal arch models, simulate the foot as a spring-damp system, working as a shock absorber. These models do not study the details of the displacements of each part of the foot during loading, like the perambulation. The FE Method can be an effective tool, because it analyses a solid model of the foot, predicting the behaviour of all its parts. In the literature, many papers already faced the problem by FE analysis (Kato et al., 1996), (Chen et al., 2003), (Cheung and Zhang, 2005), (Gefen, 2003) and (Cheung et al., 2005), but a new model for the development of the last seems to be necessary. The required input data are the geometry of each part, the constitutive laws of the materials, the applied loads and constraints (Fig. 4.4). Other parameters have to be considered to manage the process of simulation, e.g. the element size and local mesh refinement. In the following, the attention will be focused on the preprocessing phase, for which an automatic procedure is developed and will be presented. The final FE Model will be checked considering a reference loading condition of the foot.

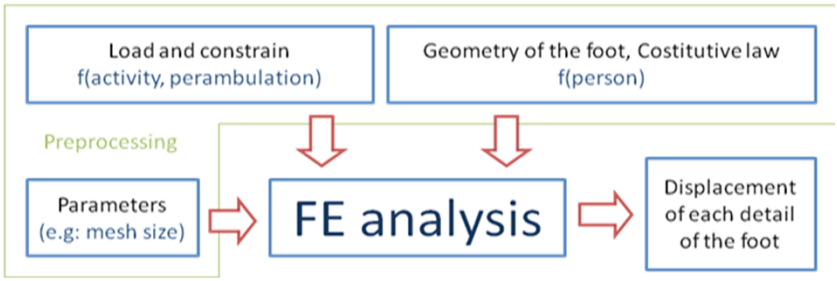

Figure 4.4: The scheme of the simulation process.

4.2 Foot Finite Element (FE) analysis: the preprocessing

The main problem of the preprocessing step (Fig. 4.4) is related to the control of the geometry and its importation into a FE program. An automatic procedure which permits to easily import and discretize the geometry was developed.

4.2.1 Data input

The information related with the shape are derived from a medical exam. At the beginning the Computerized Tomography (CT) produces a DICOM format file formed by a group of images representing the sections of the foot along the transverse and longitudinal (vertical and horizontal) directions. After the medical exam, the DICOM file is automatically converted into Solid To Layer (STL) format via commercial software. Thus, this operation transforms the two dimensional data into three dimensional data. The STL file reproduces each detail of bones shape, tendons and soft tissues and represents the external surface of each component using a set of triangles. The STL cannot be directly imported into the FE program but it must be converted into NURBS surfaces. The problem can be seen in two dimensions: whereas the STL can be figured out like a scatter of points connected by straight segments (linear functions), the NURBS curves are built up by piecewise polynomial functions with a degree higher than one. The output of this process, is a reconstructed curve.

4.2.2 Automatic procedure for building up the solid model

During the creation of the surfaces, the positioning of the seam curves is fundamental. Some commercial softwares can automatically generate the surface starting from an STL. Owing to this automatic procedure, the seam curves are located so as to minimize the error of the reconstruction (Fig. 4.5). However, this process is not always efficient if a regular mesh of the body has to be manufactured. In the preprocessing step, a compromise must be reached considering the accuracy of the reconstruction and the STL details. This starts from the seam curves which are divided into segments, whose sizes are proportional to the final size of the FE mesh. After curves segmentation, the surfaces can be meshed with triangular (or quadrilateral) mesh-only (or plane) elements. Finally, the three dimensional elements are generated starting from the 2D element mesh of the skin. Thus, considering that the quality of the mesh strongly influences the correctness and the efficiency of the FE analysis. The mesh used for building up the seam curves has a relevant impact on all stages of the FE analysis. The bones, which constitute the major volume fraction of the foot, are the most critical parts to be meshed. Two sets of seam curves have been located on the distal and proximal sections of each bone respectively (Fig. 4.5). A third set of seam curve (transversal curves), lying on section planes of the considered bone, intersects the other two. The

first observation concerns the shape of the foot bones. The major bones are elongated in one direction (Fig. 4.5). The stretched structure of the foot can be divided into two parts. The first one is composed by the bones referring to the first, second and third toe. This part also contains the first, second and third metatarsal, cuneiforms, navicular and talus bones. The second one is formed by fourth and fifth toe, fourth and fifth metatarsal, cuboid and calcaneus bones. The procedure (Fig. 4.6) to obtain the surface starts from the evaluation of the bone axes using the STL.

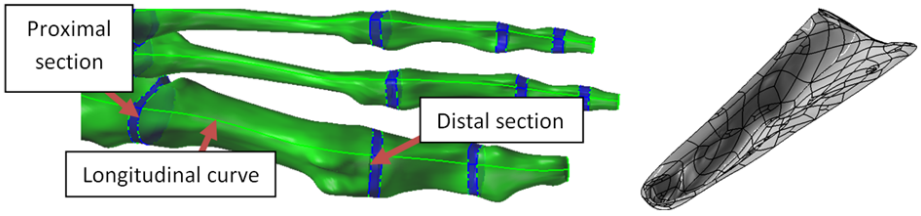

Figure 4.5: The surfaces on the frontal part of the foot and the seam curves, the name of the curves is indicated on of the first metatarsal bone (left), an example of an automatic surface reconstruction via commercial software, in black the seam curves (right).

The axes of the bones enable the definition of orthogonal sectioning planes, whose intersections with external surface define closed curves. These curves are used for the generation of the reconstructed 3D surfaces through a geometrical process called loft. The obtained surfaces represent the external shape of the component and identify the volume of the bones (Fig. 4.8). The distance between adjacent planes can be parametrically varied. Depending on the plane distance, a finer or coarser bone description can be obtained.

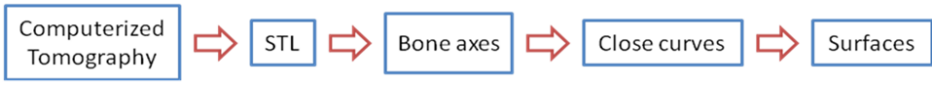

Figure 4.6: The process to obtain the solid model formed by surfaces.

4.3 Reconstruction accuracy

The surface reconstruction introduces some errors. In particular NURBS surfaces are rebuild surfaces of the STL data. The transformation can be seen as

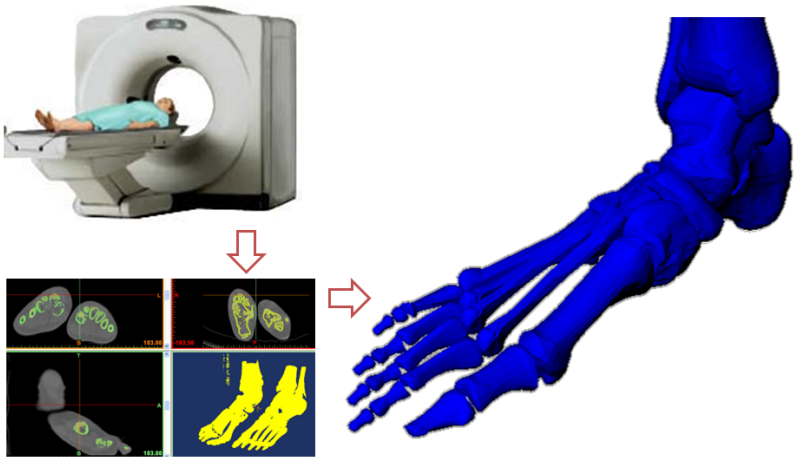

Figure 4.7: First step, from the CT to the STL.

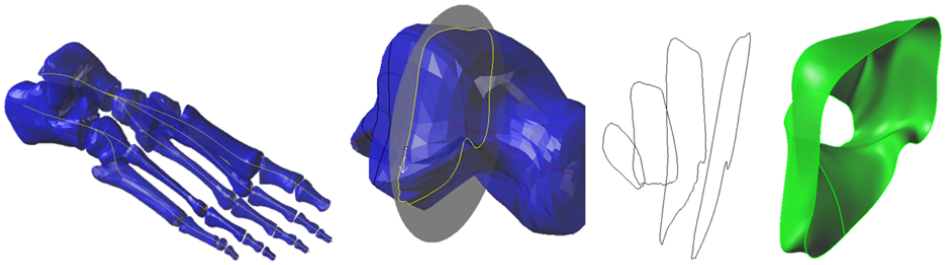

Figure 4.8: The axis bone in yellow in blue (Left), the gray plane (orthogonal to the axis) intersects the talus (center), the close curves and an example of the loft operation (right).

smoothing process. In a complex surface and, especially, in the regions characterized by strong variations of the geometry, the reconstructed surface can deviate from the original one. This deviations can be measured by carrying out a distance analysis, as shown in figure 4.9, where an example for the talus is shown. It can be observed that the deviation is prevalently within a range of 0.3 mm. The largest distance is close to the ligament capsule. In this zone the gradient is high and the adopted interpolation does not work optimally.

The result shows that the major gap is next to the sharp zone. This zone is located at the bone end and the distance can be greater than 2 mm. In

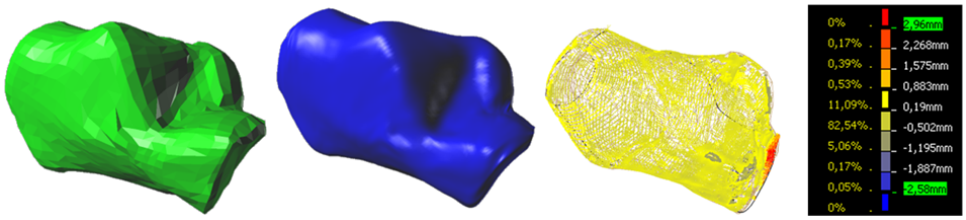

Figure 4.9: A reconstruction example on the talus, the STL and the surface (left), the distance analysis surface-STL and the statistical results.

the example, a worst case has been developed. The distance is increased using a coarse STL. On the contrary, a fine smoothed STL provides a better surface reconstruction. Thus, the finer the medical exams, the better the reconstruction. A better reconstruction of the bones shape can be also obtained by reducing the distance between the orthogonal sectioning planes and/or increasing the precision of the loft operation. The distance and precision are parameters that can be modified directly in the reconstruction algorithm.

4.4 Built up of the FE model

The solid models of the bones and soft tissues represent the basis for defining the FE model. Tendons and ligament capsules at bones ends have also to be accounted for. In the literature some papers suggest the constitutive laws and the most important tendons to be introduced in the analysis. Regard to the capsule, at the moment a simplified planar geometry of the end of each bone has been considered, permitting a simple volume identification (Fig. 4.10). A more detailed solid model of the capsule will be studied in the future.

The elements used for the simulation are 3D 10-node tetrahedral structural elements with a parametric control of the mesh size, whereas the tendons are simulated using spring elements. At this preliminary stage the capsules are represented by an elastic constitutive law, with a Young's modulus some order of magnitude smaller than of the bones in order to reproduce their lower stiffness.

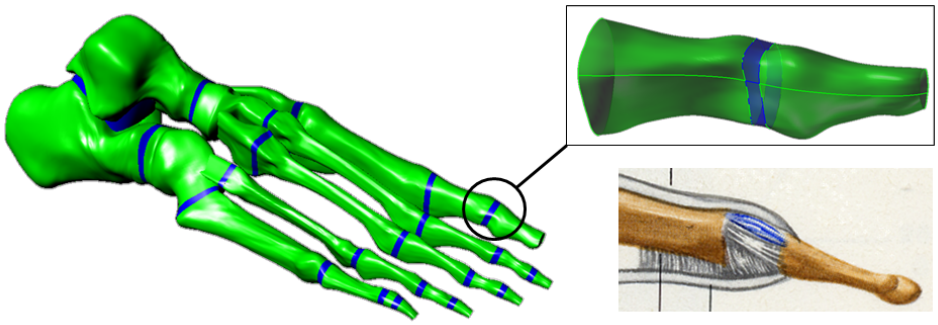

Figure 4.10: Surface reconstruciton of the ligament capsula.

4.5 Test of the preprocessing results in a FE analysis

The FE meshed model (Fig. 4.12) is adopted to perform a simple FE analysis, for which the loads are deduced considering the weight of the human body and the constraints are imposed by holding the external surface of the sole in a plane. This first analysis is a preliminary study to verify the functionality of the preprocessing. The simulation contains soft tissues, bones, ligament capsules and tendons. On the bottom part of the sole, the nodal displacements orthogonal to the sole are constrained. The loads are related to the weight of the human body and are applied on the talus and on the Achilles tendon.

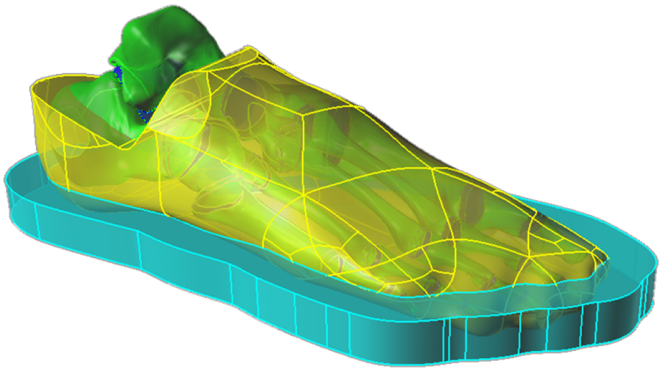

Figure 4.11: The solid model.

In the figure 4.18 shows the displacement field under load of the foot

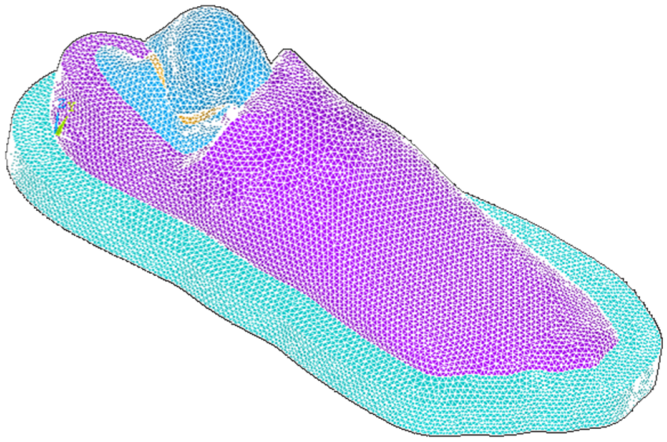

Figure 4.12: The discretization using tetraedical elements.

through colour map. The analysis of the contour plot emphasizes the reduction of the longitudinal plantar arch and the slip between the talus and calcaneus on the calcaneal articular surface. This displacement evolution seems to correctly reproduce the behaviour of the real foot.

4.6 Discussion

The development of customized lasts is acquiring a key role in the shoe design in order to improve the shoe comfort. This paper suggests a new approach to define the preprocessing of the foot FE and demonstrate the possibility to implement it using a particular surface reconstruction method. The accuracy of the reconstruction is ensured by analyzing the deviation of the initial STL from the final surface. The difference in a worst case using a coarse STL is acceptable: more than 90 % of the surface lies in the tolerances of plus minus 0.3 mm. This reconstruction procedure can be also used for other bones, e.g. collarbone. Some parts can be improved, especially with regards to the modeling of the ligament capsula. Moreover at the bones ends the sharp geometry can jeopardize the reconstruction. Some tests of the preprocessing in a simple FE analysis during the deambulation loading condition proved acceptable trends with respct to the displacement observed in real feet.

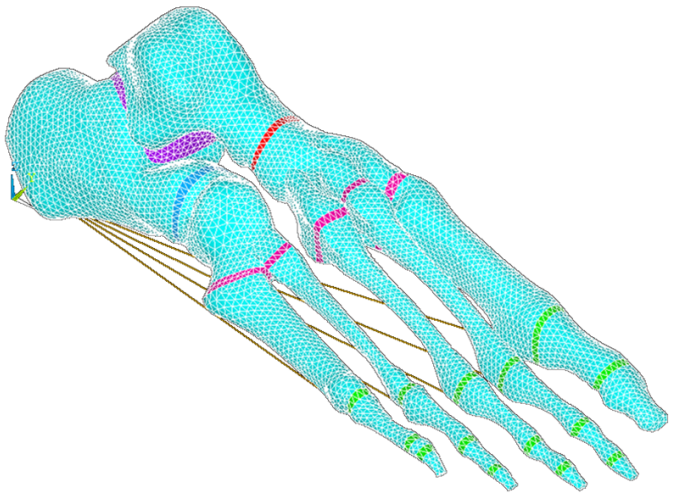

Figure 4.13: FEM model, mesh of bones, ligament capsulae and five main tendons.

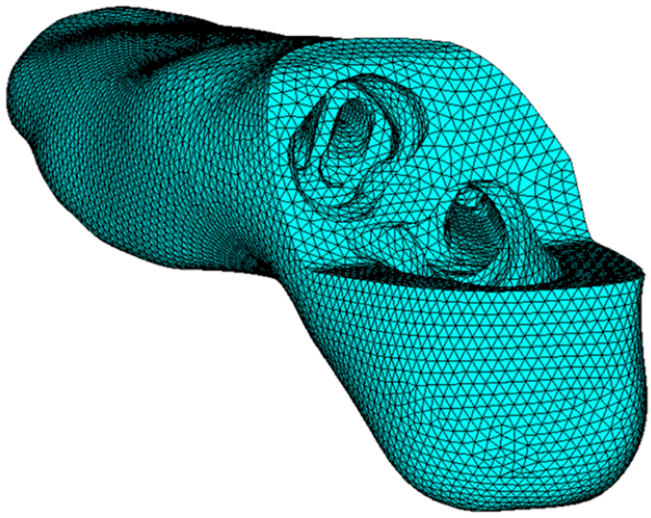

Figure 4.14: FEM model, mesh of soft tissues.

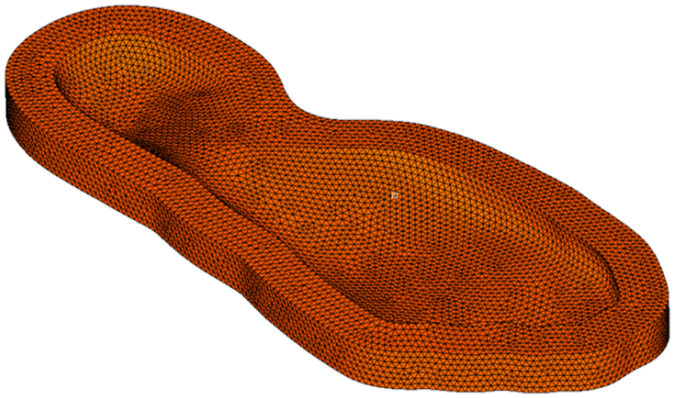

Figure 4.15: FEM model, mesh of the sole.

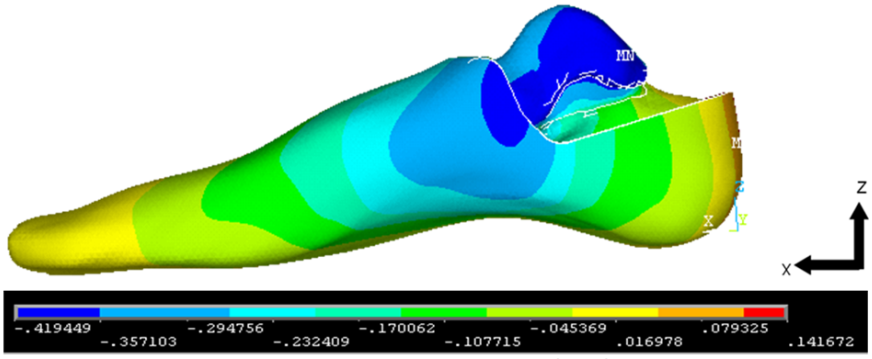

Figure 4.16: The displacement field, z direction, under load of the foot through colour map in centimeters.

4.7 Conclusion

The analysed model is formed by a mesh of circa 200000 tetrahedral elements. The time to perform the analysis is close to 24 hours. All calculated displacements are congruous with the literature. In particular, the slip of talus on calcaneum (subtalar joint) is well represented. The pitch of the plantar helix decreases under loading condition. Contact elements are not included in the analysis. The contact of the foot on the terrain was simulated using insole characterized by low mechanical characteristics (low Young modulus). This allows studying the mechanical behaviour without contact elements. The

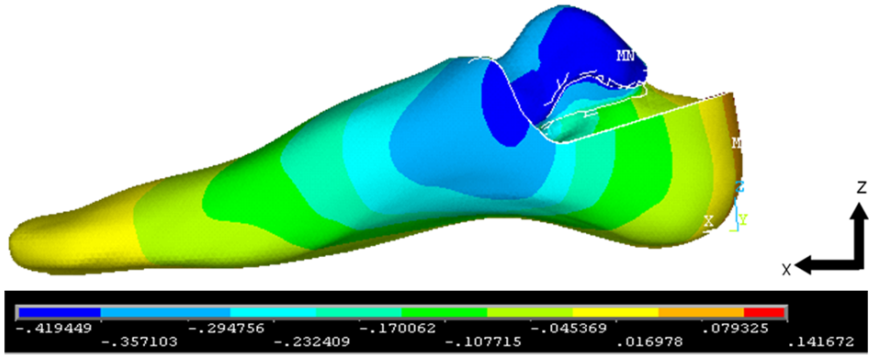

Figure 4.17: The displacement field, x direction, under load of the foot through colour map in centimeters.

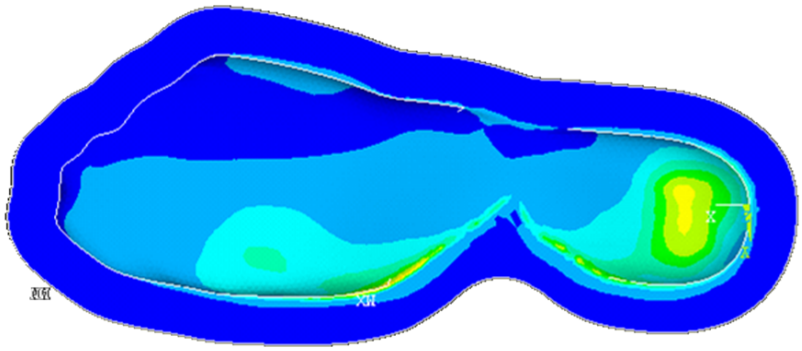

Figure 4.18: The contour map proportional to the pressure on the sole.

entire model is linear, including soft tissue. All soft tissues have the same characteristic. Ligament capsules are characterized by weak soft tissue and their geometry is approximated. It can be possible to consider the structure of the plantar arch, especially in the metatarsal zones, where the major stress is axial. In the FE model five (most important) plantar ligaments are introduced. They ensure the most important influence on the stiffness. The load is applied in two zones: the talus and the Achilles' tendon, both in vertical direction. Whatever additional complication (to obtain a more accurate FE model) increases the computer time. At the moment 24 hours for the simulation is close to the maximum tolerable. As a consequence, the development of this FE analysis was stopped. The possibility of designing wearable products

on the base of FE model was rejected. Predictive numerical analyses using FEM are effective and powerful to estimate displacements, stresses and strains but it is very difficult in a complex human part like the foot. Moreover, it seems to be necessary to study interactions between foot and shoe not only applying a static load but studying dynamical loads during the deambulation. In the literature, it is difficult to find a FE model of the foot validated with a comparison between predictive and real displacement of all the region of the foot. As a consequence works without validation are qualitative and not quantitative. In conclusion, the behaviour of the foot is influenced by many factors such as gait of the subject, speed of the deambulation, alignment of the skeleton, position of the rest of the body, etc. In the description of the foot, predictive model is not sufficient to study the interaction between foot and shoes. In the next paragraph another procedure is discussed. The purpose remains the maximization of the comfort in wearable products but a direct comparison between the external geometry of the subject and the geometry of the wearable product is preferred.

Chapter 5

Conclusion

This work aimed at determining methods and tools allowing an effective modelling of human parts, to be used in the design of the design of wearable products. Reverse Engineering (RE) and Finite Element Method (FEM) were used to gain the goal. RE instruments are the tools for the scope of designing wearable products, FEM aims at studying the displacements of the foot under loading condition.

The thesis starts with the description of a new instrument based on multi stereo vision, focusing the attention on data filtering and the generation of the solid model represented by mesh. The points cloud obtained through multiple stereo vision is the base for the representation of the external surface of the foot. For this purpose, a Matlab application, is studied to automatically filter the acquired data and to generate the solid model. The data filtering is composed of three steps: local density of points, clustering and polynomial surfaces. It is necessary to adopt this procedure because it is not possible to use available (and standard) algorithms; in many conditions points clouds, which represent the real foot, contain only few points. The ratio between correct points (that means the points really belonging to the foot surface) and outlier is unfavourable. The results of reconstructions often show a cloud formed by 1000 points characterized by 300 outlier (30% of outliers). After outliers detection the solid model can be calculated. The mesh generation is formed by Delaunay-based algorithm. Functional points are adopted to improve the reconstruction in the non-convex zones. The developed algorithm generates a solid model (represented by triangular mesh) starting from scattered points. The main characteristic of this Delaunay-based algorithm is to manage convex and non-convex zones under condition of down-sampling. Meshes are always

closed and normal directions of triangles are always internal to the foot. The multiple stereo vision instrument is able to reconstruct the foot despite the noise coming from external environment, such as light variations. In addition, all the information for the reconstruction are acquired simultaneously. All the parts of the instrument are fixed, there is no sliding rail. The instrument is open and no claustrophobic effect is produced on the patient. A socket, containing the patterns for the recognition during image analysis process must be adopted, thus the foot is covered. The foot is measured unloaded to decrease the uncertainty variables related to the percentage of weight considered and to the position of the load during the acquisition. This is a limiting condition, but it increases the repeatability of the measures, since the foot measurements under variable weight bearing percentage is not possible. Cameras are characterized by fish eye lens to reduce the size of the instrument by decreasing the distance between the foot and the cameras. The external dimensions of the multiple stereo vision instrument can be considered acceptable and ensure easy transport in a car.

Considering the obtained results, a second instrument based on the silhouette is studied. Two mirrors are used to frame the scene from another point of view. The algorithm is again implemented in Matlab and it is derived from the work of Forbes et al. (2007). The instrument is made up of only three components: 2 mirrors, 2 cameras and a background in black cotton fabric. The model acquired using silhouette method is directly represented by mesh. The obtained instrument is relatively simple and cheap. It can be adopted to estimate the volume of the foot.

These two acquisition methods, stereo and silhouette, are compared with a laser instrument available on the market. The precision of three different foot scanners is evaluated and compared. Deviations (on each part of the model) between known model and acquired model are evaluated. The first observation concerns silhouette, which is much different in comparison with the remaining techniques. The deviation of the acquired from the real model is major than 3 mm. The 3D reconstruction of the foot with respect to stereo and laser by silhouette method is insufficiently detailed, so that this method is unsatisfactory in comparison with the two others. Nevertheless the silhouette technology could support the data acquisition and filtering of other non-contact techniques. The results of both laser and multiple stereo vision scanners could be considered good enough to have a detailed 3D reconstruction of the foot. The differences between these two methods, in terms of dimension precision, are around 2 mm in length, so that they allow a good external anatomical

description of the foot, as required for tailored shoes. Both scanners show a good repeatability and a low coefficient of variation. Considering the obtained results, the multiple stereo vision scanner seems to be the better instrument to estimate the foot shape. The lightly higher coefficient of variation in length estimated from the laser scanner data can be explained considering the base of the acquisition slice step imposed (1.37 mm). This is the distance between two adjacent slices of the stripe laser. As a consequence, the maximum error could be 1.37 multiply by 2 mm. One of the most important advantages of the laser scanner technologies is the possibility of acquiring data on a foot in different weight bearing conditions. On the contrary, with the stereo vision scanner which has been tested in this work, only the unloaded foot condition is possible. One of the disadvantages in the stereo vision system is related to the adoption of the socket, which must be used because it contains the pattern for the image recognition. The deviation of the acquired from the real model was lightly high. For this reason another instrument is studied imposing, as a requirement, an error lower than that of stereo and laser techniques. The errors found during the comparison can be acceptable for the analysis of a wearable product, but are not sufficient for scientific puposes.

A fourth instrument based on range finding was developed. A lot of possible methods were analysed, than the multifrequencies, belonging to the Fringe Projection Profilometry (FPP) group, has been considered as the best compromise between precision, accuracy and elaboration times. The necessary components are a camera and a projector available on whatever electronic store. In this way the hardware of the instrument costs less than 1000 euro and the precision can be similar to the instrument available on the market, based on the same technology. The fundamental characteristic of this instrument is the capability of reconstructing a point for each pixel of the camera. The algorithm, developed in Matlab, performs the calculus of a cloud composed by 7.2 million of points in 12 seconds. It is not necessary to impose a pattern (such as the socket for the multiple stereo vision) on the object, because the pattern is directly projected. The standard deviation of the distance between correct height and reconstructed height is 0.09 mm with a precision of 0.22 mm. The proposed reconstruction algorithm can be considered up to date since it is derived from the most recent references in the literature (2010). Nevertheless the implementation of the algorithm was not straightforward but it required a fine tuning of the acquisition parameters.

At the beginning of the work, an instrument was designed to develop a RE system for the foot only. The results demonstrated that many objects,

porous materials and non-transparency liquids included, and different human parts can be reconstructed using this technique. In the future, it is also possible to develop other kinds of instruments applying the same technique, e.g. using a smaller projector and applying the FPP to a microscope. Or considering bigger instruments, the field of view could be increased using a powerful projector to reconstruct objects lenght more than 2 meter. In this case, the system for large complex shape can be adopted. The 3D shape measurement technique has been also employed to construct a complete 360 degrees object. Many reconstructions are shown, however in figure 2.38 wrinkles on the phalanges are correctly described. This is an unexpected result considering that the distance between the hand and the acquisition system was one meter. At this distance the human eye is not able to recognize details smaller than 0.4 mm.

The use of these RE techniques allows to adequately reconstruct the geometrical model of the foot; each of them as has advantages and disadvantages. Summarizing the main advantages, stereo is instantaneous, laser can also measure the loaded foot, silhouette is low cost and FPP is very precise; regarding the main disadvantages, stereo needs patterns, laser needs relative movements between acquisition apparatus and object, silhouette is imprecise and FPP is not instantaneous.

After RE study, a FE analysis is performed to estimate the deformation of the foot under loading conditions. The developed model is linear and contains about 200000 elements. The time to perform the analysis is close to 24 hours. All calculated displacements are congruous with the literature. In particular, the slip of talus on calcaneum (subtalar joint) is well represented and the pitch of the plantar helix decreases under loading condition. Contact elements are not included in the analysis. The contact of the foot with the terrain was simulated using insole characterized by (low Young modulus). This allows studying the mechanical behaviour without contact elements. Ligament capsules are characterized by weak soft tissue and their geometry is approximated. Any additional complication aimed at obtaining a more accurate FE model, increases the computational time. At the moment, 24 hours for the simulation is close to the maximum tolerable. Predictive numerical analyses using FEM are effective and powerful to estimate displacements, stresses and strains but it is very difficult in a complex human part like the foot. Moreover, it seems to be necessary to study interactions between foot and shoe not only applying a static load, but also studying dynamical loads during the deambulation. In the literature, it is difficult to find a FE model of the foot validated with a com-

parison between predictive and real displacement in all the regions of the foot. In conclusion, the behaviour of the foot is influenced by many factors such as gait of the subject, speed of the deambulation, alignment of the skeleton, position of the rest of the body, etc. In the description of the foot, predictive model is not sufficient to study the interaction between foot and shoes. For these reasons, it looked worthy to address further efforts to a direct matching between the acquired geometry and the shape of the wearable product. A function, capable to carry out the matching between foot and shoe, is developed and a coefficient called comfort index is calculated. The comfort index considers many factors. Two of them are proposed in following: the zone of metatarsal head must totally match the shoe and whatever differences in the ball girth cause a non-comfort feeling. The function can vary depending on the characteristics of each company. In particular, often customers prefer to test the shoes for aesthetic motivations. For this reason the measurement system can be a powerful tool for total customized footwear, given that the shoe is developed only for the measured foot and the aesthetic aspect is secondary. Considering this concept the measurement system is especially indicated for medical purposes. In medical field, measurements are fundamental and the custom product is made directly from the dimensions useful for the correction of the pathology. Measurements are also fundamental monitoring pathologies, e.g. the diabetic foot.

The thesis describes the development of engineering methods and tools based on biometrics, anthropometry and biomechanics aimed at designing wearable products. In the future, improvement of the FPP instrument is planned. In particular two ways can be followed. First, the projector can be substituted by other devices able to provide light sources and to generate the fringes, in this way the projection system will be improved. Second, the implementation can be carried out in another programming language; at the moment, the calibration is implemented in Python and the elaboration time is halved, the remaining parts are implemented in Matlab. These two improvements could allow to measure the displacements of the foot under loading conditions validating the FE analysis. It must be noted that these techniques could be also used in other fields, such as safety (facial scanner) or quality control in industrial processes.

Bibliography

Arndt, A., Westblad, P., Winson, I., Hashimoto, T., and A., L. (2004). Ankle and subtalar kinematics measured with intracortical pins during the stance phase of walking. *Foot Ankle Int.*, 25(5):357 – 364.

Barnard, S. T. and Fischler, M. A. (1982). Computational stereo. *Computing Surveys*, 14(4):553 – 572.

Ben Gal, I., Maimon, O., and Rockach, L. (2005). *Outlier detection, a Complete Guide for Practitioners and Researchers*. Kluwer Academic Publishers.

Besl, P. J. (1988). Active, optical range imaging sensors. *Machine Vision and Applications*, 1:127–152.

Bouguet, J.-Y. and Perona, P. (1999). 3d photography using shadows in dual-space geometry. *International Journal of Computer Vision*, 35:129–149.

Brown, M., Burschka, D., and Hager, G. (2003). Advances in computational stereo. *Pattern Analysis and Machine Intelligence, IEEE Transactions on*, 25(8):993 – 1008.

Cavanagh, P., Morag, E., Boulton, A., Young, M., Deffner, K., and Pammer, S. (1997). The relationship of static foot structure to dynamic foot function. *Journal of biomechanics*, 30(3):243 – 250.

Cavanagh PR, Rodgers MM, I. A. (1987). Pressure distribution under symptom-free feet during barefoot standing. *Foot Ankle*, 7(5):262 – 276.

Chen, W.-P., Ju, C.-W., and Tang, F.-T. (2003). Effects of total contact insoles on the plantar stress redistribution: a finite element analysis. *Clinical biomechanics*, 18(6):17–24.

Cheung, J. T.-M. and Zhang, M. (2005). A 3-dimensional finite element model of the human foot and ankle for insole design. *Archives of physical medicine and rehabilitation*, 86(2):353 – 358.

Cheung, J. T.-M., Zhang, M., Leung, A. K.-L., and Fan, Y.-B. (2005). Three-dimensional finite element analysis of the foot during standing a material sensitivity study. *Journal of biomechanics*, 38(5):1045 – 1054.

Curless, B. (1999). From range scans to 3d models. *SIGGRAPH Comput. Graph.*, 33:38–41.

Daentzer, D., Wuelker, N., and Zimmermann, U. (1997). Observations concerning the transverse metatarsal arch. *Foot Ankle Surgery*, 3(1):15 – 20.

D'Apuzzo, N. (2006). Overview of 3d surface digitalisation technologies in europe. In *Three-Dimentional Image Capture and Applications VI, Proc. of SPIE-IST Electronic Imagin.*

Dey, T., Giesen, J., and Hudson, J. (2001). Delaunay based shape reconstruction from large data. In *Parallel and Large-Data Visualization and Graphics, 2001. Proceedings. IEEE 2001 Symposium on*, pages 19 –146.

Dhond, U. and Aggarwal, J. (1989). Structure from stereo-a review. *Systems, Man and Cybernetics, IEEE Transactions on*, 19(6):1489 –1510.

Du, H. and Wang, Z. (2007). Three-dimensional shape measurement with an arbitrarily arranged fringe projection profilometry system. *Optics Letters*, 32:2438–2440.

Forbes, K., Nicolls, F., de Jager, G., and Voigt, A. (2006). Shape-from-silhouette with two mirrors and an uncalibrated camera. *Computer Vision ECCV 2006, Lecture Notes in Computer Science*, 3952:165–178.

Gefen, A. (2003). Plantar soft tissue loading under the medial metatarsals in the standing diabetic foot. *Medical engineering physics*, 25(6):491–499.

Goonetilleke, R., Witana, C., Zhao, J., and Xiong, S. (2009). The pluses and minuses of obtaining measurements from digital scans. 5620:681–690.

Gorthi, S. S. and Rastogi, P. (2010). Fringe projection techniques: Whither we are? *Optics and Lasers in Engiering*, 48(2):133–140.

Grauman, K., Shakhnarovich, G., and Darrell, T. (2008). Inferring 3d structure with a statistical image-based shape model. In *statistical image-based shape model. In Ninth International Conference on Computer Vision, ICCV 2003, Nice, France.*

Hebert, M. (2000). Active and passive range sensing for robotics. In *Robotics and Automation, 2000. Proceedings. ICRA '00. IEEE International Conference on*, volume 1, pages 102 –110.

Huang, P. S., Zhang, S., and Chiang, F.-P. (2005). Trapezoidal phase-shifting method for three-dimensional shape measurement. *Optical Engineering*, 44(12).

ISO10360-2 (2001). *Acceptance and reverification tests for coordinate measuring machines (CMM)- Part 2: CMMs used for measuring size.* Geometrical Product Specifications.

ISO10360-4 (2000). *Acceptance and reverification tests for coordinate measuring machines (CMM) - Part 4: CMMs used in scanning measuring mode.* Geometrical Product Specifications.

Kapandji, I. A. (1977). *Fisiologia articolare.* Marrapese Editore, Roma.

Kato, H., Takada, T., Kawamura, T., Hotta, N., and Torii, S. (1996). The reduction and redistribution of plantar pressures using foot orthoses in diabetic patients. *Diabetes research and clinical practice*, 31(1):115 – 118.

Kolev, K. and Cremers, D. (2008). Integration of multiview stereo and silhouettes via convex functionals on convex domains. *Computer Vision ECCV 2008, Lecture Notes in Computer Science*, 5302:752–765.

Laurentini, A. (1994). The visual hull concept for silhouette-based image understanding. *IEEE Trans. Pattern Anal. Mach. Intell.*, 16:150–162.

Lee, S., Muller, C. C., Stefanyshyn, D., and Nigg, B. M. (1999). Relative forefoot abduction and its relationship to foot length in vitro. *Clinical Biomechanics*, 14(3):193 – 202.

Lerch, T., Mac Gillivray, M., and Domina, T. (2007). 3d laser scanning: A model of multidisciplinary research. *Journal of Textile and Apparel, Technology and Management*, 5(4):1 – 22.

Lin, Y.-P., Wang, C.-T., and Dai, K.-R. (2005). Reverse engineering in cad model reconstruction of customized artificial joint. *Medical Engineering Physics*, 27(2):189 – 193.

Lorensen, W. E. and Cline, H. E. (1987). Marching cubes: A high resolution 3d surface construction algorithm. *SIGGRAPH Comput. Graph.*, 21:163–169.

Lundberg, A. (1989). Kinematics of the ankle and foot. in vivo roentgen stereophotogrammetry. *Acta Orthop Scand Suppl*, 233:1–24.

Luximon, A., Goonetilleke, R., and Zhang, M. (2005). 3d foot shape generation from 2d information. *Ergonomics*, 48:625–641.

Mahaisavariya, B., Sitthiseripratip, K., Tongdee, T., Bohez, E. L. J., Vander Sloten, J., and Oris, P. (2002). Morphological study of the proximal femur: a new method of geometrical assessment using 3-dimensional reverse engineering. *Medical Engineering Physics*, 24(9):617 – 622.

Marr, D. C. and Poggio, T. (1976). A computational theory of human stereo vision. In *Proceedings of the Royal Society of London*, pages 301 – 328.

Morag, E. and Cavanagh, P. (1999). Structural and functional predictors of regional peak pressures under the foot during walking. *Journal of biomechanics*, 32(4):359 – 370.

Moseley, L., Smith, R., Hunt, A., and Gant, R. (1996). Three-dimensional kinematics of the rearfoot during the stance phase of walking in normal young adult males. *Clinical Biomechanics*, 11(1):39 – 45.

Mundermann, L., Mundermann, A., Chaudhari, A. M., and Andriacchi, T. P. (2005). Conditions that influence the accuracy of anthropometric parameter estimation for human body segments using shape-from-silhouette. In *Procedings of Videometrics VIII, San Jose, CA*.

Paparella and Treccia, R. (1978). *Il piede dellúomo*. Verduci Editore.

Pisani, G. (1976). Calcanean and astragalic foot [piede calcaneale e piede astragalico]. *Minerva Ortopedica*, 27(3):110–113.

Popov, I. and Onuh, S. O. (2009). Reverse engineering of pelvic bone for hip joint replacement. *Journal of Medical Engineering Technology*, 33(6):454–459.

Salvi, J., Pags, J., and Batlle, J. (2004). Pattern codification strategies in structured light systems. *Pattern Recognition*, 37(4):827 – 849.

Sarrafian, A. and Shahan, K. (1993). Biomechanics of the subtalar joint complex. *J Clinical Orthopaedics and Related Research*, 240(1):17 – 26.

Schmid, C. and Zisserman, A. (1997). Automatic line matching across views. In *Computer Vision and Pattern Recognition, 1997. Proceedings., 1997 IEEE Computer Society Conference*, pages 666 –671.

Schreiber, W. and Notni, G. (2000). Theory and arrangements of self-calibrating whole-body three-dimensional measurement systems using fringe projection technique. *Optical Engineering*, 39(1):159–169.

Seitz, S., Curless, B., Diebel, J., Scharstein, D., and Szeliski, R. (2006). A comparison and evaluation of multi-view stereo reconstruction algorithms. In *Computer Vision and Pattern Recognition, 2006 IEEE Computer Society Conference on*, volume 1, pages 519 – 528.

Szeliski, R. (2010). *Computer Vision: Algorithms and Applications (Texts in Computer Science)*. Springer.

Takeda, M., Ina, H., and Kobayashi, S. (1982). Fourier-transform method of fringe-pattern analysis for computer-based topography and inteferometry. *Journal of the Optical Society of America*, 72:156–160.

Tomasi, C. and Kanade, T. (1992). Shape and motion from image streams under orthography: a factorization method. *International Journal of Computer Vision*, 9:137–154.

Viceconti, M., Zannoni, C., Testi, D., and Cappello, A. (1999). Ct data sets surface extraction for biomechanical modeling of long bones. *Computer Methods and Programs in Biomedicine*, 59(3):159 – 166.

Vlasic, D., Baran, I., Matusik, W., and Popovic, J. (2008). Articulated mesh animation from multi-view silhouettes. *ACM Transactions on Graphics*, 27(3):1 – 9.

VoMinh, Wang, Z., Thang, H., and Nguyen, D. (2010). Flexible calibration technique for fringe-projection-based three-dimensional imaging. *Opt. Lett.*, 35.

Wang, Z., Nguyen, D. A., and Barnes, J. C. (2010). Some practical considerations in fringe projection profilometry. *Optics and Lasers in Engineering*, 48(2):218 – 225. Fringe Projection Techniques.

Witana, C., Feng, J., and Goonetilleke, R. (2004). Dimensional differences for evaluating the quality of footwear fit. *Ergonomics*, 47:1301–1317.

Witana, C., Xiong, S., Zhao, J., and Goonetilleke, R. (2006). Foot measurements from three-dimensional scans: A comparison and evaluation of different methods. *International Journal of Industrial Ergonomics*, 36(9):789 – 807.

Xiong, S., Goonetilleke, R. S., Zhao, J., Li, W., and Witana, C. P. (2009). Foot deformations under different load-bearing conditions and their relationships to stature and body weight. *Anthropological Science*, 117(2):77–88.

Yemez, Y. and Wetherilt, C. (2007). A volumetric fusion technique for surface reconstruction from silhouettes and range data, computer vision and image understanding. *Computer Vision and Image Understanding*, 105(1):30–41.

Zhang, S. (2010). Recent progresses on real-time 3d shape measurement using digital fringe projection techniques. *Optics and Lasers in Engineering*, 48(2):149 – 158.

Zhang, Z. (2000). A flexible new technique for camera calibration. *Pattern Analysis and Machine Intelligence, IEEE Transactions on*, 22(11):1330 – 1334.

Appendix A

Anatomy

In this appendix, a variety of basic terms to describe body positions, or motions, used in this thesis, are mentionded.

Cardinal planes:

Frontal Plane describes the plane dividing the front of the body and the back of the body.
Sagittal Plane describes the plane dividing the left hand and right hand portions of the body.
Transverse Plane describes the plane dividing the top portion and bottom portion of the body.
Figure planes

Orientation:

Medial describes the location of something closer to the midline of the body. For example, the big toe is medial to the little toe.
Lateral describes the location of something further from the midline of the body. For example, the little toe is lateral to the big toe.
Dorsal means the top of the foot.
Plantar means the bottom of the foot or the sole.
Anterior means the front of the body. For example, your shin bone is anterior to your Achilles Tendon.
Posterior means the back of the body. For example, your heel bone lies posterior to your toes.

Motions:

Adduction describes the motion of bringing something towards the midline of the body. For example, if the big toe were oriented so it was pointing away from the second toe and towards the opposite foot, it would be adducted.
Abduction describes the motion of taking something away from the midline of the body. For example, if the big little toe were oriented so it was pointing away from the other toes, it would be abducted.
Inversion describes the motion of the foot where the foot is rolling over towards the medial, or inside portion, of the foot. (See illustration below.)
Eversion describes the motion of the foot where the foot is rolling over towards the lateral, or outside portion, of the foot. (See illustration below.)
Pronation is a complicated motion involving all three cardinal planes. Pronation involves movement of the arch in a plantarflexed, adducted and everted position.
Supination is the opposite of pronation. Supination involves movement of the arch in a dorsiflexed, abducted and inverted position.

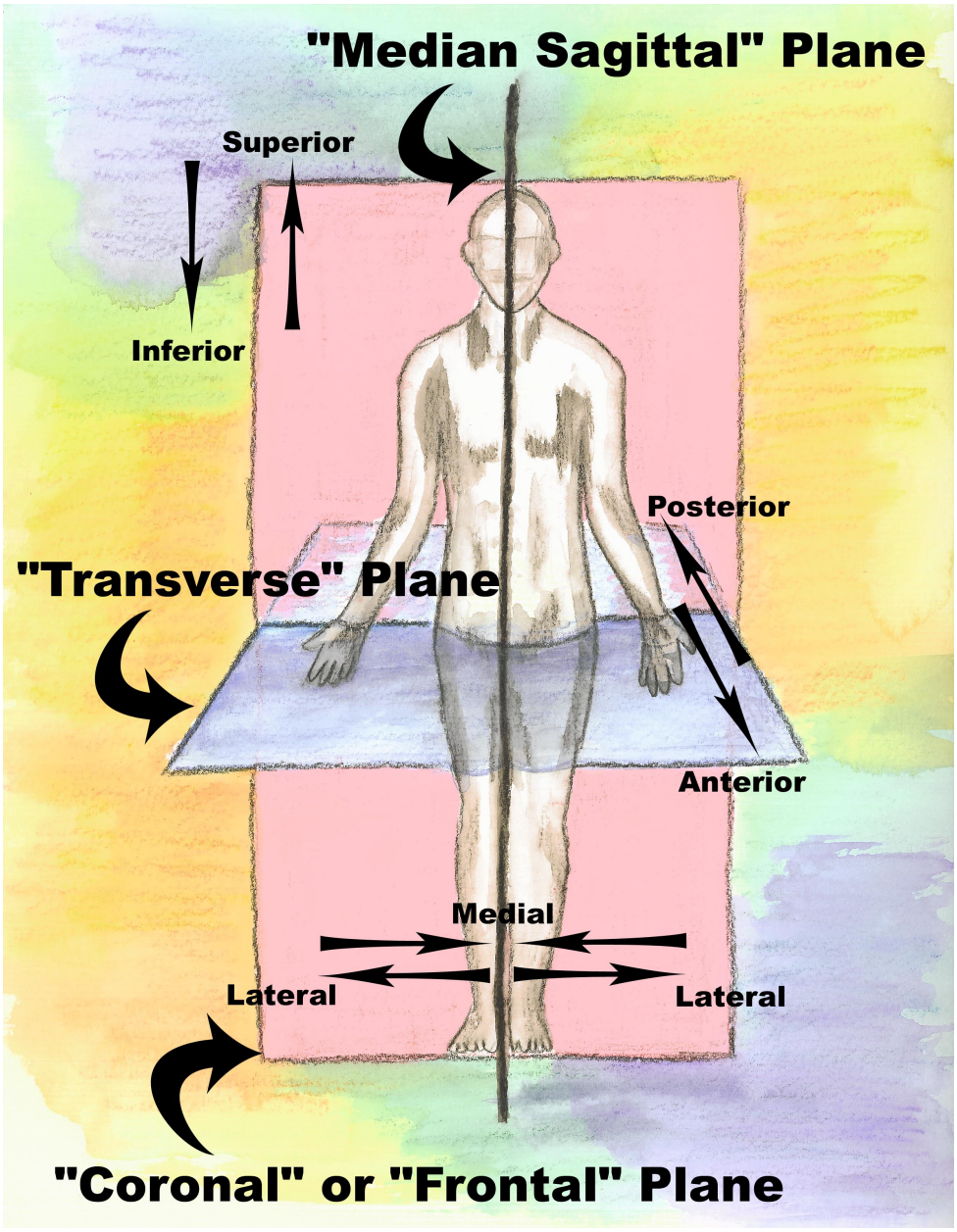

Figure A.1: Cardinal planes.

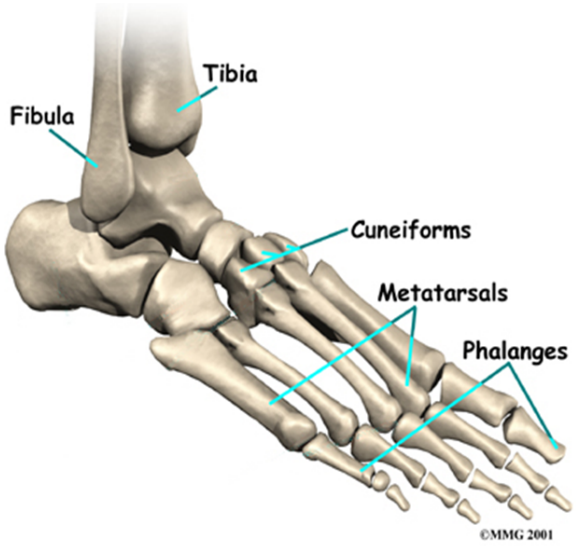

Figure A.2: Fundamental bones parts.

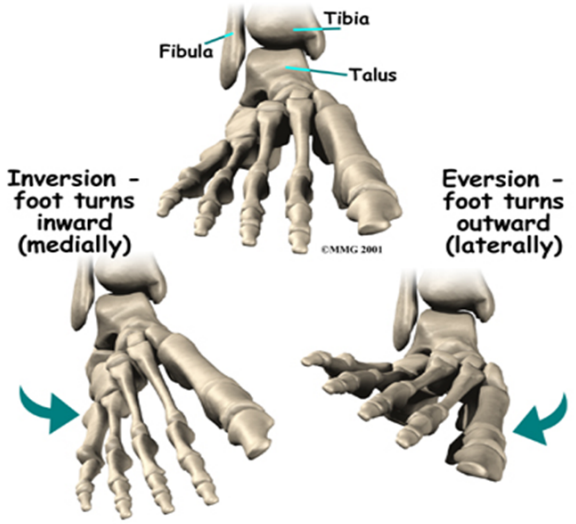

Figure A.3: Inversion and eversion.

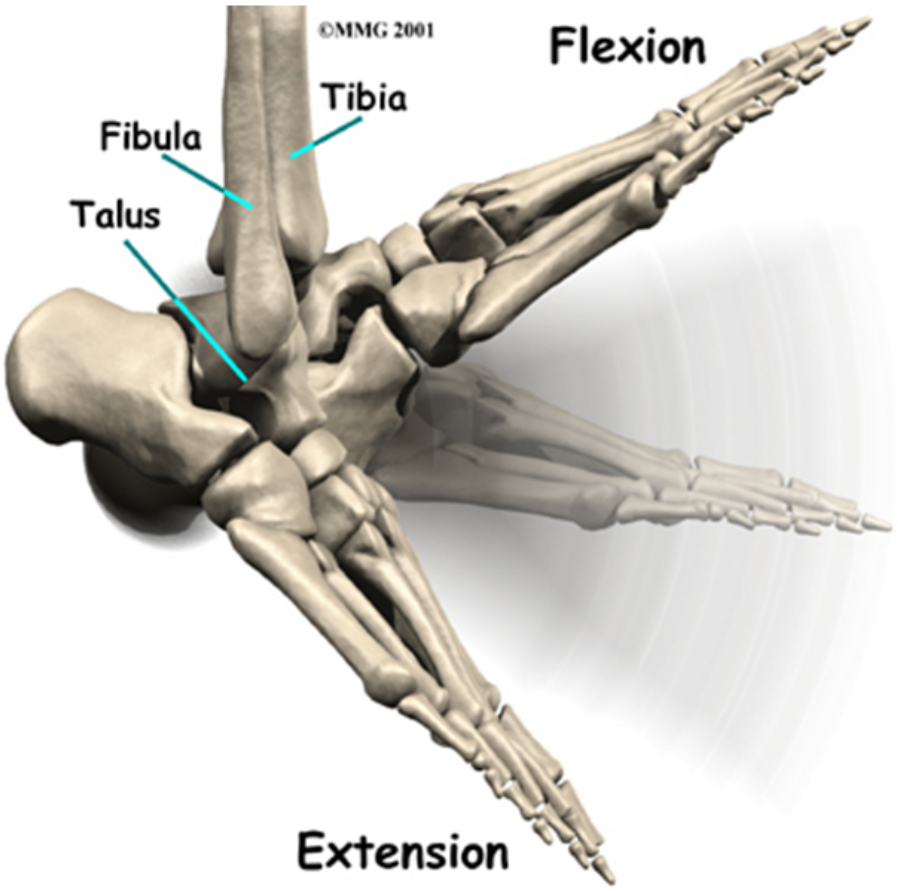

Figure A.4: Flexion and extension.

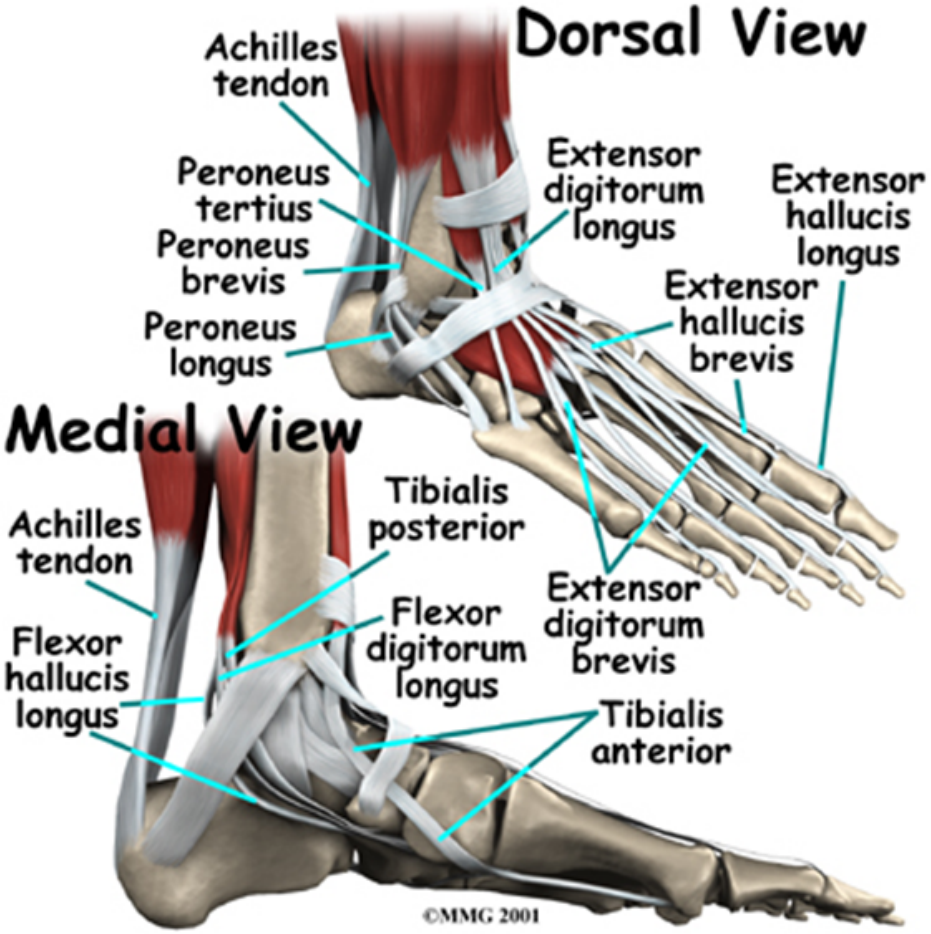

Figure A.5: Ligament and tendons.

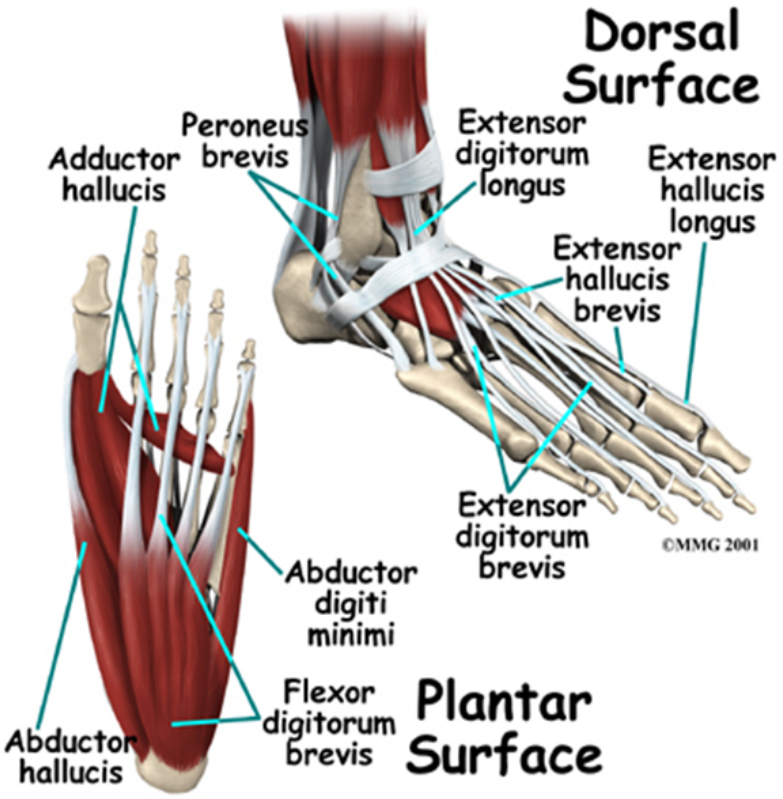

Figure A.6: Muscles.

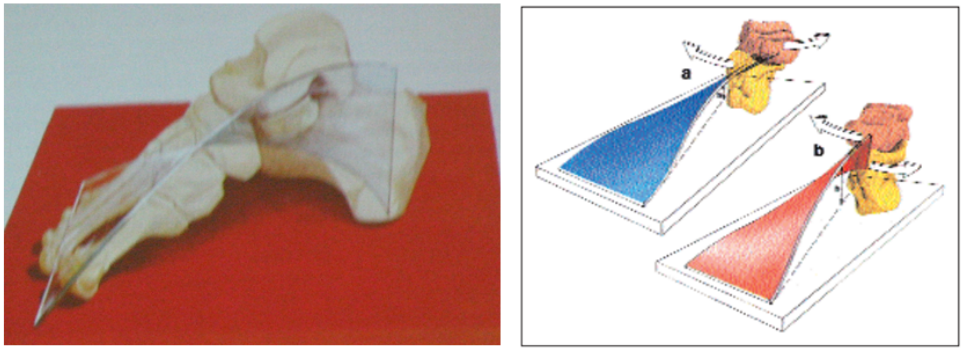

Figure A.7: The helix model theorized by Paparella.

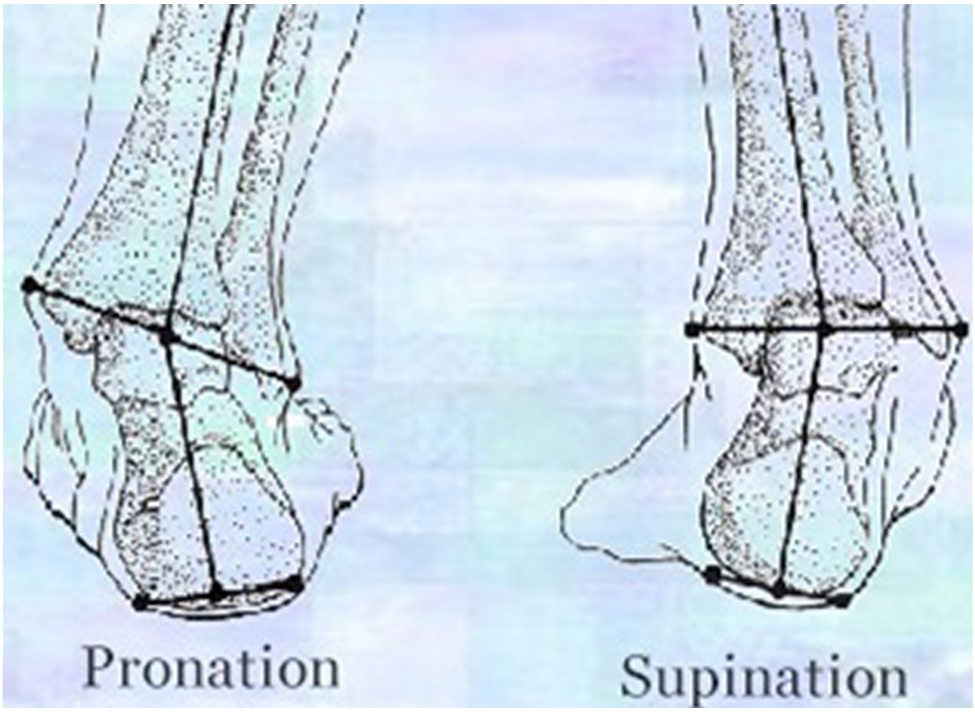

Figure A.8: Pronation and supination.